ISSN 1016-3115

wgn

27 - 6
december 1999

bimonthly journal of the international meteor organization

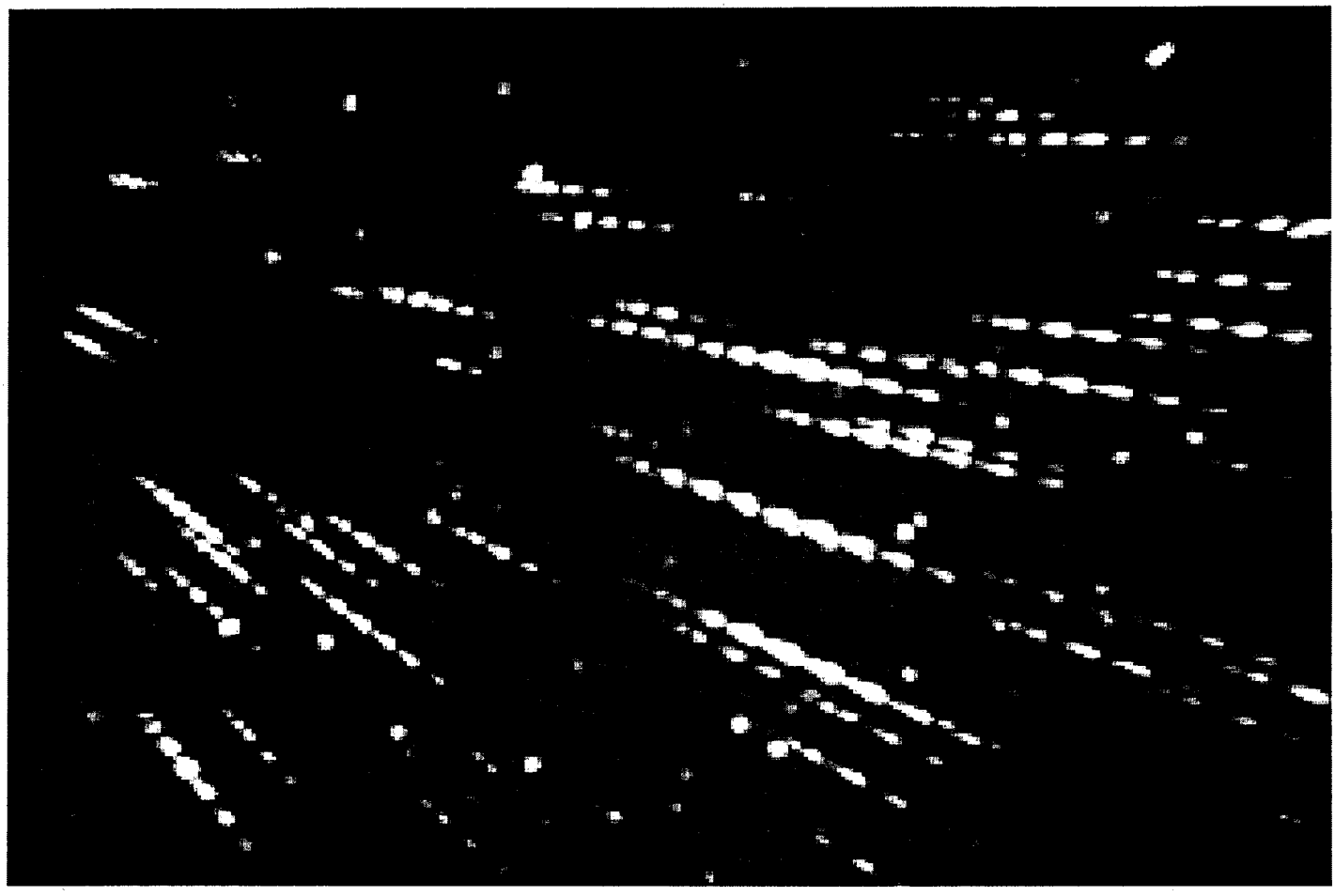

Composite picture of Leonid meteors taped by the image-intensified video system CARMEN on November 18, 1999, between 2^h00^m and 2^h15^mUT. The camera was operated by the German *Arbeitskreis Meteore* members Jürgen Rendtel and Sirko Molau north of Malaga in southern Spain. The camera shutter breaks the meteor path into single "droplets",a distinct effect of the Leonids' high entry velocity. The bright star on the top right is β Ursae Majoris, the star near the lower left corner, behind a meteor, is α Lyncis.

In this issue:

In case of non-delivery, return postage guaranteed. Please return to:
v.u.: Marc Gyssens, Heerbaan 74, B-2530 Boechout, Belgium

WGN, Vol. 27, No. 6, December 1999, pp. 263–338

Contents

Useful Information

The February issue *(WGN 28:1)*

The *February issue* will be mailed around mid-February. Contributions are due on *January 28* at the latest. They should be sent to *Marc Gyssens*.

Subscriptions and ordering of publications

Volume 28 (2000) of *WGN* will contain at least 240 pages and costs 35 DEM or 17.90 EUR, including non-airmail delivery. Ordering other *IMO* publications is done in the same way as paying subscription/membership fees. More information can be found in this issue. Changes of address and complaints about not receiving *WGN* should be addressed to the Treasurer, Ina Rendtel.

All addresses can be found on the inside of the back cover.

From the Editor-in-Chief

Marc Gyssens

The Leonids of last November may now be over a month behind us, and the Geminids have already made their annual appearance meanwhile, but the excitement over the storm that was witnessed has not quite subsided yet, and there is good reason for that!

Except perhaps for a happy few that witnessed the 1966 event, none of the observers of this year's Leonid peak saw meteor activity of this magnitude before in his or her life. Also never before, the meteor observing community felt so much like a family: thanks to modern means of communication, mainly the Internet and mobile phones, observers reported what they saw almost in real time. I wish to thank all the observers who took the effort of phoning or e-mailing in their first raw data; this enabled our Organization to disseminate reliable information based on a good lot of observations within hours after the event. When I was doing some rough analyses on these data to compile the Leonid Meteor Shower Bulletins that I sent around, I really had like never before the warm feeling of belonging to a world-wide network of friends striving toward a common goal.

The peak time predicted by Asher and McNaught was confirmed within minutes, and while the observed activity was a couple of times higher, it was of the right order of magnitude. Observations of likely Leonid meteorite impacts on the Moon complete the picture: indeed, the Moon was much more in the "line of fire" than the Earth, this year!

Meanwhile, information on almost a quarter of a million visually observed Leonids has been processed, and, although the events of last month seem to give us a feeling that, at last, we are starting to understand the dynamics of meteor storms, awareness has grown that a lot of challenges are still facing us. For instance, the Leonids during the storm peak had a very strange magnitude distribution, with a deficiency of both very bright and *very faint meteors! Also, local activity profiles show a lot of significant secondary peaks around the main maximum, but matching these profiles is not straightforward—it seems a three-dimensional approach may be necessary...*

Of course, such endeavor is not feasible in the span of five weeks. Nevertheless, we do present you with first results on visual and video observations of the 1999 Leonids, along with some eye-witness impressions, also of possible lunar Leonid impacts! In addition to a preliminary analysis of 1999 Leonid data, we also offer you a comprehensive analysis of the 1998 Leonids! I wish to express special thanks to our Visual Commission Director, Rainer Arlt, for making it possible to bring you this material still in the December issue.

For once, it is not so much other commitments as our desire to incorporate first results of the Leonids that explains the delay in the production of this issue. Usually, we try to be especially early with the December issue to avoid the annually returning seasonal jam in the mail, so it feels a bit strange for me to write this editorial on Christmas Day. Nevertheless, it feels very appropriate at the same time to reflect on the world-wide family of meteor workers and the cooperation, understanding, and friendships among them on a day on which so many people all over the globe refuse to accept the inevitability of armed conflict and renew their hope for a world-wide peace. A pleasant, but important side-effect of the excitement surrounding the Leonids is that several observers from whom we heard little or nothing during several years apparently re-found the joy of observing and become active again. At the same time, hardly being able to cope with their own observations during the Leonid storm made several observers aware which an enormous burden on the shoulders of the relative few IMO officers the reduction of the data of all observers represents, which raises hope for the future in this respect, too.

It is with this hope that I look forward to the New Year, and with the hope that not only I but the whole International Meteor Organization *can and will serve the meteor community still better, but this goal can only be realized with your help, for the* International Meteor Organization *is an association not only of and for its members, but also* by *them!*

Enjoy reading this issue!

Renew Your IMO Membership/WGN Subscription Now!

Ina Rendtel

General information

Please help us in keeping our records straight by renewing right now. In this way, you insure that your subscription is processed well in time before the February issue has to be sent out and you save the already overloaded *IMO* officers to have to run on and off to the post office to mail back issues. All relevant information is concisely summarized below.

International payments invariantly involve costs. Therefore, if you also wish to buy other *IMO* publications (outside back cover), it is a good idea to combine this with your renewal in one order and one payment. *New* IMO *publications* are Report 11 containing the 1998 visual observations, and the Proceedings of the 1998 and 1999 *IMC*s, the latter of which will appear shortly and can already be ordered. You can also pay your subscription for *two* years, by which you can avoid a possible increase in dues for 2001! Finally, you can **become a supporting member** by adding at least 15 DEM (7.67 EUR) or 10 USD per year to your membership.

Payment instructions

Please, send your payments to the Treasurer or one of her assistants as indicated below:

- **in Europe:** pay in *German Marks* or *Euro* to *Ina Rendtel* by transferring to the account number 547234107 at Postbank 10916 Berlin, bank code 10010010. (Please send **no bank checks**!—If you must pay by check, pay to Robert Lunsford as indicated below.)
- **in the United Kingdom:** proceed as above, or pay to *Alastair McBeath*, 12A Prior's Walk, Morpeth, Northumberland NE61 2RF, England.
- **in Japan:** pay to *Masahiro Koseki*, 4-3-5 Annaka, Annaka-shi, 379-01 Gunma-ken, Japan.
- **All others** pay in *US Dollars* to *Robert Lunsford*, 161 Vance Street, Chula Vista, California 91910, USA.

All people insisting on paying by check should pay to Robert Lunsford in US Dollars, as indicated above. Make checks payable to Robert Lunsford, not to the IMO!

Price list

Type of subscription	2000	2000 + 2001
Regular subscription (*WGN*)	35 DEM (17.90 EUR) or 25 USD	70 DEM (35.79 EUR) or 50 USD
Combined subscription (*WGN*, *FIDAC* News, Report)	70 DEM (35.79 EUR) or 50 USD	140 DEM (71.58 EUR) or 100 USD
Also possible outside Europe:		
Regular subscription with airmail delivery	70 DEM (35.79 EUR) or 50 USD	140 DEM (71.58 EUR) or 100 USD
Combined subscription with airmail delivery for *WGN* only	110 DEM (56.24 EUR) or 80 USD	220 DEM (112.48 EUR) or 160 USD

Letters to WGN

compiled by Marc Gyssens

On possible lunar impacts of Leonid meteorites

At the risk of sounding like a crackpot or perhaps an eight-year old boy who received a new telescope for his birthday, I should like to report my observance of numerous transient lunar phenomena during the Leonid meteor display on the night of November 17-18, 1999. I submitted this same report to David Darling, Coordinator for Lunar Transient Phenomena for *ALPO*, by electronic mail at 12^h26^m UT on November 18, at a time when I was yet unaware of what had been seen of the shower by European observers.

I observed with a 16″ $f/6$ Newtonian, equatorially mounted and driven, made by Parallax Instruments, at a nominal magnification of 240×, using a 20-mm "Ultrascopic" eyepiece (from Orion) with a 2× Barlow lens. The seeing was 3 on the *ALPO* scale, and transparency was excellent (limiting magnitude 6.53 after moonset later in the night). The ambient temperature was about 0° C. My observatory is located near Wrens, Georgia, USA, at $\lambda = 82°31'30''.3$ W, $\varphi = 33°09'36''.3$ N, and $h = 100$ m.

I began observing the dark side of the Moon visually at 2^h00^m UT. The dark lunar limb was barely visible and there was considerable glare in the field, from the sunlit portion of the Moon, which was completely out of the field of view. I saw nothing unusual until about 2^h15^m UT, when I noted a few brief star-like flashes occurring. These were not meteoric streaks, of course, but were brief stationary points of light. Color could not be determined. They increased in frequency steadily until about 2^h30^m UT, when their frequency began to decrease. They decreased to near zero at 2^h45^m UT, but then there was another increase, peaking at 2^h46^m UT, and tapering to zero at 2^h52^m UT. I saw none thereafter, and quit observing at 2^h57^m UT, exhausted by the intense concentration. Maximum frequency was at about 2^h30^m UT, at which time there were about four flashes

per minute, on average. The flashes were mostly about as bright as stars of 12th to 11th magnitude, with just a few—perhaps three during the entire session—as bright as 10th magnitude. The 12th-magnitude ones were near the limit of detectability in the glare. This magnitude estimate is difficult due to the conditions, but is the best that I can do. The duration of the flashes was 0.25 to 0.75 seconds, the brighter ones lasting longer than the fainter ones. They were difficult to see, and I think that I would have missed them were I using a smaller telescope or one less well baffled against stray light.

During the observing period, I was very sensitive to the possibility of cosmic ray hits on my retina or other ectopic phenomena that may cause a flash of light. I did experience these during the session. By continuously moving my gaze around the field of view, I was able to distinguish the flashes from ectopic phenomena, since the flashes remained stationary despite eye motion, while ectopic phenomena move.

I had begun observing with a low-light video camera at 1^h45^m UT, but it became evident that glare from the sunlit portion of the Moon was washing out the view, so I switched to visual at 2^h00^m UT.

The time of peak flash activity that I report—2^h30^m UT—does not correspond with the peak time of 2^h05^m UT reported by European naked-eye observers. Interestingly, the Moon was downstream from the Earth in the path of the Leonids, and it could be expected that it would encounter the stream of meteors somewhat later than the Earth did.

Roger Venable, November 21, 1999

Many other observations of possible lunar impacts of Leonid meteoroids on the Moon have also been reported, and a number of them were confirmed by video observations from different sites. A summary of what is currently known about these suspected Leonid impacts on the Moon can be found in the last paragraph of the preliminary analysis of the 1999 Leonids in this issue.

The 2000 International Meteor Conference

Pucioasa, Romania, September 21–24, 2000

communicated by Marc Gyssens

Wonderful Fireball
(to the *International Meteor Organization*)

"What a magnitude!"—
Said the visual observer.
"What a color!"—
Said the photographic observer.
"What a wave!"—
Said the radio observer
"What an aspect!"—
Said the telescopic observer.
"What a celestial document!"—
Said the video observer.

But I kept silent
Because I knew
That its real brightness
Will be recorded
By our souls.

Andrei Dorian Gheorghe

It was decided at the 1999 *IMC* to have the 2000 *International Meteor Conference* in Pucioasa, Romania, from September 21 (Thursday evening) to September 24 (Sunday noon). It will be organized by the *Romanian Society for Meteors and Astronomy* (*SARM*). Pucioasa is a spa town, located at an altitude of 400 m, about 100 km to the northwest of Bucharest, and only 23 km to the northwest of Târgovişte. There are direct trains and buses from the Bucharest airport/train station to Pucioasa, but the organizers plan to offer an additional shuttle service.

Accommodation will be provided in double rooms, and all meals will be served at the hotel restaurant, at 150 m from the conference site. The conference is organized in cooperation with the Town Authorities. The full conference fee will be 170 DEM (86.92 EUR). (Reductions for Eastern European participants are possible.)

A registration is provided on the next page. You may also consult the *IMO* Web pages at `http://www.imo.net` or contact Andrei Dorian Gheorghe of the *Romanian Society for Meteors and Astronomy*. We expect a more elaborate article on the 2000 *IMC* in the February 2000 issue.

International Meteor Conference

Pucioasa, Romania, September 21–24, 2000

Registration Form

Each individual participant should fill out a form and return it to *Ina Rendtel, Mehlbeerenweg 5, 14469 Potsdam, Germany*, as soon as possible. Your registration will be guaranteed only after Ina Rendtel has received the minimum pre-payment of 100 DEM (51.13 EUR). If you wish to participate, but cannot yet decide, simply return this form with the proper option checked to stay on the mailing list for further circulars.

Name: _____ Birth date: _____

Address: _____

_____

_____

Phone: _____ Fax: _____ E-Mail: _____

- ○ wishes to register for the 2000 *IMC* from September 21 to 24;
- ○ intends to participate, cannot yet register, but wishes to stay on the mailing list.

I intend to travel by _____, together with _____

Additional requests:

- ○ I need travel information from _____ to Pucioasa;
- ○ I wish to stay in Romania before or after the *IMC* and require additional information re. this matter.

For participants wishing to contribute to the program:

Lecture: _____

Duration: _____min. Required equipment: _____

Workshop or discussion: _____

Poster presentation: _____ Space: _____ m^2

Either the entire fee of 170 DEM (86.92 EUR) or a pre-payment of at least 100 DEM (51.13 EUR) should be sent to the Treasurer, *Ina Rendtel*. Follow the payment instructions below. Participants paying only 100 DEM (51.13 EUR) have to pay the remaining 70 DEM (35.79 EUR) upon arrival in Pucioasa.

Date and signature: _____

Please send your payment to the Treasurer or one of her assistants as indicated below:

- in Europe: pay in DEM or EUR to Ina Rendtel, account number 547234107 at Postbank 10916 Berlin, bank code 10010010. No bank checks, please! (Bank checks can only be sent to Robert Lunsford, see below).
- in the UK: proceed as above or pay to Alastair McBeath, 12A Prior's Walk, Morpeth, Northumberland NE61 2RF, England.
- in Japan: pay to Masahiro Koseki, 4-3-5 Annaka, Annaka-shi, 379-01 Gunma-ken, Japan.
- all others pay in USD to Robert Lunsford, 161 Vance Street, Chula Vista, California 91910, USA. In case you pay by bank check, make it payable to Robert Lunsford, *not* the *IMO*!

People wishing to pay in other currencies should contact the appropriate IMO *contact person for exchange rates.*

1998 and 1999 Leonids

Bulletin 14 of the International Leonid Watch: Visual Results and Modeling of the 1998 Leonids

Rainer Arlt and Peter Brown

A comprehensive analysis of the 1998 Leonid meteor shower is given, based on 70 800 Leonids recorded by 473 observers. The activity profile is characterized by two distinct maxima of different origin: a strong, broad component of particles ejected a few tens of revolutions ago, centered at $\lambda_\odot = 234.^\circ528 \pm 0.^\circ006$ (November 17, 1998, $1^h55^m \pm 9^m$ UT) with a maximum equivalent ZHR of 357 ± 11, and a short-lived component rich in smaller particles at $\lambda_\odot = 235.^\circ311 \pm 0.^\circ007$ (November 17, 1998, $20^h33^m \pm 10^m$ UT), which is near the Earth's passage of the orbital node of the parent comet, 55P/Tempel-Tuttle. All solar longitudes refer to equinox J2000. The maximum equivalent ZHR at this nodal peak was 136 ± 5. The early peak has a maximum flux of 0.015 ± 0.001 meteoroids brighter than magnitude +6.5 per square kilometer and per hour. The second maximum has a peak of 0.028 ± 0.03 meteoroids brighter than magnitude +6.5 per square kilometer and per hour. Model calculations integrating the motion of more than a million particles ejected up to 2000 years ago show very good agreement with the time of the observed component of bright meteors. Due to a preference for larger particles in the simulations, the nodal peak is not visible in the model. We suggest the most probable source for the nodal peak particles are the ejections from 1965, 1932, and/or 1899 with Leonids having higher ejection velocities and smaller meteoroids being dynamically preferred for delivery to Earth.

1. Observational records

After the first global analysis of the 1998 Leonids had been published in [1], the number of Leonids seen during observations archived in the *Visual Meteor Database* (*VMDB*) increased from about 47 000 to 70 800. This significant enlargement of the dataset allows for another analysis showing more detail than the previous one.

The enormous number of 473 observers reported their Leonid observations to the *VMDB* enabling us to perform the most detailed activity analysis of a meteor shower ever. We are most indebted to the following observers for their contributions:

Ghazalaha Al-Abed (ABEGH, $5^h.95$), Jasmel Acosta (ACOJA, $0^h.97$), Ilidio Afonso (AFOIL, $3^h.00$), Iyad Ahmad (AHMIY, $1^h.83$), Seishi Akagi (AKASE, $17^h.50$), Stephen Alden (ALDST, $4^h.00$), Ahmad Al-Niamat (ALNAH, $5^h.00$), Kohta Aoyama (AOYKO, $0^h.83$), Rainer Arlt (ARLRA, $0^h.78$), Kaori Asahara (ASHKA, $0^h.83$), Joseph D. Assmus (ASSJO, $3^h.11$), Zaid Ata (ATAZA, $5^h.00$), Juan Alberto Aveledo (AVEJU, $1^h.20$), Julia Babina (BABJL, $3^h.28$), Pierre Bader (BADPI, $22^h.85$), Halim Baituk (BAIHA, $2^h.30$), Moshe Bain (BAIMO, $2^h.00$), Lars Bakmann (BAKLA, $1^h.00$), Igor Baluk (BALIG, $6^h.00$), Petra Rendtel (BALPE, $10^h.71$), Ana Bankovic (BANAN, $4^h.12$), Rony Barry (BARRO, $0^h.53$), Luc Bastiaens (BASLU, $5^h.96$), Rizlane Bechar (BECRI, $1^h.67$), Sanae Bechar (BECSA, $1^h.67$), Luis R. Bellot Rubio (BELLU, $4^h.97$), Pavel Belov (BELPA, $2^h.15$), Vladimir Belchenko (BELVL, $2^h.55$), Abdelaziz Bennouna (BENAB, $1^h.08$), Orlando Benítez Sanchez (BENOR, $2^h.72$), Felix Bettonvil (BETFE, $7^h.22$), Stephen Binks (BINST, $2^h.98$), Nicolas Biver (BIVNI, $2^h.22$), Jim Blanksby (BLAJI, $9^h.33$), Miroslav Blaho (BLAMI, $6^h.81$), Boncho Bonev (BONBO, $1^h.00$), Neil Bone (BONNE, $1^h.97$), Michael Boschat (BOSMI, $4^h.00$), Louisa Bowman (BOWLO, $10^h.11$), Chris Briggs (BRICH, $10^h.13$), Iwan Brukhanov (BRUIW, $1^h.98$), Joana M. Brunet (BRUJO, $4^h.99$), William Burton (BURWL, $0^h.97$), Marija Cajetinac (CAJMA, $5^h.75$), Arturo Carvajal R. (CARAR, $0^h.50$), Jens J. Carlsen (CARJE, $7^h.15$), Tal Carmon (CARTA, $0^h.04$), Andrew Casely (CASAN, $1^h.00$), Neophite Chanev (CHANE, $4^h.34$), Yuk-lun Chan (CHAYU, $5^h.22$), Qu Chengxu (CHEQU, $1^h.63$), Koen Clement (CLEKO, $1^h.25$), Antonio Coelho (COEAN, $3^h.50$), Claudia Colonnelo (COLCL, $2^h.00$), Matthew Collier (COLMA, $0^h.24$), Tim Cooper (COOTI, $1^h.00$), Pedro Correa (CORPD, $1^h.00$), Uroš Čotar (COTUR, $1^h.03$), Camilla Coverty (COVCA, $9^h.14$), Stefano Crivello (CRIST, $5^h.78$), Hani Dalee (DALHA, $4^h.00$), Luigi d'Argliano (DARLU, $2^h.64$), Mark Davis (DAVMA, $7^h.50$), Johan de Hert (DE JO, $1^h.50$), Marc de Lignie (DE MA, $15^h.13$), Goedele Deconinck (DECGO, $4^h.58$), Sergey Dedik (DEDSE, $3^h.75$), Benoit Dejust (DEJBE, $2^h.00$), Kurt Dequick (DEQKU, $3^h.00$), Vincent Desmarais (DESVI, $2^h.20$), Peter Detterline (DETPE, $5^h.06$), Asdai Díaz Rodriguez (DIAAS, $2^h.00$), Anton Dimitrov (DIMAN, $2^h.14$), Elena Dimovski (DIMEL, $4^h.35$), Zhao Dongjuan (DONZH, $2^h.51$), Dariusz Dorosz (DORDA, $2^h.08$), Juan Jose Downes (DOWJU, $0^h.87$), John Drummond (DRUJO, $2^h.50$), Sergey Dubrowsky (DUBSE, $1^h.02$), Jarosław Dygos (DYGJA, $20^h.00$),

Tonis Eenmae (EENTO, 3h07), Maurizio Eltri (ELTMA, 4h82), Frank Enzlein (ENZFR, 2h69), Frantisek Erben (ERBFR, 2h59), Bert Everaert (EVEBE, 5h16), Tomasz Fajfer (FAJTO, 1h00), Juan Gabriel Fernandez (FERJU, 2h00), Sharon Fletcher (FLESH, 3h00), Tamás Fodor (FODTA, 1h93), Anneleen Fransen (FRAAN, 4h95), Keiiti Fukui (FUKKE, 17h51), Nobuyuki Fukuda (FUKNO, 6h64), Siniti Fukuhara (FUKSI, 4h16), Ofer Gabzo (GABOF, 0h24), Atanas Gavrailov (GAVAT, 3h02), Christoph Gerber (GERCH, 17h17), Jaroslav Gerboš (GERJA, 8h50), Ivanka Getsova (GETIV, 3h52), Suchitra Ghosh (GHOSU, 5h00), Tom Giguere (GIGTO, 3h28), George Gilbart-Smith (GILGE, 9h08), Maarten Gillis (GILMA, 2h92), David Girling (GIRDA, 13h25), George W. Gliba (GLIGE, 3h25), Orly Gnat (GNAOR, 0h17), Shelagh Godwin (GODSH, 5h74), Amit Gokhale (GOKAM, 2h05), Sagar Gokhale (GOKSA, 1h03), Yeshodhan Gokhle (GOKYE, 3h68), Alexandra Golova (GOLAL, 3h28), Dennis Goodman (GOODE, 3h00), Prerana Gore (GORPA, 2h67), Roberto Gorelli (GORRO, 8h20), Lew Gramer (GRALE, 11h22), Valentin Grigore (GRIVA, 6h00), Matthias Growe (GROMA, 3h16), Gong Guanghui (GUAGO, 2h50), Monica de la Guardia (GUAMO, 4h36), Qin Guoming (GUOQI, 1h51), Cathy Hall (HALCA, 3h87), Michal Haltuf (HALMI, 0h17), Torsten Hansen (HANTO, 1h98), Hiromi Harada (HARHI, 7h83), Takema Hashimoto (HASTA, 23h32), Roberto Haver (HAVRO, 5h12), Alana Hawkens (HAWAL, 8h50), Kim Hay (HAYKI, 2h73), Steven M. Hayward (HAYST, 0h83), Amera Hemsy (HEMAM, 5h33), Santiago Hernández (HERSA, 0h56), Veerle Herrygers (HERVE, 1h18), Motoyasu Higuchi (HGCMT, 2h00), Nathalie Hontelé (HONNA, 2h81), Kamil Hornoch (HORKM, 3h39), Mitsuhiro Igarashi (IGRMT, 2h50), Isamu Iidsuka (IIDIS, 0h83), Oomi Iiyama (IIYOO, 3h50), Hiromi Imai (IMAHR, 0h83), Osamu Imamura (IMAOS, 2h17), Hikaru Ishida (ISDHI, 4h30), Iori Ishiyama (ISHIO, 1h66), Kaoru Ishii (ISHKA, 2h34), Megumi Isii (ISIMG, 3h00), Masaharu Ishizaki (ISZMS, 2h96), Akira Ito (ITOAK, 4h16), Daiyu Ito (ITODA, 9h58), Nobuhisa Itou (ITONB, 0h83), Shigeharu Ito (ITOSG, 1h67), Rositsa Ivanova (IVARO, 2h02), Shun-ichi Iwamoto (IWAS , 7h50), Yumi Iwasaki (IWSYU, 4h17), Hiroki Izumoto (IZMHI, 1h00), Kiyoshi Izumi (IZUKI, 14h96), Yumi Izuhara (IZUYU, 1h58), Helle Jaaniste (JAAHE, 3h35), Jan Janssens (JANJA, 5h50), Steve Jaworiwsky (JAWST, 1h50), Vibor Jelic (JELVI, 4h52), Ilhame Jemmah (JEMIL, 0h50), Simon Jenner (JENSI, 2h00), Carl Johannink (JOHCA, 16h35), Ivan Jokic (JOKIV, 2h20), Kevin Jones (JONKE, 6h35), Kurt Jonckheere (JONKU, 2h34), Wojciech Jonderko (JONWO, 1h09), Javor Kac (KACJA, 9h09), Primož Kajdič (KAJPR, 2h09), D. Kalayda (KALDU, 3h33), Toshio Kamimura (KAMTO, 6h50), Dmitrij Karkach (KARDM, 3h28), Niladri Kar (KARNI, 3h72), Junichi Kasai (KASJU, 1h50), Jun Kataoka (KATJU, 1h00), Kenya Kawabata (KAWKE, 3h04), Satosi Kaya (KAYSA, 2h33), Katsuyuki Kobayashi (KBYKT, 0h50), Srdjan Keca (KECSR, 3h70), Ákos Kereszturi (KERAK, 3h57), Katarina Kerekesova (KERKT, 8h78), Stephen Kerr (KERST, 1h85), Noor Al-Khateeb (KHANO, 4h44), Mark Kidger (KIDMA, 1h50), Nobuya Kikuchi (KIKNO, 0h50), Kevin Kilkenny (KILKE, 3h21), Timo Kinnunen (KINTI, 1h00), Warwick Kissling (KISWA, 5h00), Shigemi Kanbara (KNBSG, 4h50), Toshiaki Kon-no (KNNTO, 1h65), André Knöfel (KNOAN, 17h53), Masata Kobayashi (KOBMA, 2h06), Wakaba Kobayashi (KOBWA, 13h00), Antoon Koegels (KOEAN, 0h83), Daniel Köhn (KOHDA, 1h46), Hideki Koide (KOIHI, 2h58), Khalil Konsul (KONKH, 5h50), Marcin Konopka (KONMA, 2h00), Detlef Koschny (KOSDE, 1h88), Nobuyuki Kosiyama (KOSNO, 3h00), Marija Kotur (KOTMA, 0h91), Jakub Koukal (KOUJA, 22h35), Zoran Kraljevic (KRAZO, 2h23), Nikola Kresojevic (KRENI, 5h55), W. Gary Kronk (KROGA, 6h50), Hideo Kusakai (KSKHI, 5h50), Tom Kucharski (KUCTO, 2h42), Brigitte Kuneth (KUNBR, 1h00), Werfried Kuneth (KUNWE, 1h00), Karimu Kuragaki (KURKA, 9h75), Takehisa Kuwabara (KWBTA, 0h83), Maciej Kwinta (KWIMA, 10h00), Sylvio Lachmann (LACSY, 1h15), Marco Langbroek (LANMA, 18h71), Zsolt Lantos (LANZS, 2h98), Alberto Latini (LATAL, 4h49), Trevor Law (LAWTR, 3h00), Anne-Laure Lebacq (LEBAN, 1h71), Adrian Lelyen (LELAD, 1h00), Anna S. Levina (LEVAN, 6h57), Semion Levin (LEVSE, 3h66), Mihir Limaye (LIMMH, 1h18), Alister Ling (LINAL, 1h38), Romulo Liporacci (LIPRO, 0h83), Vladimir Lukić (LUKVL, 9h20), Robert Lunsford (LUNRO, 16h40), Hartwig Lüthen (LUTHA, 10h08), Kathy Machin (MACKA, 7h84), Kimio Maegawa (MAEKI, 2h17), Kouji Maeda (MAEKO, 0h77), Shane Majoros (MAJSH, 5h96), Mirjana Malarić (MALMR, 5h00), Katuhiko Mameta (MAMKA, 54h67), Roman Manak (MANRO, 4h47), Adam Marsh (MARAD, 18h85), David Martinez Delgado (MARDA, 2h01), José Alfonso dos Reis Martins (MARJO, 2h88), Khalid Marwat (MARKH, 2h48), Pierre Martin (MARPI, 4h65), Takuya Maruyama (MARTA, 0h67), Antonio Martinez (MARTI, 4h42), Tony Markham (MARTO, 6h49), Edgardo Ruben Masa Martín (MASED, 3h96), Yukihisa Matumoto (MATYU, 2h50), Alastair McBeath (MCBAL, 7h05), Bruce McCurdy (MCCBR, 1h38), Stephen McCann (MCCST, 0h23), Tom McEwan (MCETO, 0h69), Kieron McGrath (MCGKI, 3h00), Kevin McKeown (MCKKE, 1h00), Norman McLeod (MCLNO, 4h85), Lukas Mecir (MECLU, 0h13), Mark Mikutis (MIKMR, 15h20), Ana Milovanovic (MILAA, 0h91), Iris Miljački (MILIR, 2h65), Vjera Miovic (MIOVJ, 1h17), Koen Miskotte (MISKO, 23h01), Shigeo Mitsuma (MITSH, 4h22), Hidekatu Mizoguchi (MIZHI, 4h29), Naoko Minigawa (MNGNA, 2h00), Amruta Modani (MODAM, 2h66), Marilena Molaco (MOLMA, 3h36), Sirko Molau (MOLSI, 14h17), Michael Morrow (MORMI, 4h00), Sigehiro Mori (MORSI, 1h58), Takako Mori (MORTK, 0h83), William Morgan (MORWI, 1h16), Erick Mota Perez (MOTER, 2h90), Ken-ichi Mohri (MOUKE, 1h55), Krzysztof Mularczyk (MULKR, 3h00), Darshan Mundada (MUNDA, 1h28), Minoru Muraki (MURMI, 21h39), Yoshikane Murakami (MURYO, 4h00), Joanne Muskarovsky (MUSJO, 13h38), Sin Nakayama (NAKSI, 7h76), Koji Naniwada (NANKO, 3h33), Tasso Napoleao (NAPTA, 3h00), Tatsunori Naruke (NARTA, 0h92), Toru Naruse

(NARTO, 4h49), Sven Näther (NATSV, 12h35), Jonathon Newton (NEWJH, 6h00), John Newton (NEWJO, 9h00), Kevin Nicasi (NICKE, 3h67), Dalibor Nikolic (NIKDA, 2h46), Markku Nissinen (NISMA, 7h01), Prakash Nitsure (NITPR, 4h05), Yumiko Nobukiyo (NOBYU, 6h17), Jarosław M. Nocoń (NOCJA, 1h00), Tooru Nishino (NSNTO, 0h50), Mohammad Odeh (ODEMO, 4h15), Ibrahim Odwan (ODWIB, 4h75), Eran Ofek (OFEER, 3h45), Hiroshi Ogawa (OGAHI, 1h50), Masamichi Ohno (OHNMA, 1h66), Hiroyuki Okayasu (OKAHI, 4h98), Masayuki Oka (OKAMA, 5h34), Dragana Okolić (OKODR, 5h38), Marcelo Oliveira (OLIMA, 2h50), Matt Orsie (ORSMA, 6h00), Elke Ortmanns (ORTEL, 2h82), Kazuhiro Osada (OSAKA, 66h99), Kazuhiko Osaki (OSKKA, 6h67), Jesus Otero (OTEJE, 1h00), Fumio Oyama (OYMFM, 4h77), Ketan Pendse (PENKE, 1h33), Miroslav Penev (PENMI, 2h15), Alfredo Pereira (PERAF, 5h71), Dusan Perovic (PERDU, 3h59), Radame Perez (PERRA, 1h00), Suyin Perret-Gentil (PERSU, 1h52), Natasa Petelin (PETNA, 3h22), Furio Pieri (PIEFU, 4h73), Mila Popović (POPMI, 1h20), Dubravko Potkrajac (POTDU, 1h08), Tushar Purohit (PURTU, 2h85), William Pyke (PYKWI, 4h75), Zhao Qingshan (QINZH, 1h92), Daniela Rapava (RAPDA, 7h09), Pavol Rapavy (RAPPA, 8h34), Simona Rapava (RAPSI, 5h85), Ina Rendtel (RENIN, 1h08), Jürgen Rendtel (RENJU, 21h68), Francisco Reyes Andrés (REYFR, 1h03), Janko Richter (RICJA, 0h88), Ian Rigney (RIGIA, 2h88), José Ripero (RIPJO, 2h68), Mileny Roche Lamas (ROCMI, 1h00), Beriozka Rodriguez (RODBE, 0h68), Francisco Rodriguez Ramirez (RODFR, 5h05), Juan Rodríguez (RODJU, 4h86), Dirk Rombouts (ROMDI, 0h83), Martin Rudd (RUDMR, 12h29), Jelyl Rufat (RUFJE, 1h00), Victor Ruiz Ruiz (RUIVI, 3h91), Etsuko Saito (SAIET, 4h00), Mitsue Sakaguchi (SAKMI, 14h53), Andy Salmon (SALAN, 1h00), Jeffery Sandel (SANJE, 9h53), K.V. Sankaranarayanan (SANKV, 2h50), Masanori Sano (SANMK, 0h83), Koetu Sato (SATKO, 6h45), Mikiya Sato (SATMK, 1h00), Tatuo Sato (SATTA, 6h75), Richard Schmude (SCHRI, 2h75), René Scurbecq (SCURE, 4h22), Harald Seifert (SEIHA, 1h07), Abderazak Sersouri (SERAB, 1h67), Miguel Serra Martin (SERMI, 2h66), Shashank Shalgar (SHASH, 4h03), Masumi Shimizu (SHIMA, 2h33), Brian Shulist (SHUBR, 3h10), Yasuo Shiba (SIBYA, 2h33), Hendrik Sielaff (SIEHE, 5h65), Hiroyuki Sioi (SIOHI, 6h16), Kazuaki Siotani (SIOKA, 2h42), Andrzej Skoczewski (SKOAN, 1h17), Vesna Slavković (SLAVE, 2h65), Keiko Shimada (SMDKE, 0h83), Alton Smith (SMIAL, 2h00), Amanda Smith (SMIAM, 9h76), James N. Smith (SMIJN, 15h26), Steven Smith (SMIST, 4h58), Makoto Shimamune (SMMMA, 0h83), Kiko Soares (SOAKI, 3h50), Andrey Solodovnik (SOLAD, 3h05), Manuel Solano Ruiz (SOLMA, 1h25), Je Soub-park (SOUJE, 2h59), Willian Souza (SOUWI, 0h50), George Spalding (SPAGE, 4h92), Ulrich Sperberg (SPEUL, 5h76), Yoshihisa Seshimo (SSMYS, 5h50), Mark Stafford (STAMA, 1h82), Octaaf Steen (STEOC, 4h39), Enrico Stomeo (STOEN, 2h12), Niko Štritof (STRNI, 3h04), Moomi Suen (SUEMO, 3h54), Kazuhiro Sumie (SUMKA, 11h33), Paul Sutherland (SUTPA, 1h67), Masafumi Suzuki (SUZMA, 1h00), Máximo Svárez Tejera (SVAMX, 4h21), David Swann (SWADA, 1h92), Eva Szabados (SZAEV, 0h90), Konrad Szaruga (SZAKO, 2h30), Richard Taibi (TAIRI, 4h42), Akihiro Takeda (TAKAK, 2h64), Hiromi Takai (TAKHR, 0h83), Masaaki Takanasi (TAKMA, 0h67), Mika Takanasi (TAKMI, 4h49), Keiko Tanaka (TANKE, 1h77), Sizuka Tanaka (TANSI, 0h50), Syoiti Tanaka (TANSY, 5h38), Lance Taylor (TAYLA, 1h40), Khaled Tell (TELKH, 10h47), István Tepliczky (TEPIS, 1h53), Kazumi Terakubo (TERKA, 1h00), Michiaki Taguchi (TGCMI, 0h67), Neelima Thatte (THANE, 5h90), Axel Thomas (THOAX, 5h66), Chiro Takahashi (TKHCH, 0h83), Ysohinori Takahashi (TKHYS, 1h66), David Todd (TODDA, 1h92), Masayuki Toda (TODMA, 5h58), Robert Togni (TOGRO, 4h95), Marko Toivonen (TOIMA, 3h50), Danilo Tomic (TOMDA, 2h40), Yasuhiro Tonomura (TONYA, 8h08), Michael Toomey (TOOMI, 2h49), Tamas Tordai (TORTA, 4h10), Hamid Touma (TOUHA, 1h17), Daniel Trainor (TRADA, 15h79), Gabrijela Triglav (TRIGA, 0h93), Josep M. Trigo Rodriguez (TRIJO, 1h07), Mihaela Triglav (TRIMI, 5h33), Aleksander Trofimowicz (TROAL, 3h00), Paweł Trybus (TRYPA, 1h00), Arnold Tukkers (TUKAR, 15h41), Megan Turner (TURME, 11h14), Shigeo Uchiyama (UCHSH, 4h58), Toshihiko Ueno (UENTO, 3h83), Akira Umetsu (UMEAK, 1h66), Tadasi Usui (USUTA, 1h25), Birgit Van Opstal (VANBI, 3h64), Caroline van Dissel (VANCA, 8h00), Erwin van Ballegoy (VANER, 4h92), Glenn Van Olmen (VANGL, 2h97), Hendrik Vandenbruaene (VANHE, 1h93), Jan Vansteelandt (VANJJ, 1h97), Michel Vandeputte (VANMC, 5h51), Steven Van Impe (VANST, 4h11), Vishnu Vardhan (VARVI, 10h50), Trent Veitch (VEITR, 2h71), Cis Verbeeck (VERCI, 2h08), Daniel Verde (VERDA, 9h81), Jan Verbert (VERJN, 6h43), Ivaylo Videv (VIDIV, 2h30), Miquel A. Villalonga Vidal (VILMQ, 1h36), Myriam Vingerhoets (VINMY, 4h30), Catarina Vitorino (VITCA, 3h35), Helio Vital (VITHE, 3h00), Marija Vlajic (VLAMA, 2h40), Roger Vodicka (VODRO, 2h25), Björn Voß (VOSBJ, 8h60), Maja Vuckovic (VUCMJ, 1h17), Song Wanfang (WANSO, 7h80), Richard Ward (WARRI, 3h53), Anne van Weerden (WEEAN, 9h03), Thomas Weiland (WEITH, 4h41), Barbara Wilson (WILBA, 5h24), Vaya Willemen (WILVA, 1h50), Jean-Marc Wislez (WISJE, 3h46), Jeff Wood (WOOJE, 12h18), Noriko Watanabe (WTNNR, 2h66), Liu Xiaoyan (XIALI, 9h43), Zhou Xingming (XINZH, 0h90), Yasuo Yabu (YABYA, 0h99), Masayuki Yamamoto (YAMMA, 2h67), Yoko Yamashita (YAMYK, 0h83), Yoshio Yamada (YMDYS, 2h33), Hisamoto Yamaguchi (YMGHI, 5h50), Miyoko Yamamoto (YMMMI, 0h83), Motohiro Yamanaka (YMNMO, 10h00), Ruka Yamashita (YMSRK, 4h58), Yasuyuki Yonekura (YONYA, 1h67), Kazuko Yosino (YOSKA, 22h98), Noriko Yosimura (YOSNO, 0h50), Yosihito Yosida (YOSYO, 5h00), Kim S. Youmans (YOUKI, 4h00), Muneo Yoshizawa (YSZMU, 5h50), Chen Yu (YU CH, 2h37), George Zay (ZAYGE, 20h64), Su Zhiping (ZHISU, 2h00), Zhao Zhiheng (ZHIZH, 3h38), Jin Zhu (ZHUJI, 1h75), Florian Zschage (ZSCFL, 2h98), and Tomasz Żywczak (ZYWTO, 15h00).

The observers come from the following 43 countries and regions:

Australia, Austria, Belarus, Belgium, Brazil, Bulgaria, Canada, China, Croatia, Cuba, Czech Republic, Denmark, Ecuador, Estonia, Finland, France, Germany, Hong Kong, Hungary, India, Israel, Italy, Japan, Jordan, Kazakhstan, Morocco, the Netherlands, New Zealand, Pakistan, Papua New Guinea, Poland, Portugal, Romania, Slovakia, Slovenia, South Africa, South Korea, Spain, United States, United Kingdom, Ukraine, Venezuela, and Yugoslavia.

2. Overview and terminology

Many observers all around the world were taken by surprise when the Leonids started to increase their activity in the mid-UT hours of November 15-16 showing an extraordinarily large number of bright meteors and fireballs. The climax of this fireball activity was observed from western Asian and European geographical longitudes in the night of November 16-17. We will refer to this maximum as the *bright-meteor maximum*.

The meteoroid stream of the Leonids is connected with Comet 55P/Tempel-Tuttle, which returned to perihelion in February 1998. The close encounter with particles directly behind the comet led to the prediction of a short-lived activity peak near the time of Earth's passage at the descending node of the comet's orbit. Forecasts were thus based on very young material ejected only two or three cometary revolutions ago. Indeed, such an activity peak occurred, almost unnoticed by the observers, who expected a much stronger outburst, and thus "overlooked" the enhancement revealed by more detailed analysis. We will call this activity peak near the passage of the descending node of the parent comet, 55P/Tempel-Tuttle, the *nodal peak*.

These two features were superimposed over a very broad *background component* which is observable for at least 10 years near the Comet's perihelion passage. In the following, we will use the following terms to refer to the three components in the Leonid meteoroid stream discussed above:

- bright-meteor component;
- nodal component; and
- background component.

Newspapers reported that astronomers had miscalculated the peak time. In fact, it was "bad luck" in some sense that the fireball peak was caused by particles ejected many orbital revolutions ago, which were not considered in predictions before the occurrence of the 1998 Leonids. Only young stream components were taken into account, which are supposed to have a large mass index (as well as a large population index), that is, a large proportion of smaller particles, and hence produce generally faint meteors.

3. The population index profile

Generally, only those magnitude distributions are selected for the determination of population indices which fulfill the following criteria:

- At least five consecutive magnitude classes should be used to compute the r-value.
- The faintest of these magnitude classes should be more than two full magnitudes from the limiting magnitude of the sample. The reason from imposing this criterion is the increasing uncertainty in corrections towards the limiting magnitude. The probability of detecting a meteor (perception probability—not to be confused with perception coefficient) is extremely low near the limiting magnitude, and small meteor numbers seen by the observer will be corrected to very large true meteor numbers introducing large errors.
- The total number of meteors in the magnitude distribution should be at least 20.
- The true number of meteors in each magnitude class (i.e., meteor number calculated after correction for the perception probability) is larger than 3.0.

In order to derive some population indices at the far ends of the activity graph, we reduced the last criteria to a total meteor number of 5 and a minimum true meteor number of 1.0 per magnitude class for the periods before November 16 and after November 18.

Figure 1 shows the overall profile of r in the period between November 14, 7^h UT, and November 20, 1^h UT. Too few Leonids were reported outside these limits to yield meaningful population indices; in fact, these dates are beyond the activity period suggested by the *IMO* for visual observations. Throughout, solar longitudes refer to equinox J2000. The two main features of this graph are the abrupt dip in r near $\lambda_\odot = 234\overset{\circ}{.}5$ and the characteristic peak of r near $\lambda_\odot = 235\overset{\circ}{.}3$, close to the nodal passage.

The small error bars near these features suggest that even smaller bins could give information about the small-scale structure in the population index. Figure 2 shows the profile between November 16, 18^h00^m UT and November 18, 0^h50^m UT, with finer bins.

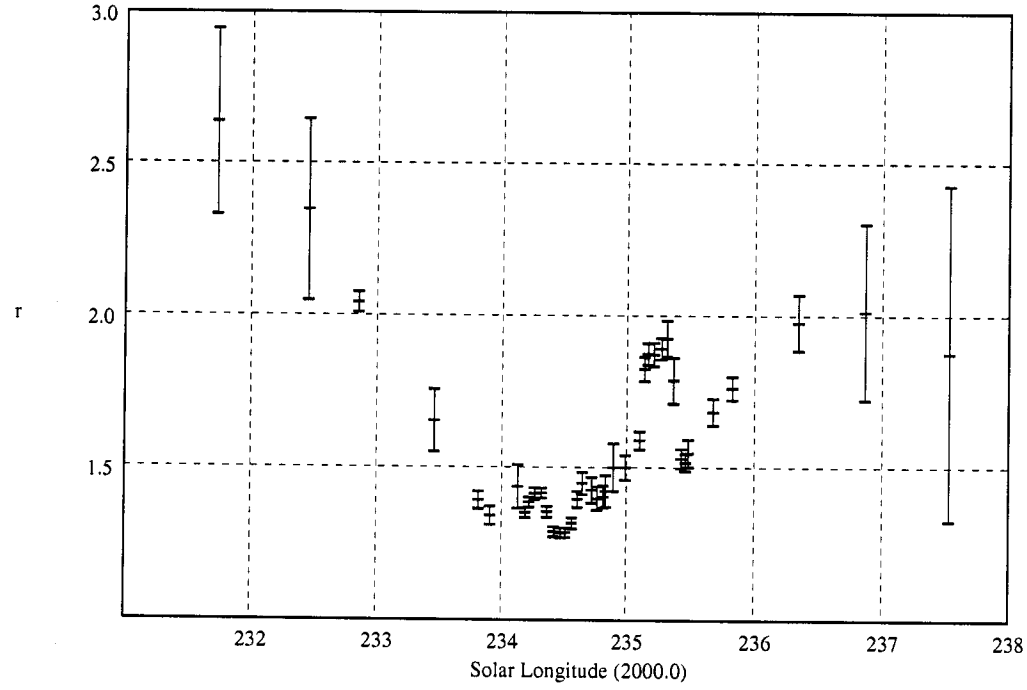

Figure 1 – Entire profile of the population index r of the 1998 Leonids.

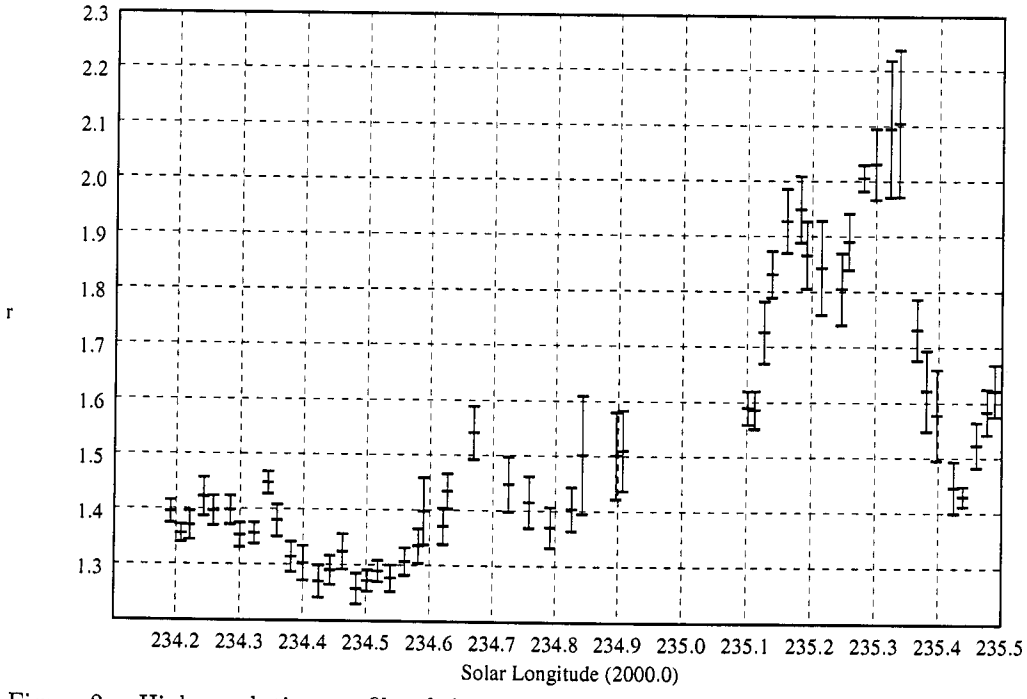

Figure 2 – High-resolution profile of the population index r of the 1998 Leonids covering the period of highest activity.

The bin sizes used for the population index profile in Figure 2 are shown in Table 1.

Table 1 – Bin sizes for the population index profile in Figure 2.

Range in $\lambda_\odot$	Width	Shift
234°.18–234°.60	0°.04	0°.02
234°.60–234°.86	0°.08	0°.04
234°.86–235°.12	0°.20	0°.10
235°.12–235°.50	0°.04	0°.02

All population indices above have been calculated with the regression-line method which fits a linear function through the logarithmic, extrapolated true meteor numbers as a function of magnitude. Another method provides an even finer resolution of the profile and has been introduced in [2]. The average magnitude difference between the meteors and the stellar limiting magnitude is a unique function of the population index and can be converted into r, thereby enabling a lookup table to be constructed which involves the numerical integration of sample magnitude distributions. We present the population index profile near the nodal peak with a fine binning in Figure 3. Both methods provide comparable results, the method of mean-magnitude distances delivering slightly higher population indices. The method runs into problems during the bright-meteor maximum, since a substantial number of meteors brighter than magnitude -6 are all archived in the -6 class of the *VMDB*, since -6 is the brightest class stored. The average magnitude difference will be affected, whereas the regression line will not, unless class -6 is used. Therefore, we only give a highest-resolution graph for the nodal peak, when $r > 1.5$.

A significant triple maximum in the population index is evident: one of the maxima—the highest—coincides with the maximum in ZHR activity at $\lambda_\odot = 235°.338 \pm 0°.010$. The times, however, do not match exactly: the population index maximum time is 0°.027 in solar longitude or 38 minutes after the ZHR maximum.

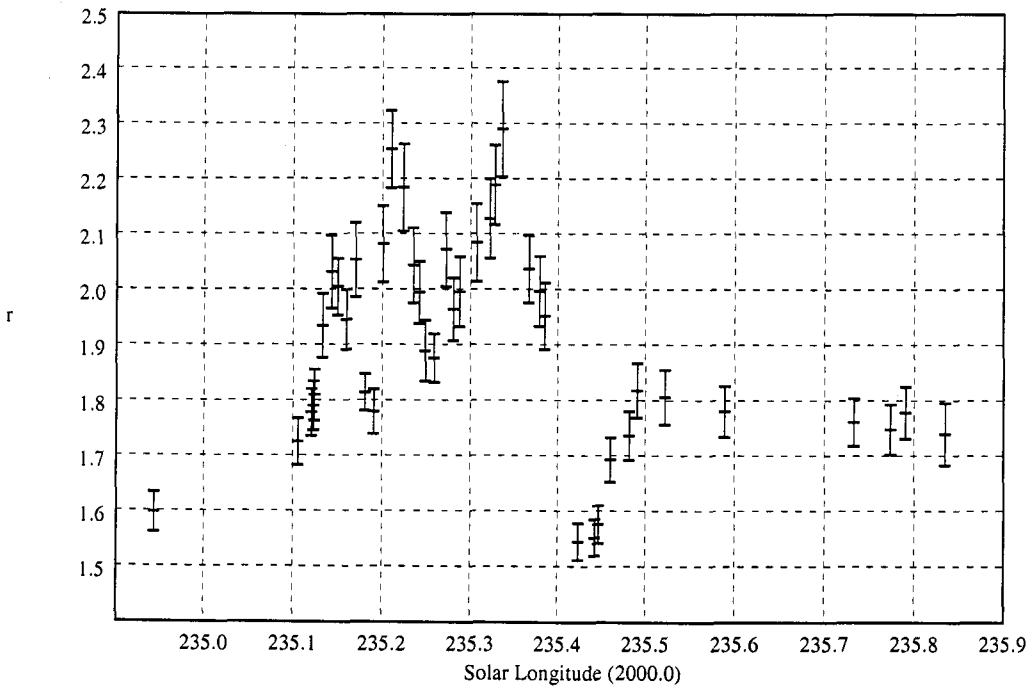

Figure 3 – Profile of the population index with even higher resolution than in Figure 2 as obtained from the average distance of meteor magnitudes from the limiting magnitude.

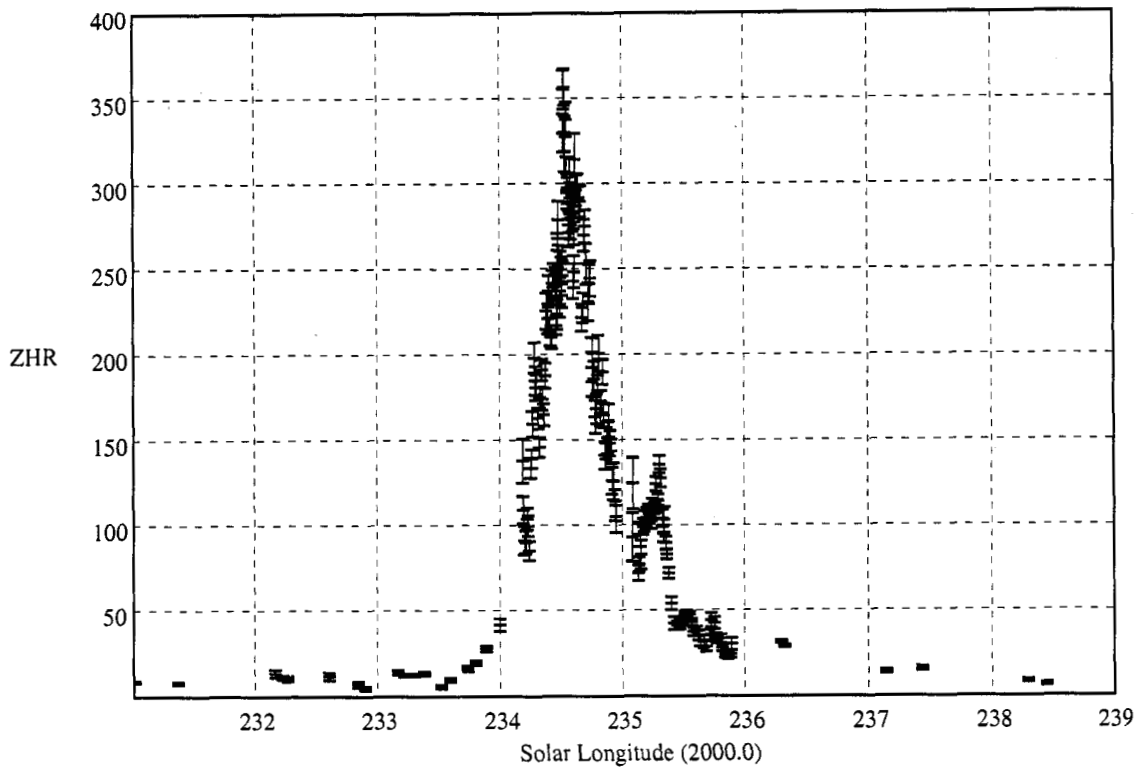

Figure 4 – Entire ZHR-profile of the 1998 Leonids. Left and right margins of the graph correspond to November 12.6 and 21.6 respectively.

A population index as high as $r = 2.3$ is unusual for major-shower maxima (which generally consist of older ejections), indicating that very recently ejected material dominates the particle mass distribution. A considerable number of meteors from the bright-meteor component might also have been incorporated into this measure of the population index; thus, if we could separate the bright-meteor component from the nodal component, the population index might be even higher.

4. The ZHR profile

The smooth population index profile of Figure 1 was used for the corrections of observations to the zenithal hourly rate (ZHR). The high-resolution profiles might amplify ZHR variations and increase the noise. We applied the following criteria for individual ZHR values to be used for averages:

- minimum radiant elevation of 20°; and
- maximum correction factor $r^{(6.5-\mathrm{lm})}F/\sin h_{\mathrm{R}} < 5$,

where lm is the stellar limiting magnitude, F the correction for possible obstructions of the field of view, and h_{R} the radiant elevation above the horizon.

The bright-meteor maximum

The very large sample of observations, particularly for the first maximum characterized by many bright meteors and fireballs, provides us with an extraordinary resolution in the activity profile. Observers mostly from western Asia, southern and western Europe, and from several parts of America contributed greatly to this excellent coverage.

It is non-trivial to find the optimum bin size for averaging a quantity like the ZHR. Large bins may suppress short-lived structures in the time series, while smaller bins may produce much larger error bars than the fluctuations they reveal, and the profile will be less reliable. Some examples of bin-size estimates include that of Brooks and Carruther (cf. [3]) with

$$k \leq 5 \times \log n,$$

where n is the number of individual ZHR values and k the suggested number of bins. We may apply this relation to the part of the activity graph between $\lambda_\odot = 234.^\circ46$ and $\lambda_\odot = 234.^\circ62$ (November 17, 0^h20^m–4^h10^m UT) where we obtained 544 individual ZHR estimates. The bin-size relation allows a maximum of 14 classes. Sturges [4] gives

$$k = 1 + 3.32 \log n,$$

resulting in only 10 classes. Heinold and Gaede [5] suggest

$$k \approx \sqrt{n}$$

giving a maximum of 23 bins. The ZHR profile in Figure 4 consists of 16 non-overlapping bins in the period considered, which is certainly near the upper limit for resolving the small-scale structure of the shower. If we look at the magnification in Figure 5 for this period, we find a clear maximum of the bright-meteor peak at $\lambda_\odot = 234.^\circ528 \pm 0.^\circ006$ corresponding to November 17, $1^h55^m \pm 9^m$ UT. This time, and the peak ZHR of 357 ± 11, agree well with the preliminary analysis in [1]. Given the fairly small error margins for the ZHR values, resulting from the large numbers of Leonids involved in each average, the variability of the activity appears significant. Clear sub-peaks can be spotted, such as at $\lambda_\odot = 234.^\circ281 \pm 0.^\circ010$, $\lambda_\odot = 234.^\circ398 \pm 0.^\circ010$, $\lambda_\odot = 234.^\circ481 \pm 0.^\circ005$, $\lambda_\odot \approx 234.^\circ63 \pm 0.^\circ01$, and $\lambda_\odot = 234.^\circ700 \pm 0.^\circ010$. Due to the variability of the ZHR-profile, the full width at half maximum (FWHM) is difficult to measure. It is found to be in the range $0.^\circ440$–$0.^\circ565$ corresponding to $10^h.5$–$13^h.5$. The individual sub-peaks in the ZHR-profile exhibit much smaller time-scale variations. The additional upper panel in Figure 5 shows the average limiting magnitude for each ZHR average; the absence of a clear correlation of individual ZHR peaks with sky conditions supports the physical reality of the variations. In 12 hours, the Earth travels 1.3 million km, but not perpendicularly through the stream. We thus get a smaller perpendicular extent of the bright-meteor component of about 380 000 km—the distance of the Moon.

Table 2 – Bin sizes for the ZHR profile in Figures 4–6.

Range in $\lambda_\odot$	Width	Shift
–232.°00	2.°00	1.°00
232.°00–234.°10	0.°20	0.°10
234.°10–234.°46	0.°04	0.°02
234.°46–234.°62	0.°01	0.°005
234.°62–235.°35	0.°02	0.°01
235.°35–236.°00	0.°04	0.°02
236.°00–	1.°00	0.°50

The nodal peak

The activity maximum near the time when the Earth passes close to the descending node of the parent comet's orbit was supposed to be the strongest period of activity based on predictions for 1998. The actual ZHR fell below most expectations, though a clear peak was observed by several groups in eastern Asia. The peak time at $\lambda_\odot = 235.^\circ311 \pm 0.^\circ007$ (November 17, $20^h33^m \pm 10^m$ UT) is 75 minutes after the nodal passage. The maximum ZHR was 136 ± 5 which is lower than obtained in the preliminary analysis of [1]. The nodal maximum nearly coincides in time with the highest population index observed. This agrees with the assumption that the nodal peak is formed by particles recently ejected from the comet, probably no earlier than three revolutions ago. The ZHR-profile of the nodal peak (magnified in Figure 6) is skew with the steeper gradient following the maximum; the skewness is even retained when subtracting the activity of the far end of the broad bright-meteor component.

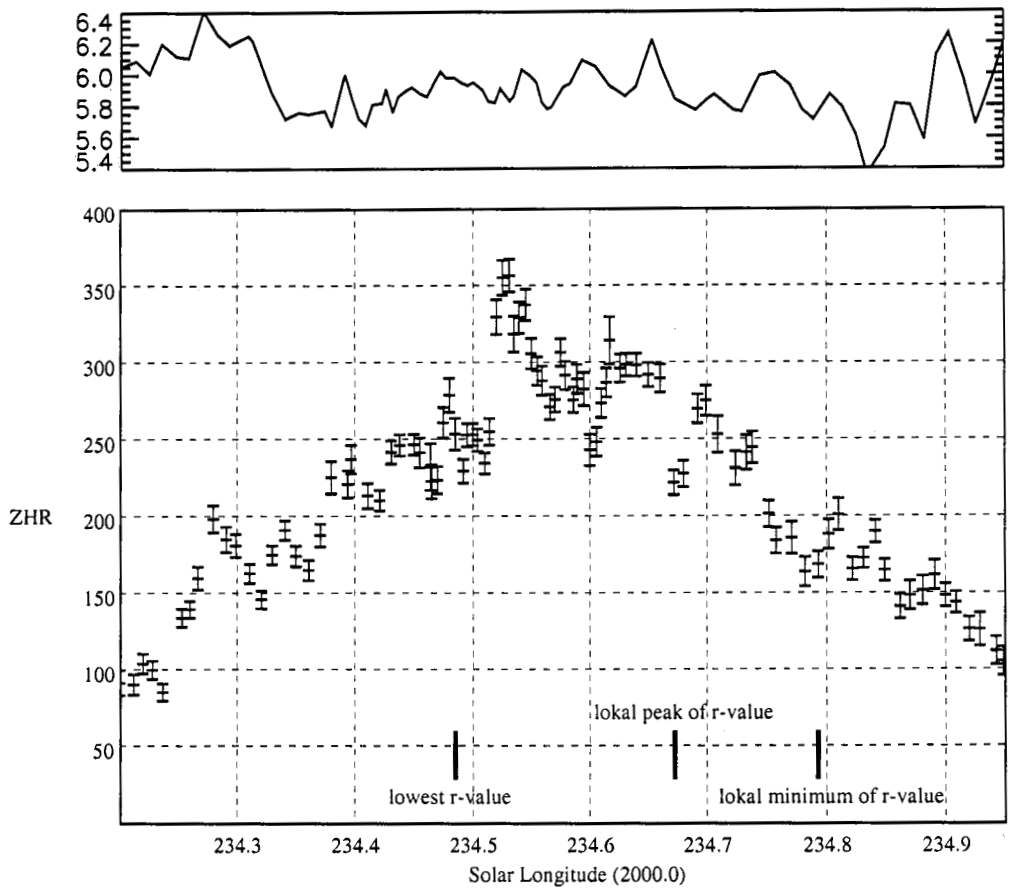

Figure 5 – Magnification of the 1998 ZHR-profile of the Leonids near the maximum characterized by low population indices. The upper panel shows the average limiting magnitude for each ZHR value.

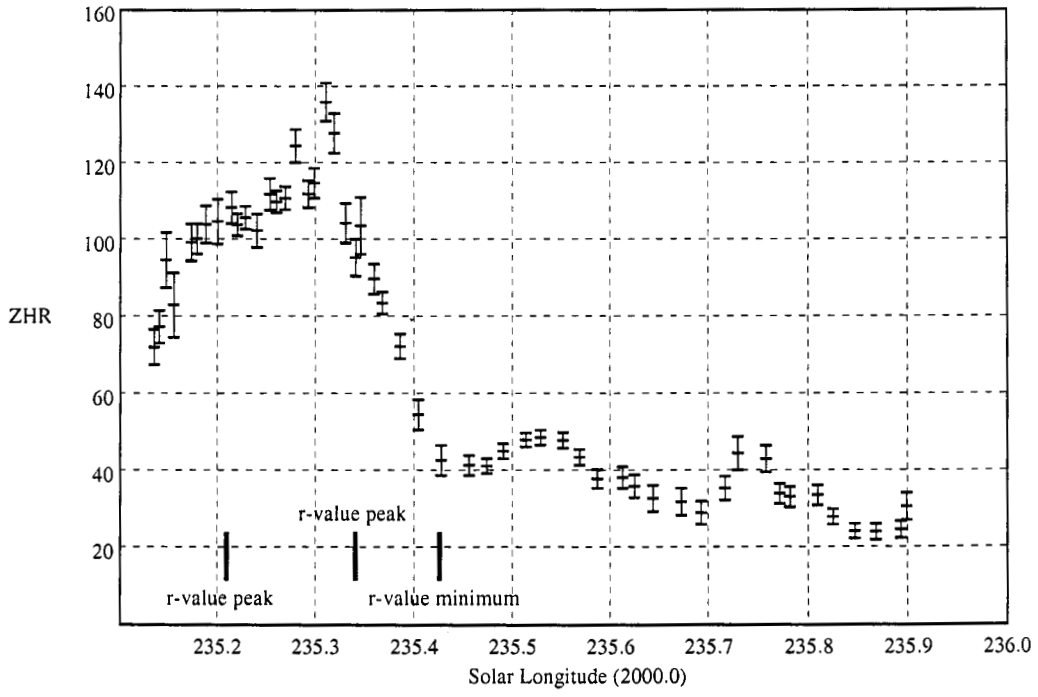

Figure 6 – Magnification of the 1998 ZHR-profile of the Leonids near the nodal maximum.

In order to produce a stand-alone profile of the nodal peak structure, we try to subtract the influence of the bright-meteor maximum (index 1) and the relatively weak background component (index 2) of more than a day duration.

We compute a combination of two Gaussian profiles

$$\mathrm{ZHR} = C_1 \exp\left(-\frac{(\lambda_\odot - \lambda_1)^2}{2\sigma_1^2}\right) + C_2 \exp\left(-\frac{(\lambda_\odot - \lambda_2)^2}{2\sigma_2^2}\right),$$

where C_1 and C_2 are the amplitude of the two profiles, λ_1 and λ_2 are their centers, and σ_1 and σ_2 are the Gaussian standard deviations representing the width of the individual component. Note that the two Gaussian profiles do *not* correspond to the two maxima, but, instead, refer to the bright-meteor component and the background component, respectively.

The fit ran from $\lambda_\odot = 233°$ to $\lambda_\odot = 236°$, excluding the period of the nodal peak, $\lambda_\odot = 235\overset{\circ}{.}00$–$235\overset{\circ}{.}45$. We obtained $C_1 = 225$, $C_2 = 66$, $\lambda_1 = 234\overset{\circ}{.}567$, $\lambda_2 = 234\overset{\circ}{.}841$, $\sigma_1 = 0.216$, and $\sigma_2 = 0.764$. Figure 7 shows the ZHR profile in the period under consideration with the double-Gaussian fit in the upper panel and the reduced ZHR profile near the nodal passage in the lower panel. The peak ZHR of the reduced nodal maximum is 80, and the skewness is retained. Neglecting the shoulder before $\lambda_\odot = 235\overset{\circ}{.}25$, we get a FWHM of $0\overset{\circ}{.}11$ or $2\overset{\mathrm{h}}{.}6$. This time corresponds to a traveling distance of 280 000 km and a perpendicular extent of the nodal peak—the thickness—of 82 000 km.

We should recall that the maximum population index occurred 38 minutes after the ZHR maximum. High r-values of $r > 2.0$ were observed up to 4 hours before the ZHR maximum, whereas a sudden decrease in r was observed less than 2 hours after the r-peak and $2\overset{\mathrm{h}}{.}6$ after the ZHR maximum.

Statistical means to study the shape of distributions are the momenta

$$m_q = \frac{\sum_{i=1}^{N} (\lambda_i - \overline{\lambda_\odot})^q \, \mathrm{ZHR}_i}{\sigma^q \sum_{i=1}^{N} \mathrm{ZHR}_i},$$

where λ_i is the independent distribution variable, ZHR_i are the corresponding rates, $\overline{\lambda_\odot}$ is the average solar longitude (not necessarily the highest value), and σ is the standard deviation of the distribution belonging to $\overline{\lambda_\odot}$. The value of q determines the order of the momentum.

The skewness of the nodal peak can be estimated through the third momentum ($q = 3$) of the ZHR distribution versus solar longitude. The nodal maximum delivers a skewness of $m_3 = -0.15 < 0$, confirming the right-weighted asymmetry in the profile; a positive third moment would have implied a left-weighted profile. The bright-meteor maximum has $m_3 = +0.02$ indicating a highly symmetric distribution of rates.

The fourth momentum ($q = 4$) measures the "excess" of the profile compared with a Gaussian distribution. A positive value means the profile is too steep, the maximum is too high, and the wings are under-represented. A negative value indicates a bump-like profile with too low a maximum and strong wings. We get $m_4 = -0.9$ for the nodal peak indicating an excess of the wings. A triangular distribution has $m_4 = -0.6$, a rectangular distribution has $m_4 = -1.2$. These momenta were applied to the reduced ZHR profile, after subtraction of the bright-meteor background affecting the nodal peak. The bright-meteor component has $m_4 = -0.9$, probably because of its roughly bimodal structure at maximum.

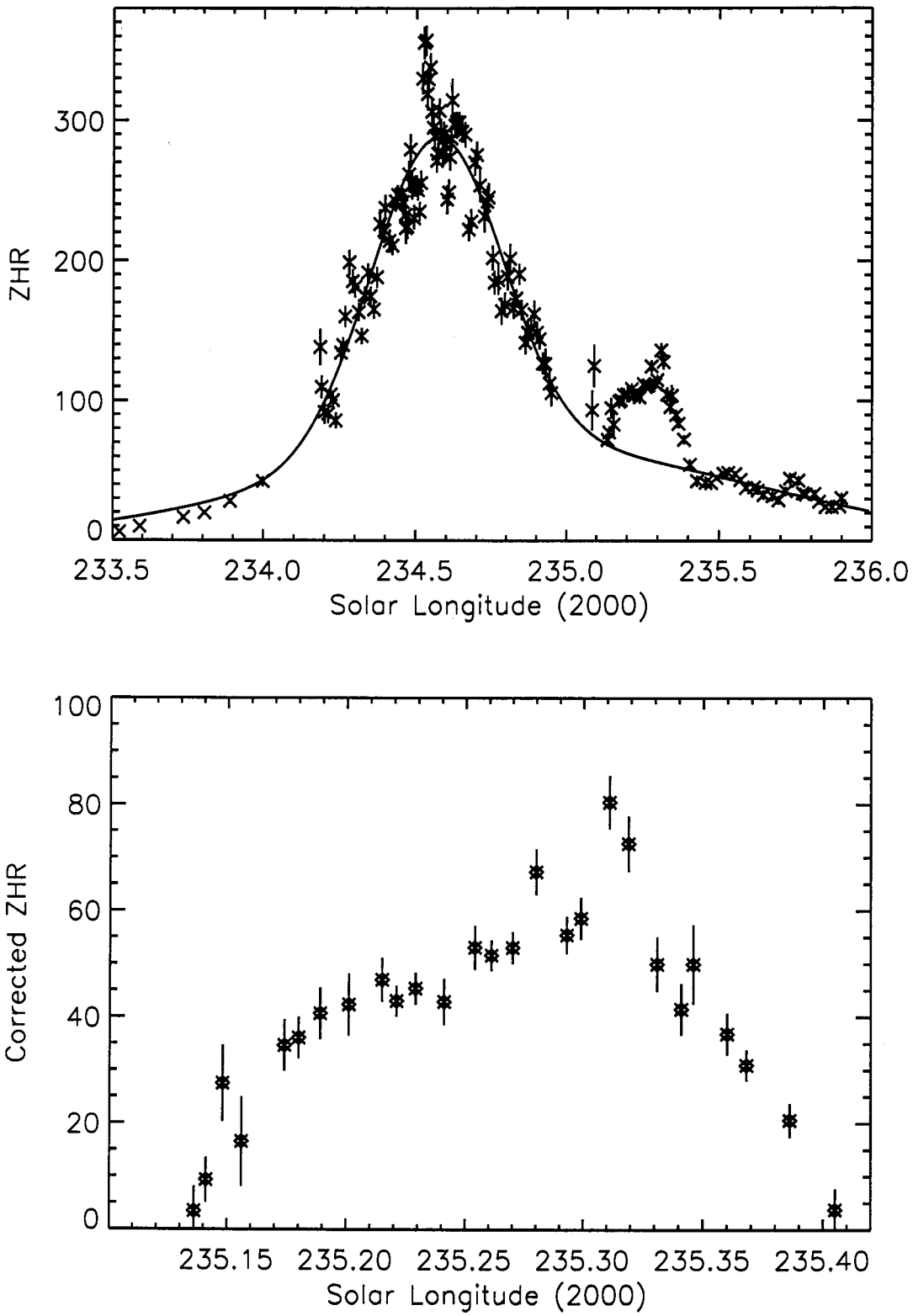

Figure 7 – Best fit by a sum of two Gaussians, representing the bright-meteor component and a weak background component, to the ZHR profile excluding the nodal-peak range $\lambda_\odot$ = 235°.0–235°.45 (*top*). Reduced nodal peak profile with the double-Gaussian fit subtracted (*bottom*).

5. Leonid meteoroid flux

The ZHR is an observational measure for the shower's activity as seen by an average observer on Earth. Physically, it is more interesting to investigate the actual number density of particles in space. For this purpose, we have to determine the volume monitored by the observer which can be approximated by the area size of a fixed layer—the meteor layer—in the atmosphere. This area physically depends on the elevation of the observer's field of view, since at lower elevations a larger atmospheric volume is monitored, and on the population index, since meteors will be far away at low elevation and their magnitudes thus significantly reduced. The normalization to a standard "monitoring" area (collecting area A_{red}) of an average observer towards the zenith has been previously computed [6]. Only observations with a given center of field of view were used for the flux density profile shown in Figure 8.

The error bars were obtained using error propagation of the Poissonian error of meteor numbers and the error of the population index which affects the flux density not only through the ZHR, but also through the the standard collecting area and the extrapolation to the true number of meteors. The striking feature of the flux density graph in Figure 8 is the completely reversed amplitude of the peaks: the fireball maximum is less pronounced than the nodal peak. This is an observational effect. The monitored area increases with the zenith distance of the field, and, thus, an observer could see more meteors at low elevations; but the distance to these meteors increases with the zenith distance of the field, and the meteor intensity decreases with the square of this distance. The question whether the increased monitoring area balances with the magnitude loss is controlled by the population index. During the 1998 fireball maximum these effects combined to produce a huge excess of meteors in fields not towards the zenith—the actual number density of particles, however, was lower than during the nodal peak. In fact, many observers reported that it was their impression that looking towards low elevations was best for detecting the greatest number of meteors.

Different populations constitute different fractions of the full sample of particles. The upper panel of Figure 8 shows the flux density for particles causing meteors brighter than magnitude +6.5 which corresponds to a mass of 2.2×10^{-5} g according to the conversion [7,8]

$$m = 40 - 2.5 \log \left(2.732 \times 10^{10} M^{0.92} V_{\mathrm{G}}^{3.91}\right),$$

where m is the meteor magnitude, M the meteoroid mass in grams, and V_{G} the geocentric velocity of the meteoroids. The fireball maximum is much more prominent in the flux if larger particles are exclusively considered. The nodal peak is still visible in the graph of the flux for meteors up to medium magnitudes. It is completely absent when examining fireball-class events alone.

A second feature is the varying peak time with varying mass limit. Large particles have their highest flux earlier than smaller particles within the fireball maximum. The difference in peak time as derived from the top and bottom panels of Figure 8 is $0^{\circ}.11$, corresponding to about 2.6 hours. The fact that the population index has a minimum an hour *before* the bright-meteor maximum and climbs gradually during times of highest activity (as already presented in Section 3) foreshadowed this apparent mass sorting.

6. Comparison with particle simulations

In an effort to interpret the overall characteristics of the shower in 1998 (i.e., large, broad fireball peak and smaller, larger r peak near nodal passage), we have examined some modeled Leonid distributions in detail. We make use of the numerical model previously developed in detail for the Perseids and described by Brown and Jones [9].

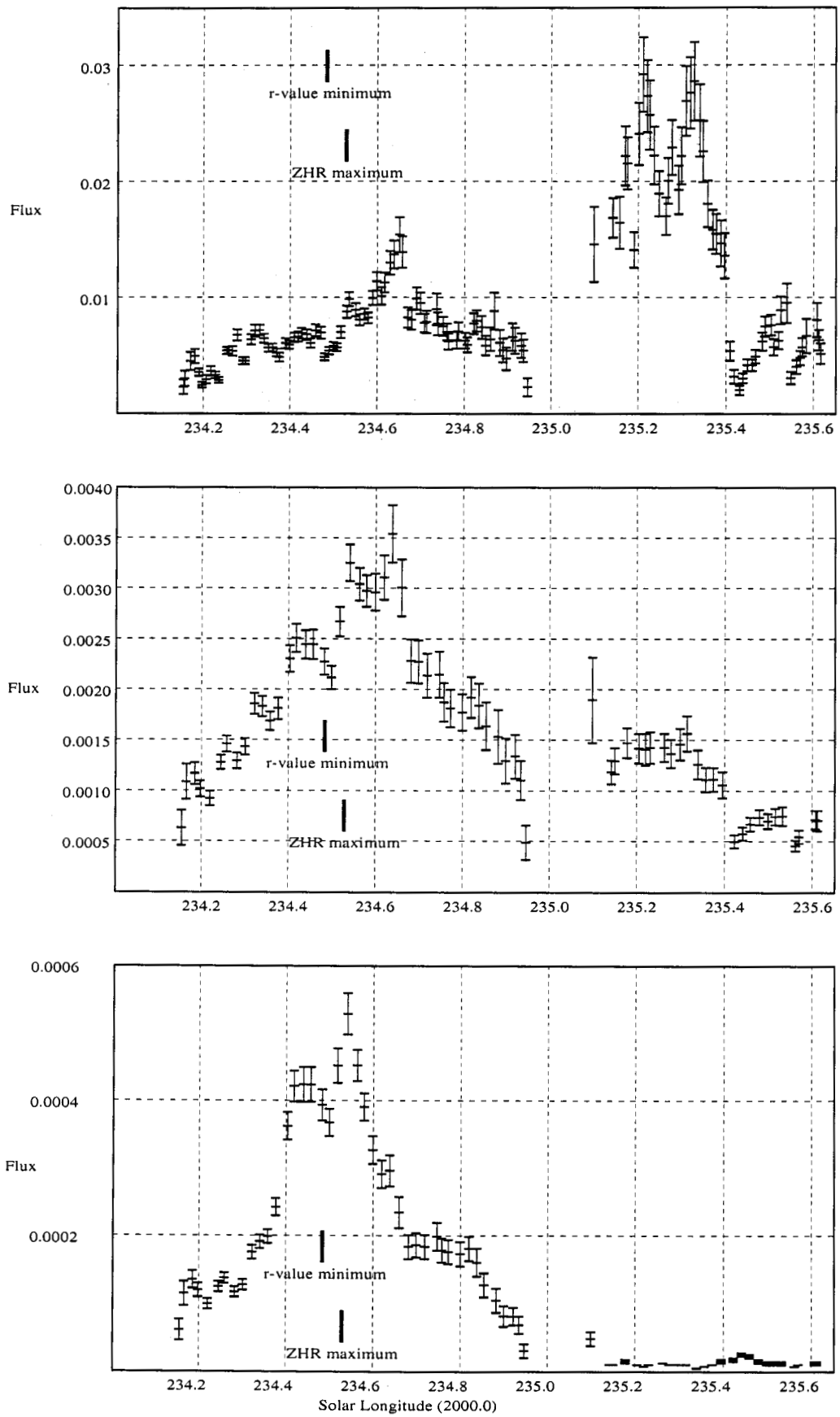

Figure 8 – Flux density profiles of the 1998 Leonids for various particle populations: particles causing meteors brighter than magnitude +6.5 (heavier than 2.2×10^{-5} g) (*top*), than magnitude +2.7 (heavier than 1 mg) (*middle*), and −4.2 (heavier than 1 g) (*bottom*).

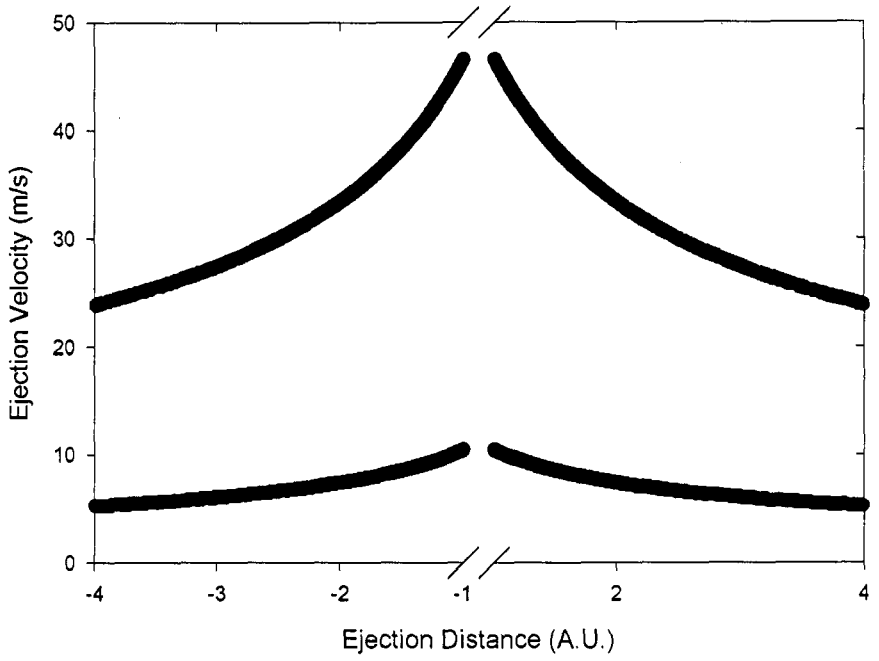

Figure 9 – Range of total ejection velocities as a function of the Comet's distance from the sun and β, the ratio of solar radiation pressure force to the sun's gravitational force. All ejection velocities lie in the band between the two curves. Negative distances mean pre-perihelion positions. Note that the abscissa skips distances closer than the perihelion distance of the Comet.

Briefly, the basic procedure consists of generating a suite of test particles close to each perihelion passage of Comet 55P/Tempel-Tuttle and following each of these through to the epoch of interest. The "daughter" Leonids are created through random ejection on the sunward hemisphere of the Comet and are distributed at random in true anomaly along the cometary arc inside 4 AU. The osculating elements for 55P/Tempel-Tuttle at perihelion are taken from Yeomans et al. [10].

A total of 10 000 test meteoroids with density 0.8 g/cm^3 are ejected in each decadal mass interval from 10 g to 10^{-5} g, for a total per perihelion passage of 70 000 test particles. This corresponds to values of β from 5×10^{-5} to 5×10^{-3} approximately separated by factors of two between each of the 7 categories. Here, β refers to the ratio of solar radiation pressure force to the Sun's gravitational force, i.e., $\beta = F_{\mathrm{rad}}/F_{\mathrm{grav}}$. This procedure is repeated for each of the last 58 perihelion passages of the Comet, so that the complete "run" consists of just over 4 million test particles.

After the initial conditions are specified in this way, each test particle is numerically integrated forward from ejection to the epoch of interest and followed until it reaches its descending node (the only point along its orbit at which it might possibly be observable from the Earth) and its Keplerian elements at the time of nodal passage are stored.

For this model, we adopt a bulk meteoroid density of 0.8 g/cm^3 over all masses and release meteoroids with velocities following the standard Whipple ejection routine [11], modified to follow an $r^{-0.5}$ heliocentric velocity dependence. More details can be found in [9]. Figure 9 shows the range of total ejection velocities as a function of distance from the Sun and β.

The final particle distributions are chosen such that the test meteoroids have nodal passage times within 1 week of the peak of the shower in 1998 (this is equivalent to taking a slice of 0.°2 width in mean anomaly along the stream orbit) and nodal distances within 2×10^{-3} AU of the Earth's orbit. All Leonid test particles which meet these two conditions are then binned in 0.°02 intervals of solar longitude (approximately 30 minutes). As the majority of the recently ejected Leonid "streamlets" (over the last 3–4 revolutions) are primarily more than 0.005 AU inside the

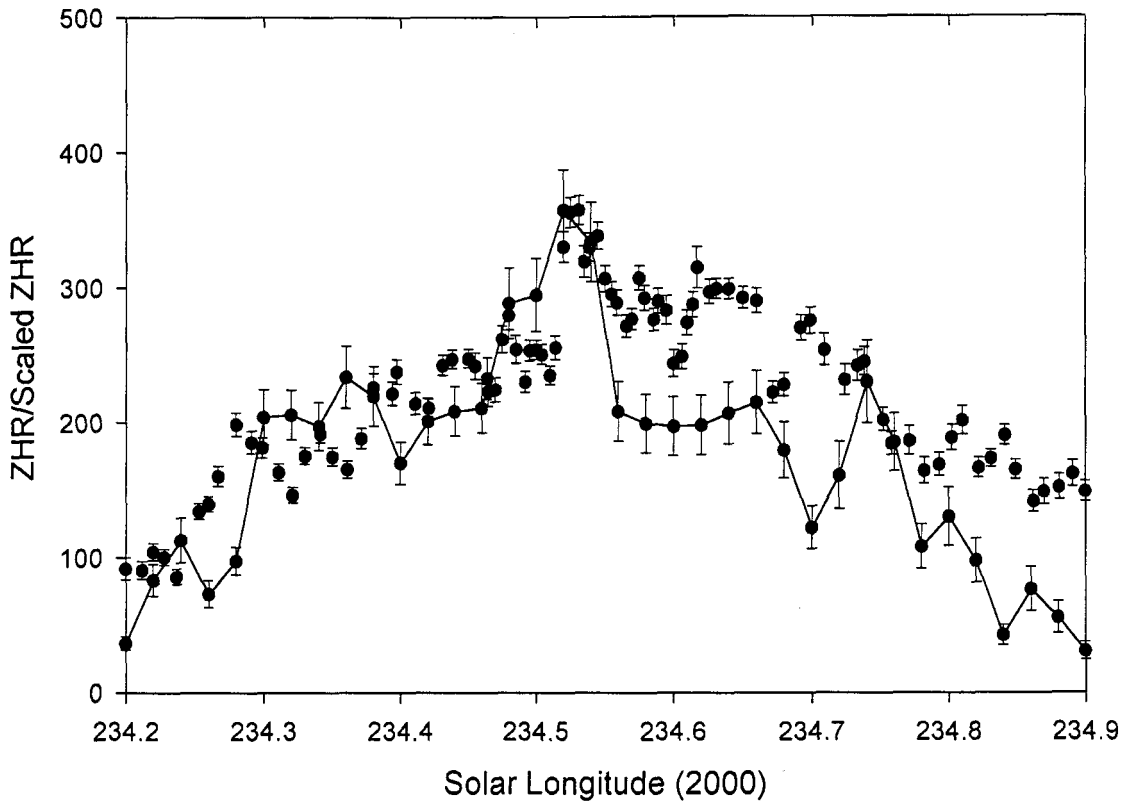

Figure 10 –Comparison of observed ZHR with a modeled "ZHR" scaled to the maximum of the observed profile.

However, the total final summed particle distributions found in this manner are not a true reflection of a ZHR-like value as all masses have been weighted equally, whereas some power-law distribution at the source must be assumed. For simplicity, we have used a mass index at the source of 1.4. The choice of this value heavily influences the final distributions and we emphasize that what follows is not a unique solution. We note that such a low value for the mass index at the source implies that we are giving more weight at the source to the large meteoroids in the distribution, as was observed during the 1998 return.

The final activity found in this manner is then scaled to the same peak ZHR as observed to compute the resulting shapes of the two curves over the solar longitude range $\lambda_\odot = 234°–235°$. This is shown, along with the ZHR values discussed previously, in Figure 10. The basic shape and profile of the two curves is remarkably similar over the range $\lambda_\odot = 234.^\circ2–234.^\circ9$ (where good observational data exist). The simulated results are still not of a fidelity to permit detailed comparison with all the fine structure in the ZHR curve, even assuming all are real features of the stream. However, two notable features are visible in each curve: the good agreement of the location of the peak activity and a plateau visible from $\lambda_\odot = 234.^\circ58–234.^\circ68$ in both. As well, the theoretical profile falls off more sharply than is observed, particularly after $\lambda_\odot = 234.^\circ8$.

Figure 11 shows the age distribution of material composing the stream over this interval. We note that the single-most prolific ejection era contributing meteoroids in 1998 was the 1333 passage of Comet 55P/Tempel-Tuttle. This has been previously noted by Asher, Bailey and Emel'yanenko [12] and was ascribed to trapping of large Leonids in the 5:14 resonance with Jupiter. However, unlike the conclusions from [12], we note considerable (almost equal) contributions from many passages within a few revolutions on either side of the 1333 ejection—particularly from 1167. The reason for the difference in final distributions between those found by [12] and here might be that the results from [12] were confined to ejection at perihelion, whereas we extend these ejection locations over almost all of the cometary arc where significant ejection activity might be expected. Unsurprisingly, removing the constraint that ejection must be precisely at perihelion allows a much greater range of initial meteoroid ejections to be "visible" in 1998.

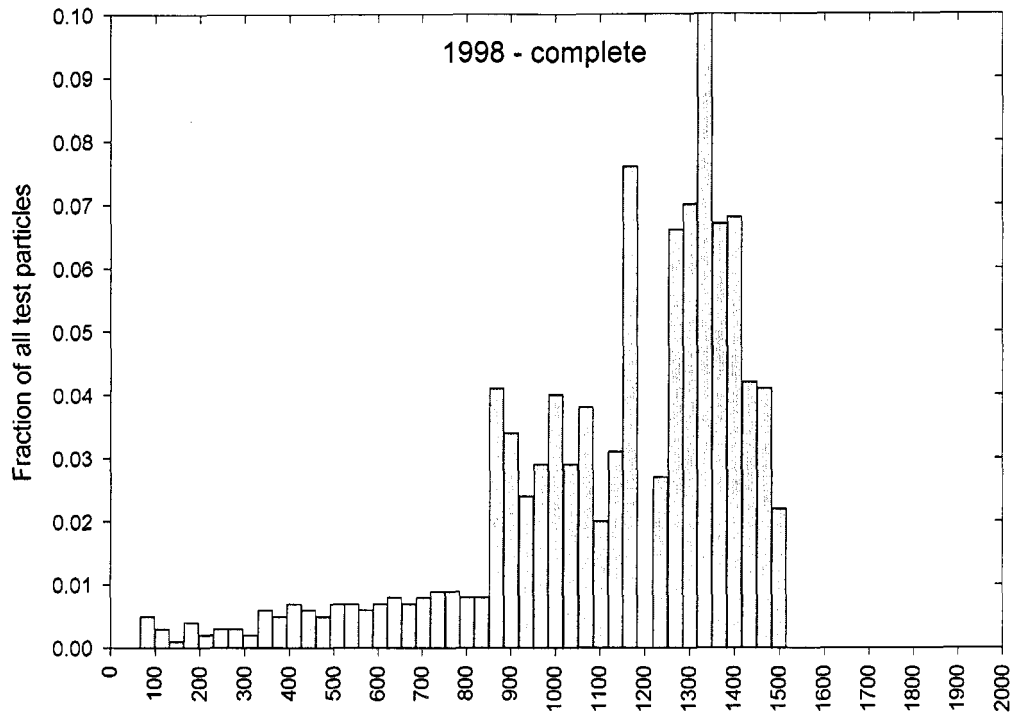

Figure 11 –Ejection years contributing to the 1998 activity profile. Test particles are counted as Leonids in 1998 if they have nodal passage times within 1 week of the shower maximum (at $\lambda_\odot = 235°.3$) and nodal distances within 0.002 AU of the Earth. Only ejected meteoroids with masses greater than 0.1 g are included.

Using this model, we may conclude that the 1998 shower was composed of material which was 500–1000 years old, but cannot confine the exact origin more precisely than this. This suggests that the fireball peak was actually composed of a series of filaments from different ejection epochs, though it is unclear that these would be necessarily separable in terms of ZHR activity as most of these ejections end up spread over nearly the same range of solar longitudes, whereas the ZHR profile shows a variety of sub-maxima.

Notable also in this figure is the drop in the numbers of accepted Leonids prior to the 833 AD epoch. A partial explanation for this may lie in the fact that 55P/Tempel-Tuttle did not enter the 5:14 resonance until around 700–800 AD. Material ejected prior to this epoch would not have such easy access to the 5:14 resonance and thus show lower transfer efficiencies at the present epoch (unlike the material from 900 AD to 1500 AD).

If we examine the age of material across the profile from $\lambda_\odot = 234°$–$235°$, we find, in general, that the material tends to become slightly older as we move to larger values of solar longitude. Figures 12 and 13 show the normalized age distribution of material over the interval from $\lambda_\odot = 234°.2$–$234°.9$ in steps of $0°.1$. The rising portion of the curve and the region around the peak are most populated by very large meteoroids ejected at the few passages of Tempel-Tuttle on either side of 1333. At the point where the plateau occurs in the theoretical and observed profiles, near $\lambda_\odot = 234°.6$, the dominant population switches to become centered around the 1167 passage of 55P/Tempel-Tuttle and moves (relatively speaking) toward smaller meteoroids. The descending portion of the profile is richer in smaller meteoroids and material of slightly older (the 1167 AD and a few nearby passages of the Comet) origin. This change in origin may also be responsible for the increase in population index starting at $\lambda_\odot = 234°.6$. Figure 14 shows the distribution of accepted particles as a function of solar longitude.

The nodal peak observed at $\lambda_\odot = 235°.3$ is almost completely lacking in these modeled results. Previous work [14] suggests that material observed near this solar longitude range is about 3 revolutions old at most (older ejections would tend to peak at different solar longitudes).

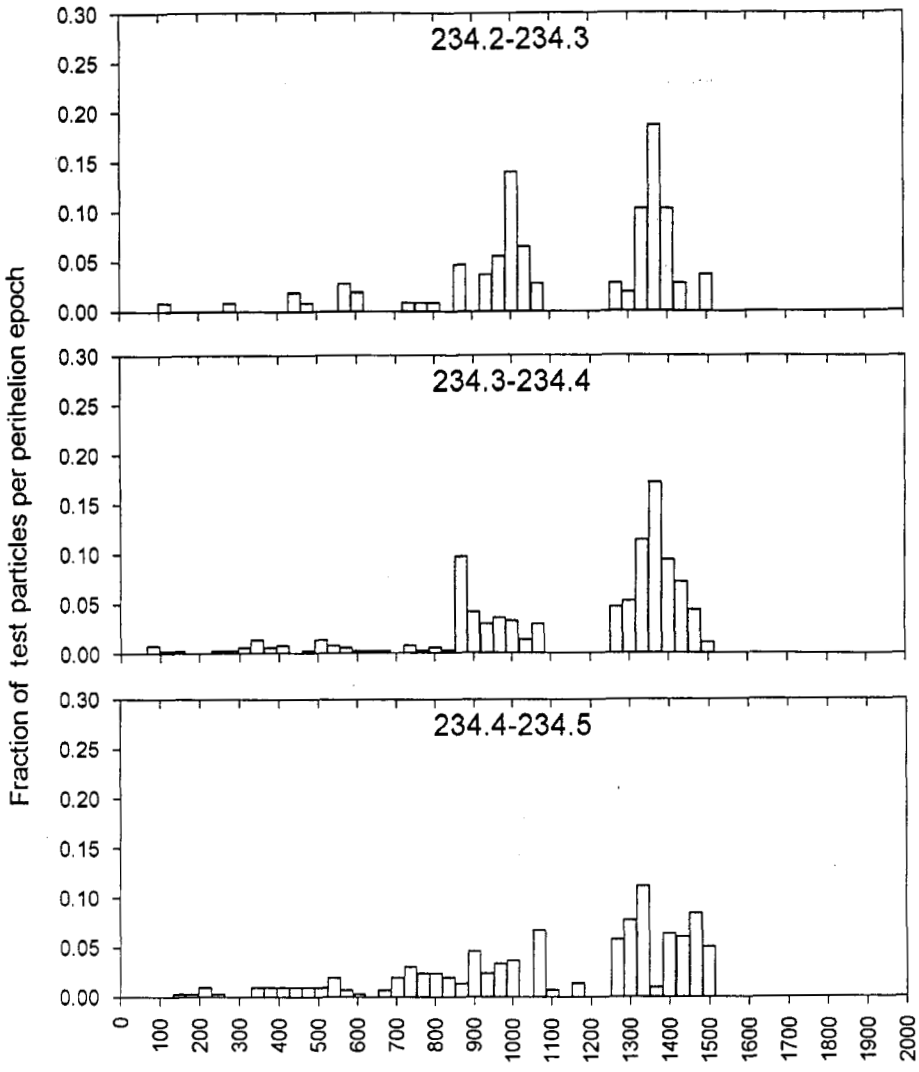

Figure 12 –Contributions of particles from various ejection years. Each of the graphs gives the perihelion epoch contributions for a 2.4-hour period of the activity profile.

We note from [13,14] that the center of these recent streamlets were approximately 0.005 AU interior to the Earth's orbit at the time of the 1998 shower. As a result, any particles from these ejection epochs which reached the Earth had significantly larger nodal distances than did the average Leonid with low ejection velocity and modest size ($\beta < 10^{-3}$).

From [14], ejection velocities in the range 15–20 m/s (with a significant transverse component) can produce an increase in the nodal radii (ignoring planetary perturbations) of more than 0.005 AU for ejections within a few tens of degrees in true anomaly of perihelion. As well, radiation pressure forces on very small particles (with $\beta \approx 10^{-2}$) can produce an increase of comparable magnitude in the nodal radii. As a result, it is reasonable to expect that the smallest meteoroids associated with the last few revolutions of the comet (namely, 1965, 1932, and 1899) would be visible (albeit in small numbers) near the current nodal longitude of the comet in 1998. From [14], the nominal ejection epoch with the greatest contribution is 1932 for this solar longitude interval (exclusively small particles), but the numbers are so small (roughly 0.01% of the initial sample) as to make the determination questionable.

In summary, all we may conclude is that very small, high ejection velocity, high β particles from some (or all) of the 1965, 1932, and 1899 ejections contributed to the nodal peak in 1998. For somewhat older trails ejected 4 to 7 revolutions ago (such as those given in [13]) with expected peaks in solar longitude between $\lambda_\odot = 235\overset{\circ}{.}6$ and $\lambda_\odot = 235\overset{\circ}{.}9$, no obvious features were visible in the 1998 ZHR profile.

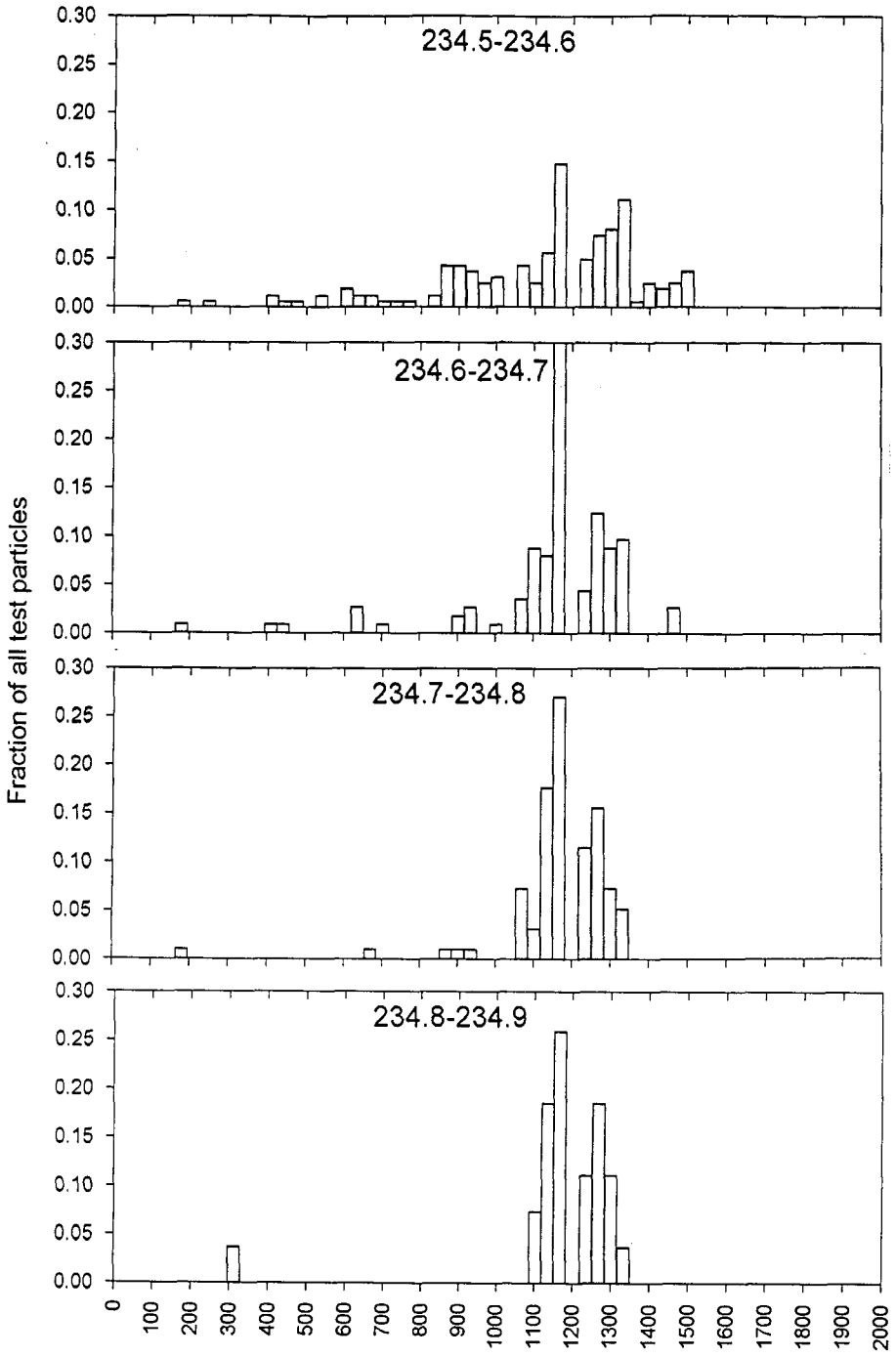

Figure 13 –Contributions of particles from various ejection years for more bins of the activity profile.

7. Conclusions

In 1998, two distinct particle components were detected in the Leonid stream. The first, was a strong, broad component of particles ejected primarily 500–1000 years ago, centered at $\lambda_\odot = 234^\circ.528 \pm 0^\circ.006$ (November 17, 1998, $1^h55^m \pm 9^m$ UT), with a maximum equivalent ZHR of 357 ± 11, and with a peak flux of 0.015 ± 0.001 meteoroids brighter than magnitude +6.5 per square kilometer and per hour. A more short-lived maximum, rich in smaller particles, occurred at $\lambda_\odot = 235^\circ.311 \pm 0^\circ.007$ (November 17, 1998, $20^h33^m \pm 10^m$ UT), which is near the Earth's passage of the orbital node of the parent comet, 55P/Tempel-Tuttle. The maximum equivalent ZHR at this nodal peak was 136 ± 5 and the peak flux was 0.028 ± 0.03 meteoroids brighter than magnitude +6.5 per square kilometer and per hour. The nodal (second) maximum is most likely composed of the high ejection velocity "tail" of smaller meteoroids released during one or possibly all of the 1965, 1932, and 1899 passages of 55P/Tempel-Tuttle.

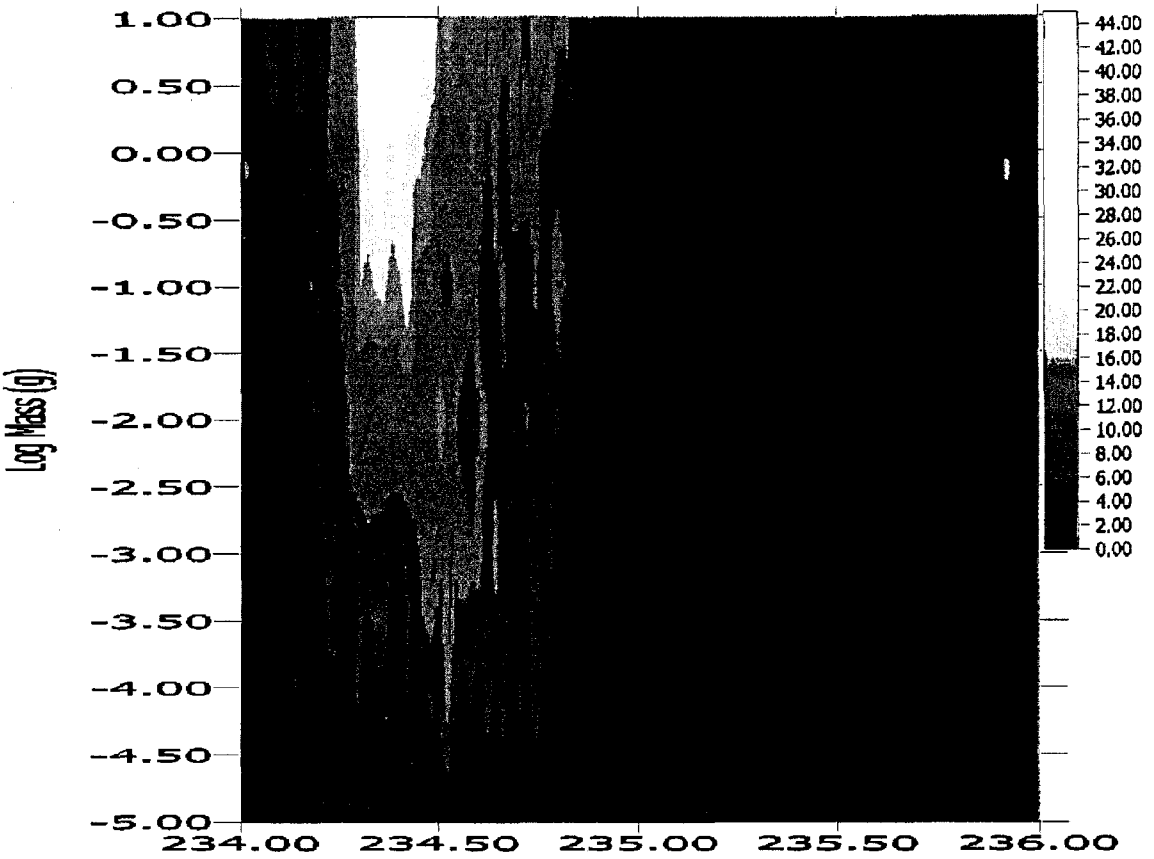

Figure 14 –Particle number density as a function of solar longitude and particle mass. The sum of values for all particle masses gives the activity profile. The maximum of the largest particles is found before the activity maximum.

Acknowledgments

We are most grateful for the numerous valuable comments by Marc Gyssens and Luis Bellot Rubio, for the enormous efforts of all observers, and for the support of national and regional coordinators in various countries.

References

[1] R. Arlt, "Bulletin 13 of the International Leonid Watch: The 1998 Leonid Meteor Shower", *WGN* 26, 1998, pp. 239–248.

[2] R. Arlt, "Global Analysis of the 1998 Perseid Meteor Shower", *WGN* 27, 1999, pp. 237–249.

[3] R. Sturm, "Wahrscheinlichkeitsrechnung, mathematische Statistik und statistische Qualitätskontrolle", Fachbuchverlag Leipzig, 7th ed., 1988, p. 86.

[4] H.A. Sturges, "The Choice of a Class Interval", *J. Amer. Statist. Assoc.* 21, 1926, pp. 65 and 66.

[5] J. Heinold, K.-W. Gaede, "Ingenieur-Statistik", Oldenbourg, München-Wien, 1972 (3rd edition).

[6] R. Arlt, "Global Analysis of the 1997 Perseids", *WGN* 26, 1998, pp. 61–71.

[7] F. Verniani, "An Analysis of the Physical Parameters of 5759 Faint Radio Meteors", *J. Geophys. Res.* 78, 1973, pp. 8429–8462.

[8] D.W. Hughes, "P/Halley Dust Characteristics: A Comparison between Orionid and Eta Aquarid Meteor Observations and Those from the Flyby Spacecraft", *Astron. Astrophys.* 187, 1987, pp. 879–888.

[9] P. Brown, J. Jones, "Simulation of the Formation and Evolution of the Perseid Meteoroid Stream", *Icarus* 133, 1998, pp. 36-68.

[10] D.K. Yeomans, K.K. Yau, P.R. Weissman, "The Impending Appearance of Comet Tempel-Tuttle and the Leonid Meteors", *Icarus* 124, 1996, pp. 407–413.

[11] F.L. Whipple, "A Comet Model. II. Physical Relations for Comets and Meteors", *Astrophys. J.* 113, 1951, pp. 464–474.

[12] D. Asher, M.E. Bailey, V.V. Emel'yanenko, "Resonant Meteoroids from Comet Tempel-Tuttle in 1333: The Cause of the Unexpected Leonid Outburst in 1998", *Mon. Not. R. Astr. Soc.* 304, 1999, pp. L53–L56.

[13] R. McNaught, D.J. Asher, "Leonid Dust Trails and Meteor Storms", *WGN* 27, 1999, pp. 85–102.

[14] P. Brown, "Evolution of Two Periodic Meteoroid Streams: The Perseids and Leonids", Ph. D. Thesis, Univ. of Western Ontario, London, Ont., 1999, pp. 171–258.

Bulletin 15 of the International Leonid Watch: First Global Analysis of the 1999 Leonid Storm

Rainer Arlt, Luis Bellot Rubio, Peter Brown, and Marc Gyssens

An overall activity profile of the 1999 Leonid meteor shower is presented based on the observations of 434 observers who reported 277 172 Leonids in 10 806 observing periods. A storm of Leonid activity was observed from western Asian, European, and African locations at a solar longitude of $\lambda_\odot = 235.^\circ285 \pm 0.^\circ001$, corresponding to November 18, 1999, $2^h02^m \pm 2^m$ UT with a peak equivalent ZHR of 3700 ± 100 based on 2.8-minute intervals. Solar longitudes refer to equinox J2000.0. The flux density of particles causing meteors brighter than magnitude +6.5 is 1.4 ± 0.3 particles per square kilometer and per hour. This corresponds to a number density of 5400 ± 1200 particles per 10^9 cubic kilometer. Additional maxima are found in the ZHR peak profile; one of them at $\lambda_\odot = 235.^\circ272$ or 1^h43^m UT can be associated with the cometary ejecta from the 1932 perihelion passage. The time of this peak as well as the main peak, which is caused by particles from the 1899 passage, are reproduced by particle simulations. A clear second activity outburst occurred at $\lambda_\odot = 235.^\circ87 \pm 0.^\circ04$ (November 18, 1999, $16^h \pm 1^h$ UT) with a maximum ZHR of 180 ± 20. The Leonid storm component is found to exhibit an unusual magnitude distribution with a lack of both very bright *and* very faint meteors.

1. Predictions and observational data

Although innumerable verbal reports would be worth reproducing, we have to restrict ourselves to the mere numbers in this overview of 1999 Leonid activity. A considerable number of meteor reports with 1-minute counts is available for the peak period; the same holds for many breakdowns of magnitude distributions. All observers who reported longer intervals during this period are highly encouraged to revisit their observations for possible shorter intervals according to their notes and tapes. Until December 8, 1999, we obtained the reports from 434 observers who logged 277 172 Leonids in a total of 10 806 observing intervals.

Predictions were attempted by three independent investigations of the stream evolution: Kondrat'eva and Reznikov [1] and Asher and McNaught [2,3] give the same peak time, November 18, 2^h08^m UT ($\lambda_\odot = 235.^\circ29$), whereas Brown [4] gives November 18, 2^h20^m UT ($\lambda_\odot = 235.^\circ30$).

In all these models, the major contribution to the peak comes from particles ejected from the parent comet in 1899. The results in [1–3] are based on the evolution of the dust trails Comet 55P/Tempel-Tuttle ejects at each perihelion passage and evaluates the encounter conditions when the Earth passes the meteoroid stream (do not confuse with the comet's tail which consists of much smaller particles). The closest encounter times given in [3] for the trails ejected in 1932 and 1965 are 1^h44^m and 1^h53^m UT corresponding to $\lambda_\odot = 235.^\circ273$ and $\lambda_\odot = 235.^\circ279$, respectively, but no significant activity was attributed to either of them. The work in [4] reports on full-stream models covering the evolution of the Leonid stream over a 2000-year history, simulating the actual number density of particles in the stream by a large number of model particles which is of the order of one million.

Locations in western Asia, Europe, and northern Africa were most favorable for witnessing a meteor storm of at least 500 meteors per hour, and many people at these locations were fully awarded with much higher rates at the exact time, weather permitting.

In addition, Emel'yanenko [5] expected that material ejected earlier than 1899 would produce enhanced rates near November 18, 17^h UT, corresponding to a solar longitude of $\lambda_\odot = 235.^\circ91$q. Brown [4] also suggested that some activity might be detectable near $\lambda_\odot = 236.^\circ0$, principally from high ejection velocity material (or, equivalently, from particles with small values of β, the ratio of the Sun's radiation pressure force to its gravity) from the 1866 ejection. Predictions in [3] were more specific and noted three possible additional peaks of activity—one near 19^h55^m UT ($\lambda_\odot = 236.^\circ04$) due to 4-revolution-old (1866) ejecta, one near 21^h59^m UT ($\lambda_\odot = 236.^\circ13$) due to 5-revolution-old (1833) ejecta and one near $236.^\circ16$ from 6-revolution-old (1799) ejecta. Throughout, solar longitudes refer to equinox J2000.0.

We are very much obliged to all observers who took part in this challenge of collecting the largest dataset of a single return of a meteor shower for their efforts in the field and their quick submission of observational reports:

Oriol Abellán, Yuuko Abe, Jonay Abril Torres, Seishi Akagi, Doblado Alarcón, Per Aldrich, José Abargues Alemán, Nuria Álvarez Rodriguez, Rubén Amayra Pacho, Alexandre Amorim, Laura Ángel Martinez, M.M. Ángel Sánchez, Barbara von Arb, Rainer Arlt, Big-ching Au, A. Barbero Roca, Joaquín Barberá, Juan Manuel Barro Santos, Marc Baró, Rony Barry, Luc Bastiaens, Nadya Baskakova, Angel Bellido Sobradelo, Ana María Beltrán Primo, Aitor Benavent, M.C. Benzal Pintado, M. Bernáldez, Felix Bettonvil, Abhay Bharad, Mikhail Bidnichenko, Louis S. Binder, Nicolas Biver, Maria de Guia Blanco, Antonio José Blanquer Cabra, F. Blanco, Neil Bone, Sara Bordowitz, Mohamed Bouazzaqui Miguiz, Hans Buchholtz, Eisse Pieter Bus, Amparo Cabezuelo López, Francisco Campos, Luna Campos, Salvador Cambres Cañigal, Jesús Cano Anguita, José Miguel Cano Pestaña, Beatriz Carreño Martinez, Gil Carmona, Raúl Ceballos Corredera, Lizardo Cejas Cejas, Carlos M. Celestrin Campa, Jakub Cerny, Chu-lok Chan, David Chan, Luke Chidester, Yeon-jong Choi, Antonio Coelho, Paola Contreras Muñoz, Gerardo José Cordero Vaca, Silvia Cordero Álvarez, Stefano Crivello, David Cuenca, Chen-zhou Cui, Luís A. da Silva Machado, Luiz Augusto da Silva, Haakon Dahle, Luigi d'Argliano, Shivinand Darbastwar, Mark Davis, Marc de Lignie, Goedele Deconinck, Ana Lucía Delgado Díaz, Werner Depoorter, Jose G. de Souza Aguiar, Prasad Deshpande, Peter Detterline, Ajitha Devarajan, Bhushan Dholakia, Asdai Díaz Rodriguez, Fernández Diaz, Antonio Díaz Pulido, Hans-Günter Diederich, José Pascual Domínguez, Manuel Domínguez Palma, Guillermo Egea, Shlomi Eini, Albert Escoda, Bella Espinar Frias, Ángela Estévez Megias, Bert Everaert, Ricardo Fagundo Rivero, Yuwei Fan, Gregori Farras, David Barba Fernández, Juan F. Fernández Ocaña, L. Fernández, Raul Fernandez, Ricardo Fernandez, Sonia Fernández Fdez, N. Flores, Edesio Edson Fortes dos Santos, Keiiti Fukui, Nobuyuki Fukuda, Kai Gaarder, Ofer Gabzo, Marcin Gajos, Martin Galea, V. García, David García Pallás, José Alberto García Quesada, Juan Carlos García, Mariano García Vilchez, Kalpana Gawhane, Li Gen, Petros Georgopoulos, Jaroslav Gerboš, Nandkishare Gite, George W. Gliba, Orly Gnat, Shelagh Godwin, Amit Gokhale, Sagar Gokhale, Yeshodhan Gokhle, Alexandra Golova, Juanjo Gómez Masmano, Marta Gómez, Manuel Gómez, Durán González, Oswaldo Gonzalez, A. González, Juan González Gonzalez, M. González, Noelia Gorrín Marrero, Prerana Gore, Laura Granell, Lew Gramer, Vered Grindberg, Rocío Guerrero Quintero, Cobos Guillén, Alejandra Gutiérrez Martinez, Antonio Gutierrez Corrales, Rafael Haag, Pavol Habuda, Cathy Hall, Wayne T. Hally, Joost Hartman, Marek Harman, Takema Hashimoto, Saurabh Hatwar, Roberto Haver, Lars Trygve Heen, Natalie Henche Saxon, Carlos Heredero, S. Hernández, Saray Herrera Arteaga, Arno Hesse, A. Hess, Pierre S. Hilaire, Michaela Honkova, Kamil Hornoch, Dave Hostetter, José Luis Iglesias, Oomi Iiyama, Maria Isaeva, Emre Isik, Daiyu Ito, Kiyoshi Izumi, Helle Jaaniste, R. Jiménez Martinez, Carl Johannink, Bhargav Joshi, Miguel Ángel Juárez, Eva María Juvé, Kapil Kanole, Stanislav Kaniansky, Kenya Kawabata, Elena Kayankina, Peter Kayankin, Alexander Kichizhiev, Marina Kichizhieva, Mark Kidger, Atusi Kisanuki, Hitomi Kisanuki, André Knöfel, Wakaba Kobayashi, Radek Kodousek, Albert Kong, Matej Korec, Detlef Koschny, Ralf Koschack, Jakub Koukal, Gábor Kövágó, Lukas Kral, Anton Krupnov, Rhishikesh Kulkarni, Vineet Kulkarni, Maris Kuperjanov, Karimu Kuragaki, Jan Kyselý, Sylvio Lachmann, Francisco Lambíes Cusí, Marco Langbroek, Alberto Latini, Kai-nang Lau, Ana Lázaro Guerrero, Anne-Laure Lebacq, Ping-chung Lee, Adrian Lelyen, Anna S. Levina, Robert Leyland, Qing Liang, Mihir Limaye, Michael Linnolt, Angel Rafael Lopez Sanchez, Armentario López Castillo, M. López, Javier López Valenciano, Juan Manuel López Álvarez, M. Ángeles López Ruiz, Sonia López, Yeray Lopez Delgado, Vladimir Lukić, Robert Lunsford, Hartwig Lüthen, Oisin MacConamhna, Kouji Maeda, Katuhiko Mameta, José Maria Martínez, José Alfonso dos Reis Martins, Nayade Martínez Molina, JM Marínez Nuñez, Pierre Martin, Rafael Carlos Martínez, C. Martínez Conesa, Fernando Martínez Ruiz, Antonio Martinez, José Luis Marínez, L. Martín, J.M. Martinez Núñez, Tony Markham, Jan Masiar, Joana Mateo Ruiz, Ketaki Matkar, Robert McNaught, Alastair McBeath, Ángeles Méndez García, Nahum Mendez Chazarra, Irene Merayo, Markko Meriniit, Marina Michailova, Alex Mikishev, Pavel Mikulka, Arjona Miranda, Koen Miskotte, Hidekatu Mizoguchi, Sui Mo, Amruta Modani, Macarena Molina de Armas, Sirko Molau, Marcelo Montagna, Soria Montesinos, Daniel Morales, José Morales Maestro, JM Morano, Judit Moreno, Leticia Mora, Moscoso Morillo, P. Morocho, Rafael Moreno Jiménez, Rivas Morán, Sergio Moreno Martínez, Francisco Munoz, María Elen Nájar, Francisco Naranjo, Sven Näther, Iván Navarro Martínez, JA Navarro Garay, Ilia Nazvanov, Marc Neijts, Jonathon Newton, John Newton, Delfi-Isabel Nieto Isabel, Pedro Nieto Martínez, A Nieto Martínez, Prakash Nitsure, Masahiko Ooba, Mohammad Odeh, Eran Ofek, Hiroshi Ogawa, Hiroyuki Okayasu, Masayuki Oka, Dragana Okolić, José Ortega, Kazuhiro Osada, Alexei Pace, Sachin Pansare, Arvind Paranjpye, Carlos Parra, Miguel Ángel Parrado Flores, JM. Pastor Hernández, Mukesh Pathak, José Vicente Pedrón Jiménez, Cedric Peinado, Ketan Pendse, Ruth Peñate Pacheco, Trevor Pendleton, Alfredo Pereira, Nataly Pershina, Silvia Pérez

Limiñana, Suyin Perret-Gentil, Alejandro Piedrabuena Delgado, Roman Pifl, Carles Pineda Ferré, Nikolay Pit, Dulce Plasencia, Isaac Plané, Granados Porras, Roberto Porcel, Fabricio Prieto Santos, Dmitry Pryadunenko, Tushar Purohit, Rui Qi, Francisca Quetglas, Roberto Carlos Ramos, E.S. Rangarajan, Pavol Rapavy, Simona Rapava, Ashutosh Rathor, Ina Rendtel, Jürgen Rendtel, Klar Gilberto Renner, Jacobo Requena Laborda, Francisco Reyes Andrés, Ian Rigney, Mayra Del Rio, Sabrina Rodríguez, Sergio Rodríguez, Paul Roggemans, Presentación Ros, Marion Rudolph, Jelyl Rufat, Antonio José Ruiz López, Roberto Carlos Ruiz Villena, Victor Ruiz Ruiz, Francisco Sáez, William Sager, Timur Sahýn, Chaitanya Salgarkar, L. Sánchez Garcia, Javier Sanchez, Nicolás Santiago Medina, Raul Santos Salcedo, Anastasia Satanova, Rocío Saucedo Núñez, Robin Scagell, Igor Schedrov, Olga Schedrova, René Scurbecq, Miguel Serra Martin, Shashank Shalgar, K. Shivasankar, Brian Shulist, Yi Shum, Anastasia Sierra Aguilar, Hiroyuki Sioi, Andrzej Skoczewski, Aaron Sluder, Kiko Soares, Milos Sochan, Mateo Soldado Sánchez, Manuel Solano Ruiz, Paqui Soriano García, George Spalding, Ulrich Sperberg, Jan Stancel, Michal Stancel, Umberto Mule Stagno, Kazuhiro Sumie, David Swann, Lai-chun Tai, Richard Taibi, Syoiti Tanaka, Honglin Tao, Khaled Tell, Manuel Tello Abolafia, Kazumi Terakubo, Neelima Thatte, Yasuhiro Tonomura, Rafael De Torres Carpio, Manuela Trenn, Josep M. Trigo Rodriguez, Satosi Uehara, Elena Valero Rodriguez, Javier Valero Rufino, José Alberto Valenciano Jiménez, Juan Valiente Soriano, Manuel Ángel Valadez López, Erwin van Ballegoy, Hendrik Vandenbruaene, Koen van Gorp, Markku Vanamo, Raúl Vázquez, I. Vega, Jose Miguel Velasco Fuentes, Cis Verbeeck, Jan Verbert, Rita Verhoef, Craig Anthony Vincent, Mark Vints, Catarina Vitorino, Helio Vital, Alenxander Voetskiy, Jan Wagner, Di Wang, Milos Weber, Thomas Weiland, Francisca Werner Marín, Margareta Westlund, Barbara Wilson, Jean-Marc Wislez, Guang-jie Wu, Dan Xia, Zhou Xingming, Masayuki Yamamoto, Kim S. Youmans, Maria Cruz Zafra, Petr Zajicek, Joseph Zammit, Eva Zapletalova, Michal Zapletal, George Zay, Ju Zhao, Jin Zhu, and Xiaojin Zhu,

who are from the following countries and regions:

Australia, Austria, Belgium, Brazil, Bulgaria, Canada, China, Cuba, Czech Republic, Denmark, Estonia, Finland, France, Germany, Greece, Hong Kong, Hungary, India, Ireland, Israel, Italy, Japan, Jordan, Korea, Malta, the Netherlands, Norway, Poland, Portugal, Slovakia, Spain, Switzerland, Turkey, United Kingdom, Ukraine, United States, Venezuela, and Yugoslavia.

As observations are still coming in, and since the amount of data is enormous, it may well be that one or another contribution has not been included yet in the following analysis. We will work hard on completing the data set and present a more in-depth analysis based on all the observational material in the course of the next year.

2. The population index problem

Usually, before going into the details of an activity profile of a meteor shower, we need information about the population index r versus time in order to correct visual counts for the sky conditions. The 1999 Leonids challenge us with unusual magnitude distributions. Two methods of population index determination, the regression line method and the conversion of an average magnitude distance from the limiting magnitude, yields completely different results. The first one obtains the population index from the slope of a best-fit regression line through the logarithmic true meteor numbers, i.e., the observed numbers extrapolated by perception probabilities [6]. The second method makes use of the uniqueness of the dependence of r on the mean magnitude *distance* from the limiting magnitude [7]. (Note that the mean magnitude alone does not deliver a unique r, because it is strongly affected by the sky conditions.)

The first method—applying a certain range of magnitudes of the distributions—gives a more or less constant population index of roughly $r \approx 2.3$ for the peak period between $\lambda_\odot = 235\overset{\circ}{.}2$ and $\lambda_\odot = 235\overset{\circ}{.}4$, whereas the second method—applying all meteors of the magnitude distribution—gives a sharp r-peak up to $r \approx 2.7$ near $\lambda_\odot = 235\overset{\circ}{.}29$ and values of 2.0 to 2.3 for the adjacent times. Both methods rely on an exponential distribution of the true number of meteors versus the magnitude. The discrepancy thus indicates a non-exponential distribution of true meteor numbers. A similar behavior was witnessed on November 16, 1998. We give a near-peak profile of the population index in Figure 1 obtained by the regression-line method over the magnitude range -1 to $+3$.

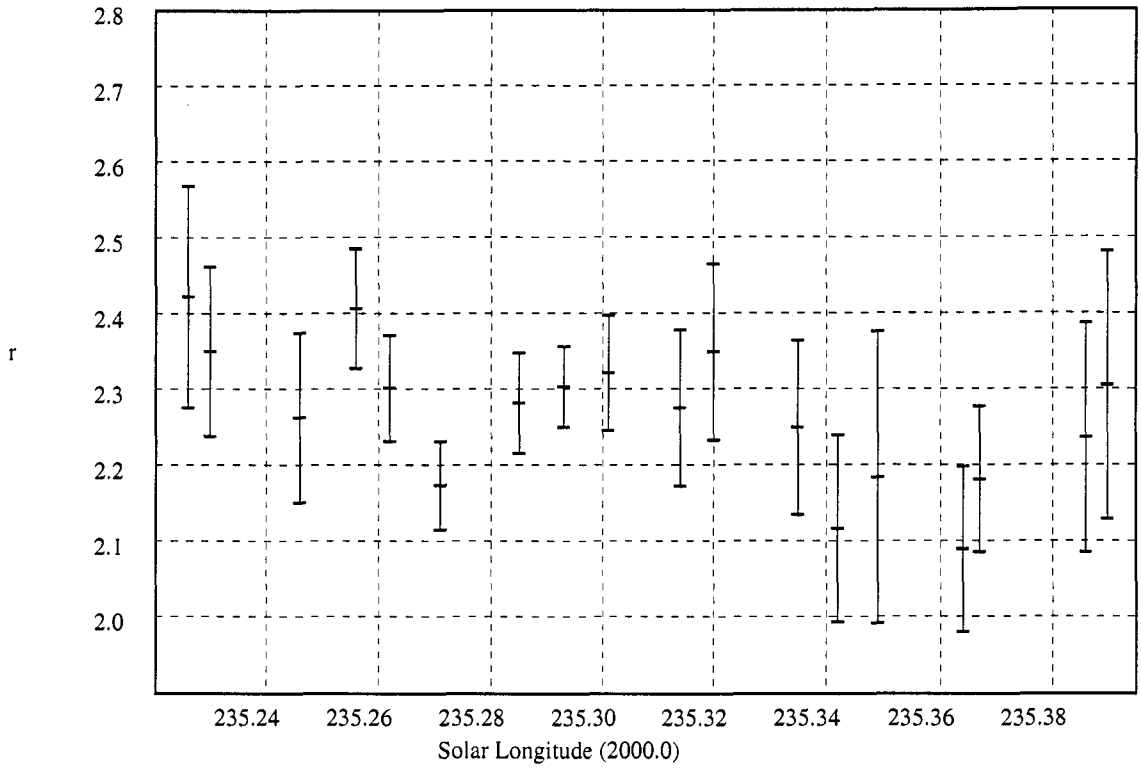

Figure 1 – Population index profile of the 1999 Leonid meteor shower peak as derived by the regression line method in the magnitude range −1 to +3. The individual r-values were averaged in bins of width 0°.02 in solar longitude, shifted by 0°.01; the mean is plotted at the average solar longitude in each bin. The error bars represent the standard deviation of the values contributing to the average.

Due to their very high geocentric velocity of 71 km/s, Leonid meteoroids as small as about 10^{-5} g are able to produce visual meteors. The distribution of true meteor numbers indeed starts to lack meteors of magnitude +4 and fainter, although the observers had the impression of an abundance of faint meteors. This impression may be subjective, however: on the one hand, due to the large total number of meteors, the number of faint ones was large, too; on the other hand, the observers noticed an obvious *lack of bright meteors*, a phenomenon many may have described *erroneously* as an *abundance of faint meteors*. Figure 2 shows the magnitude distribution of the true meteor numbers showing *both* phenomena, the lack of very faint *and* the lack of very bright meteors. The under-representation of meteors for magnitude +4 and fainter is similar to that found from video records as reported in [8]. The solid line is the total of true magnitude distributions for $\lambda_\odot = 235°.20$–$235°.30$; the dotted line refers to $\lambda_\odot = 235°.30$–$235°.40$. The deficiencies are more prominent before and during the peak than afterwards.

In view of these problems, we will adopt a population index of $r = 2.3$ for the computation of the ZHR profile and restrict the analysis to observations with limiting magnitudes between +6.0 and +7.0 to avoid large extrapolations. Even if the population index is uncertain by ±0.5, the errors introduced by the limiting magnitudes most different from +6.5 are roughly 10%. In any case, we note that the average of the individual ZHR values will be a close measure of the true activity, the large number of observations ensuring that over- and underestimated ZHRs compensate each other.

3. High-resolution activity

The great number of reports submitted to the *Visual Meteor Database* (*VMDB*) and their detailedness allow a the computation of a ZHR graph with a very fine resolution down to the order of minutes.

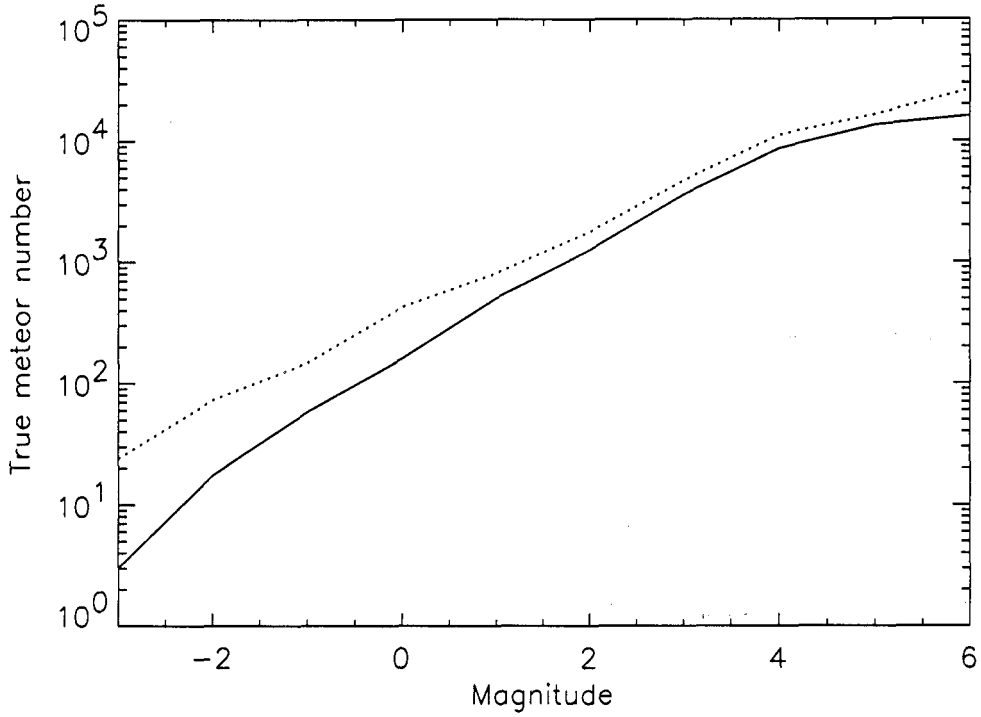

Figure 2 – Distribution of true meteor numbers corrected for perception probabilities versus magnitude for 20 experienced observers in logarithmic scale. A straight line would indicate an exponential distribution, whence the existence of a population index. The solid line refers to the period $\lambda_\odot = 235°.2$–$235°.3$; the dotted line to the period $\lambda_\odot = 235°.3$–$235°.4$.

The actual storm component in the Leonid stream is supposed to form a sheet-like structure extending approximately in the Comet's orbital plane. Since we are dealing with a temporal resolution smaller than the crossing time of the globe through this stream filament, we have to account for the actual geographic position of the observer, in order to preserve the features of the stream in the activity graph. The time shifts are called *topocentric correction*, and are described in [10]. They express the correction toward the stream encounter by the center of the Earth.

To compute this topocentric correction, each geographic position plus time is transformed into ecliptical coordinates, and the spatial offset to the direction of the center of the Earth is computed. This offset converts to a time shift given the crossing speed of the Earth through the stream.

As we encounter the stream at its descending node, the particles, which meet the Earth almost head-on, move from north to south through the ecliptic plane. Roughly speaking, southern latitudes therefore see the storm first, northern latitudes see the storm delayed. South Africa encounters the densest part 11 minutes earlier than the center of the Earth, whereas northern Scandinavia sees the peak 17.5 minutes later—6.5 minutes after topocentric encounter.

The profile near the maximum is shown in Figure 3 with a point-to-point distance of $0°.001$ in solar longitude, corresponding to 1.4 minutes. The actual binning, however, is twice as large, whence 2.8 minutes. Only observing intervals shorter than 2.8 minutes are included in each average. All activity error bars are $\mathrm{ZHR}/\sqrt{n_{\mathrm{tot}}}$, where n_{tot} is the number of Leonids involved in the average. We did not apply perception coefficients which account for personal systematic deviations of observers, since the enormous number of people ensures a reliable average. The number of individual observing intervals in each average of Figure 3 varies between 40 and 60 during the peak hours.

From Figure 3, we read the peak time as $\lambda_\odot = 235°.285 \pm 0°.001$, corresponding to November 18, 1999, $2^{\mathrm{h}}02^{\mathrm{m}} \pm 2^{\mathrm{m}}$ UT. The maximum equivalent ZHR was 3700 ± 100.

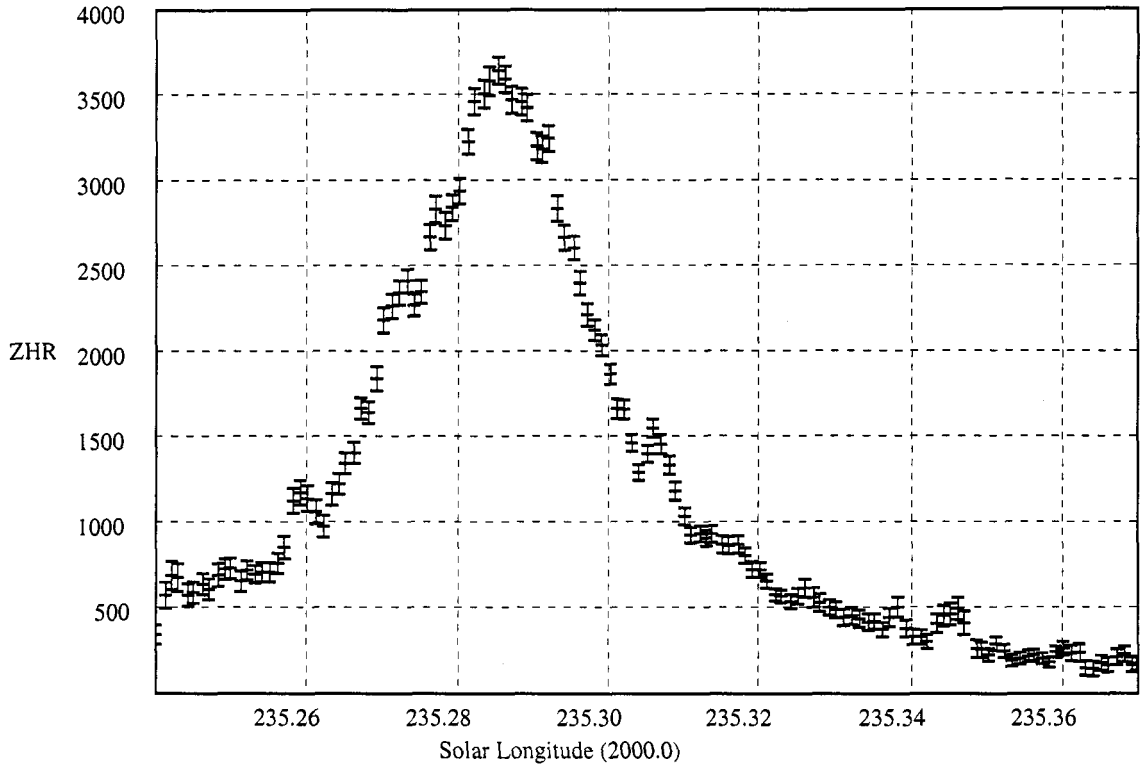

Figure 3 – ZHR-profile of the 1999 Leonid meteor storm. The time shift towards topocentric stream encounter was applied for each observing period according to [10]. Only observations with limiting magnitudes between +6.0 and +7.0 were chosen, since the derivation of a population index turned out to be almost impossible. Error bars represent $\mathrm{ZHR}/\sqrt{n_{\mathrm{tot}}}$, with n_{tot} the total number of Leonids.

Apart from the main maximum of the meteor storm shown in Figure 3, we can detect several small-scale features in the graph. Additional clear enhancements are found at $\lambda_\odot = 235\overset{\circ}{.}259$ ($1^{\mathrm{h}}25^{\mathrm{m}}$ UT), $\lambda_\odot = 235\overset{\circ}{.}272$ ($1^{\mathrm{h}}43^{\mathrm{m}}$ UT), $\lambda_\odot = 235\overset{\circ}{.}277$ ($1^{\mathrm{h}}50^{\mathrm{m}}$ UT), $\lambda_\odot = 235\overset{\circ}{.}307$ ($2^{\mathrm{h}}33^{\mathrm{m}}$ UT), $\lambda_\odot = 235\overset{\circ}{.}338$ ($3^{\mathrm{h}}17^{\mathrm{m}}$ UT), and $\lambda_\odot = 235\overset{\circ}{.}346$ ($3^{\mathrm{h}}29^{\mathrm{m}}$ UT). When grouping only locally close observing sites into "regional" profiles, these features are present in most of them. Consideration of the error bars suggests that such peaks are statistically significant with enhancements of equivalent rates of 100–300 meteors per hour above the general storm component and durations of 5 to 7 minutes. The maxima at $\lambda_\odot = 235\overset{\circ}{.}272$ and $235\overset{\circ}{.}277$ are most likely associated with the 2- and 3-revolutions-old trails, respectively, as suggested in [3], but the origin of the other, not less significant peaks remains unknown.

The full width at half maximum of the peak profile in Figure 3 is $0\overset{\circ}{.}030$ in solar longitude, or 45 minutes. This time converts to a traveling distance of the Earth of nearly 80 000 km. The extent at half number density of the storm component perpendicularly to its orbital plane is thus about 23 000 km. This value is in excellent agreement with the sizes of the trails discovered by the IRAS satellite in the wake of short-period comets at heliocentric distances of 1 AU. The Leonid ZHR was above 100 for $0\overset{\circ}{.}23$ in solar longitude, corresponding to 5.5 hours. This period is quite precisely centered on the peak time (off by only 15 minutes).

A closer look into local ZHR profiles appear to reveal structures which were not present at each site. Three examples of profiles have been compiled, grouping locations in the Near East (776 intervals with 19 089 Leonids), southern France (1110 intervals with 18 190 Leonids), and southern Spain (622 intervals with 11 116 Leonids). These examples are shown in Figure 4 with a temporal resolution of five minutes for the French and Spanish graph, and three minutes for the Near-East graph, indicating that clear differences in the structure of the profiles exist. We did not apply the time shift for topocentric stream encounter in this graph in order to preserve the original activity information provided by the observational reports.

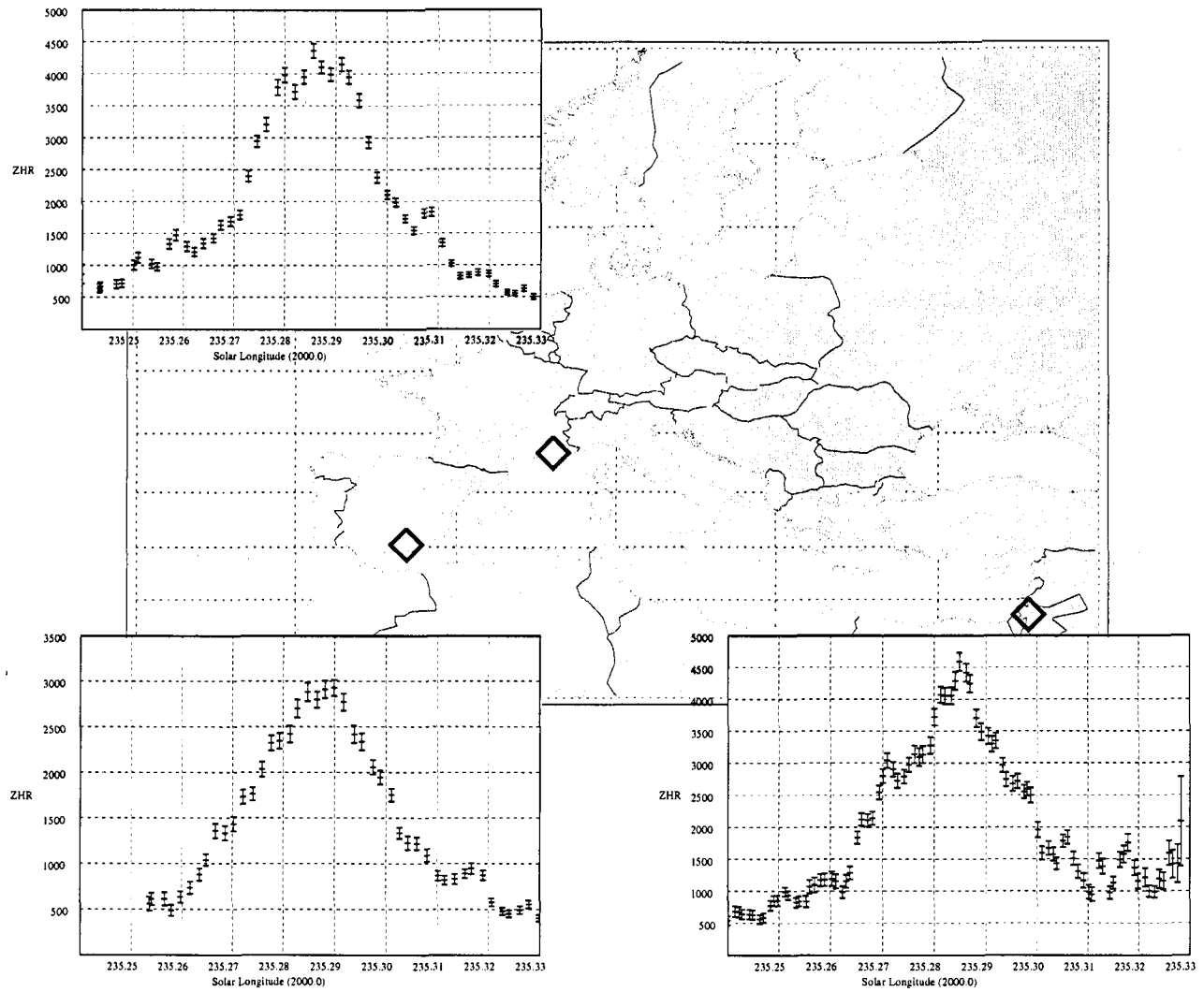

Figure 4 – ZHR profiles of peak period observer groups at different locations. The upper panel includes all observations from southern France, the lower left panel those of southern Spain, and the right panel contains all observations reported from Jordan and Israel. Again, error bars represent $\mathrm{ZHR}/\sqrt{n_{\mathrm{tot}}}$. No topocentric correction was applied to these local profiles to preserve the original results. The topocentric shifts for comparison with Figure 3 would be −1 minute (−0.°0007), −2 minutes (−0.°0014), and +0.5 minutes (+0.°0003) for southern Spain, southern France, and the Near East, respectively. Only observing intervals with limiting magnitudes between 6.2 to +6.8 are included to avoid erroneous corrections due to the non-exponential magnitude distributions.

The peak time of the Spanish and the Near-East graphs differ by over 5 minutes, which is much more than the 1.5 minutes stream encounter difference expressed by topocentric correction as given in [10]. The peak time of the French graph coincides with the Near East within the resolution of the graphs, the encounter time difference being 2.5 minutes corresponding to nearly 0.°002 in solar longitude.

By contrast, however, a broad activity plateau of about 20 minutes duration—in a higher-resolution graph even a triple peak—is found for the observers in southern France. The strong scatter in ZHRs and the larger error bars in the Near-East graph indicate dawn interference; in contrast, the western European graphs suffer from low radiant altitudes before $\lambda_{\odot} = 235.°26$.

The features of Figure 4 suggest that the activity also depends on the observer's geographical longitude and may provide valuable information on the structure of the dust trails parallel to the orbital plane. The wealth of data contained in these profiles means that a three-dimensional tomography of the dust trails may be attempted in the future by combining the regional activity curves.

A first attempt to derive the physical flux density of particles caught by the Earth delivers a peak value of 1.4 ± 0.3 particles causing meteors brighter than magnitude +6.5 per square kilometer and per hour. This flux density corresponds to a number density of 5400 ± 1200 particles per 10^9 cubic kilometers. The number density of particles with masses exceeding 1 mg is 230 ± 50 per 10^9 cubic kilometers at their peak. About 30 particles of 10 mg or more can be found within this volume. In contrast, 3800 particles of 10 mg or more were contained in 10^9 cubic kilometer during the Draconid outburst of early October 1998. The much higher velocity of the Leonids has two effects: (*i*) almost four times as many particles per time unit are caught by the Earth at the same number density, and, much more important, (*ii*) the high velocity causes much smaller, whence many more particles, to light up in the visual magnitude range. A Leonid particle of 10 mg produces a meteor of about magnitude 0, whereas the same particle in the Draconid stream can only produce a magnitude +6 meteor—so, we see only the biggest particles in the latter. Referring to absolute mass ranges, the spatial number density of particles found when crossing the Draconid stream is 100 times higher than at the Leonid encounter, although the peak ZHR was five times lower.

4. Late activity maximum

A significant activity peak was indeed observed close to the time predicted in [5]. East-Asian observers witnessed an outburst at $\lambda_\odot = 235\overset{\circ}{.}87 \pm 0\overset{\circ}{.}04$ (November 18, $16^h \pm 1^h$ UT) with peak ZHRs at about 180 ± 20. The actual peak value in Figure 5 comprises only six individual observing periods. A more certain value for the maximum ZHR is subject to a full analysis once all data have been utilized. When subtracting a background profile decreasing from ZHR = 55 at $\lambda_\odot = 235\overset{\circ}{.}6$ to ZHR = 30 at $\lambda_\odot = 236\overset{\circ}{.}4$, we get a full width at half maximum of $0\overset{\circ}{.}28$ in solar longitude, corresponding to 4.3 hours.

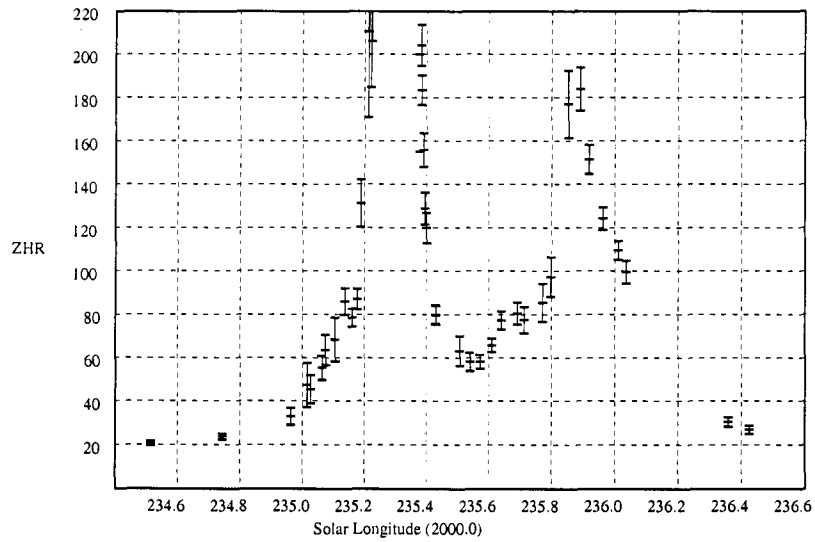

Figure 5 – ZHR-profile of the Leonids excluding their maximum.

5. Modeling of the 1999 Leonids

To attempt to reproduce the observed activity profile, the same modeling procedure used in [9] was applied to the 1999 return. The main storm profile was made up of ejecta from 1899 and 1932 only—it is possible to basically match the ZHR profile using these two ejections alone—no other epoch contributes significantly. Note that we were not able to match the observed profile using either 1899 or 1932 alone—both returns appear to have significantly contributed to the activity in 1999, within the limitations of our modeling. The ejection velocities and locations from both 1899 and 1932 epochs which resulted in Leonids close to Earth in 1999 are shown in Figure 6. All test particles within 0.002 AU of Earth's orbit (as in [9]) and one degree in mean anomaly about the nodal passage time of Earth through the stream are included.

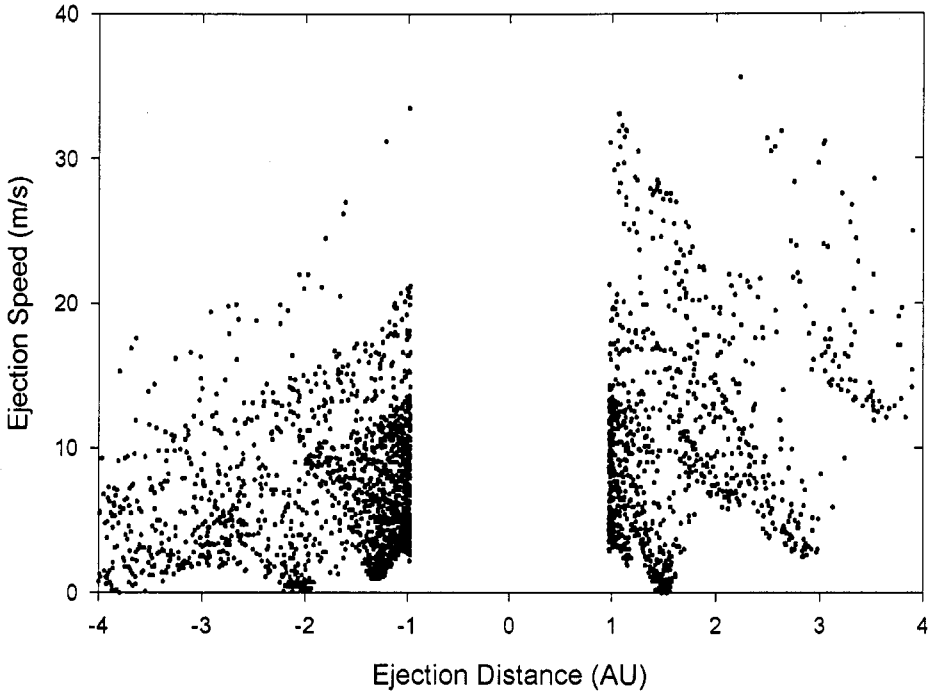

Figure 6 – Distribution of ejection velocities depending on the Comet's distance from the Sun. Negative numbers mean pre-perihelion distances. Distances closer than the perihelion distance cause the white area in the middle.

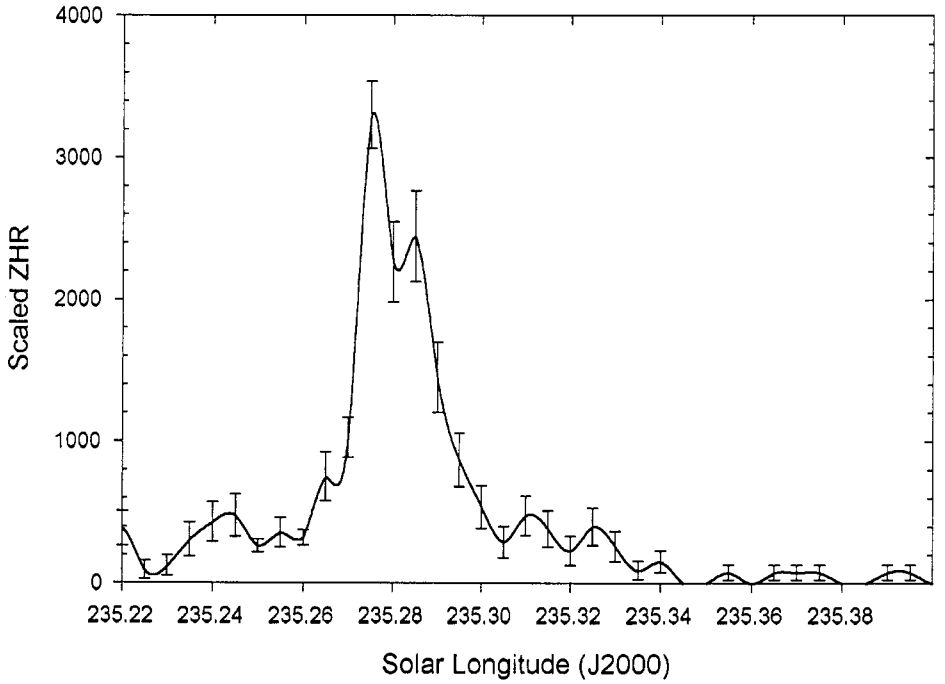

Figure 7 – Modeled ZHR profile consisting of 1899 and 1932 ejecta.

The resulting synthetic ZHR profile is found by scaling the relative activity to the observed peak ZHR in bins of $0^{\circ}.005$ width in solar longitude, and is shown in Figure 7. To find the relative activity from the total number of test particles accepted in each solar longitude bin, a cometary weighting exponent of 1.7 was used, as was found for Comet Halley's coma (which, for a young storm/shower, should be most appropriate—cf. [11]). The shape of the profile in this instance is relatively insensitive to the choice of the weighting exponent. We note that the model overestimates the ZHR near the early peak (due to 1932 ejecta), underestimates at the observed time of the peak, while the width of the total profile is narrower in the modeling than

is observed. As we have made a deliberate choice in the distribution of initial ejection velocities (we found that a good fit in terms of the observed profile width and timing can be obtained from a distributed coma production model using a meteoroid density of 0.8 g/cm^3—see [12] for more details), one could easily make a better fit simply by using a population with slightly larger average ejection velocities than is shown in Figure 6.

Ideally, model results which are independent of an assumed initial ejection velocity distribution could best define the delivery efficiency of material for a given ratio β and ejection velocity from 1899 and 1932. Indeed, by forcing the simulated profile to match the observed profile, it may be possible to invert results of such a simulation to obtain directly an estimate of the ejection velocities/locations which might have produced the 1999 storm, a procedure currently being examined.

Postscript: Possible lunar impacts from Leonid meteoroids

Several dedicated observers have reported possible lunar impacts caused by Leonid meteoroids (cf. the letter of Roger Venable elsewhere in this issue). Dunham [13,14] reports 6 confirmed possible impact events, mostly near the center of the Moon's dark limb. The events were registered by at least two observers and recorded on video. The 6 events occurred between 3^h05^m and 5^h16^m UT and reached magnitudes as estimated from the video frames between +3 and +7. There is still ongoing discussion on the likely sizes and masses of the meteoroids having caused these events, but it seems unlikely that they produced craters visible from Earth. Notice the discrepancy between the times of the events reported by Venable and the events reported by Dunham; there need not be a contradiction between both, however, as Venable ceased observing before the occurrence of the first event reported by Dunham. More information on the events reported by Dunham, as well as video images, can be found at `http://iota.jhuapl.edu`.

Interestingly, Asher [14] calculated that the minimal distance between the Moon and the core of the 3-revolutions-old (1899) trail was +0.0002 AU (outside the trail's orbit), compared to −0.0064 AU for the Earth (inside the trail's orbit). This makes the encounter geometry for the Moon quite comparable with that for the Earth during the 1833 and 1966 storms! Therefore, the Moon experienced a substantially higher Leonid flux than the Earth in 1999. According to Asher, the Moon's closest approach to the core of the 3-revolutions-old trail occurred 161 minutes after the Earth's closest approach. Adding this to the peak time obtained from this analysis yields November 18, 4^h43^m UT, as the time of peak encounter for the Moon.

References

[1] E.D. Kondrat'eva, E.A. Reznikov, "Comet Tempel-Tuttle and the Leonid Meteor Swarm.", *Sol. Syst. Res.rm 19*, 1985, pp. 96–101.

[2] D. Asher, "The Leonid Meteor Storms of 1833 and 1966", *Mon. Not. R. Astr. Soc.* 307, 1999, pp. 919–924.

[3] R.H. McNaught, D.J. Asher, "Leonid Dust Trails and Meteor Storms", *WGN* 27, 1999, pp. 85–102.

[4] P. Brown, "Evolution of Two Periodic Meteoroid Streams: The Perseids and Leonids", Ph. D. Thesis, Univ. of Western Ontario, London, Ont., 1999, pp. 171–258.

[5] V. Emel'yanenko, *personal communications*, November 1999.

[6] R. Koschack, J. Rendtel, "Determination of Spatial Number Density and Mass Index from Visual Meteor Observations (II)", *WGN* 18, 1990, pp. 119–140.

[7] R. Arlt, "Global Analysis of the 1998 Perseid Meteor Shower", *WGN* 27, 1999, pp. 237–249.

[8] S. Molau, J. Rendtel, M. Nitschke, "First Results of Video Observations during the 1999 Leonid Storm", *WGN* 27, 1999, pp. 296–300.

[9] R. Arlt, P. Brown, "Bulletin 14 of the International Leonid Watch: Final Results of the 1998 Leonid Meteor Shower", *WGN* 27, 1999, pp. 267–285.

[10] R.H. McNaught, D.J. Asher, "Variation of Leonid Maximum Times with Location of Observer", *Meteorit. Planet. Sci.* 34, 1999, pp. 975–978.

[11] P. Brown, J. Jones, "Simulation of the Formation and Evolution of the Perseid Meteoroid Stream", *Icarus* 133, 1998, pp. 36–68.

[12] J.A.M. McDonnell, G.C. Evans, S.T. Evans, W.M. Alexander, W.M. Burton, J.G. Firth, E. Bussoletti, R.J.L. Grard, M.S. Hanner, Z. Sekanina, "The Dust Distribution within the Inner Coma of Comet P/Halley 1982 *i*–Encounter by Giotto's Impact Detectors", *Astron. Astrophys.* 187, 1987, pp. 719–741.

[13] *IAU Circular* 7320, November 26, 1999.

[14] D. Dunham, *electronic communication* through various mailing lists, December 1999.

[15] D. Asher, *personal communications*, December 13, 1999.

First Results of Video Observations During the 1999 Leonid Storm

Sirko Molau, Jürgen Rendtel, and Mirko Nitschke

A preliminary analysis of meteors recorded during the 1999 Leonid meteor storm by three different intensified video cameras is presented. Two of these were located in southern Spain, the third operated from Tenerife. The radiant as derived from a period of 4 hours around the peak period is $\alpha = 153\overset{\circ}{.}6 \pm 0\overset{\circ}{.}1$ and $\delta = +21\overset{\circ}{.}9 \pm 0\overset{\circ}{.}1$ (at $\lambda_\odot = 235\overset{\circ}{.}29$, eq. J2000.0). The population index decreases from $r \approx 3.0$ for meteors of magnitudes 0 to +2 to $r \leq 2.0$ for Leonids of magnitude about +3. We find a turning point in the magnitude distribution, indicating that Leonids fainter than +5 were less abundant. The activity shows fluctuations based on three-minute count intervals with the most prominent peaks at 1^h58^m and 2^h11^m UT.

1. Introduction and equipment

The 1999 Leonids were eagerly awaited because recent model calculations (e.g., [1,2]) indicated a sharp and high activity peak on November 18, close to 2^h UT. Almost all of Europe as well as the Middle East and large parts of Africa were the optimal observing regions. Unreliable weather conditions in central Europe forced observers of the German *Arbeitskreis Meteore* (*AKM*) to choose more southern locations, namely the Canary Islands (although quite far west for the predicted storm time) and southern Spain.

Two intensified video cameras were operated by Sirko Molau and Jürgen Rendtel near Alfarnatejo, north of Malaga, ($\lambda = 4°20'$ W, $\varphi = 36°57'$ N), and another one by Mirko Nitschke near Vilaflor on Tenerife ($\lambda = 16°40'$ W, $\varphi = 28°12'$ N). A summary image obtained from one of the cameras is shown in Figure 1. The parameters of the video systems are given in Table 1.

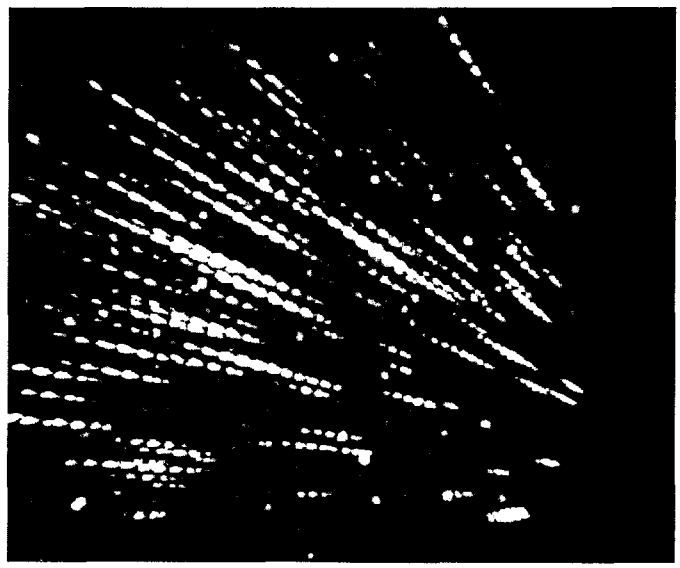

Figure 1 – Leonids recorded with the intensified video meteor camera CARMEN on November 18, 1999, between 1^h44^m and 2^m15^m UT.

Table 1 – Parameters of intensified video cameras operated by *AKM* members during the 1999 Leonid storm. The given limiting magnitude refers to stars.

Camera	Operator	Lens	Field	Lm	Location
AVIS	Sirko Molau	$f/1.5$, $f = 100$ mm	15°	+9	Alfarnatejo
CARMEN	Jürgen Rendtel	$f/1.8$, $f = 28$ mm	35°	+6	Alfarnatejo
VK-1	Mirko Nitschke	$f/0.75$, $f = 50$ mm	20°	+8	Vilaflor

The field centers of AVIS and CARMEN were identical, so that we recorded the same area with different limiting magnitudes. The idea was to derive data about stream particles in different mass ranges obtained under identical conditions. The third camera was operated separately with the field center adjusted in such a way that the Leonid trails were orthogonal to the trails recorded by the first two cameras. This yielded a better spatial distribution for radiant analyses.

All data were recorded on VHS tape and analyzed with the METREC software [3,4], which allowed a very efficient and fast access to the meteor data.

2. Radiant position

Single-station meteor trails and their angular velocities obtained with good accuracy make it possible to determine the precise radiant position of a given meteor shower. We made use of 633 meteor trails recorded by the three cameras. As mentioned before, the trails are well-distributed around the radiant, so that there is only little bias to one particular direction. The Leonid plot obtained with the software RADIANT [5] and shown in Figure 2 reveals a pin-point radiant at $\alpha = 153^\circ.6 \pm 0^\circ.1$ and $\delta = +21^\circ.9 \pm 0^\circ.1$ (at solar longitude $\lambda_\odot = 235^\circ.29$; eq. J2000.0).

This radiant differs by $0^\circ.3$, mainly in right ascension, from the position given by Ueda and Fujiwara [6], and by $0^\circ.4$, mainly in declination, from the position given by Suzuki et al. [7]. Further investigations may point out whether there is a difference between this radiant of the storm component and the regular background Leonids, or between the meteoroids produced by different returns of the parent comet, 55P/Tempel-Tuttle.

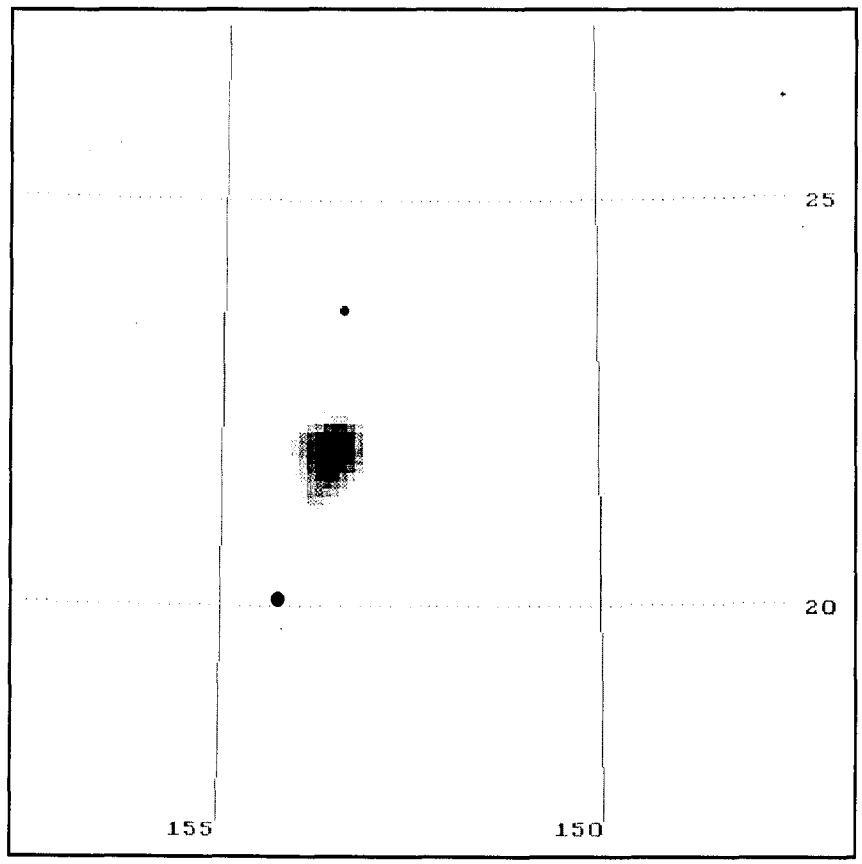

Figure 2 – Radiant plot calculated from 633 single-station video meteors observed between 0^h00^m and 4^h00^m UT on November 18, 1999. The stars above and below the radiant are ζ and γ Leonis, respectively.

3. Magnitude data

Determination of magnitudes from intensified video camera images is still not satisfactory solved. Meteors brighter than about 5 magnitudes above the limiting magnitude show severe saturation on the video recordings. Furthermore, the cameras have a high sensitivity in the near-infrared region [8], which makes their recordings difficult to compare with visual data. Detailed investigations are under processing in the *AKM*. Here, we refer to preliminary data of the two video cameras operated at the Alfarnatejo site, observing the same field centered at 54° azimuth and 43° elevation. Hence, the meteoroids of our sample enter the Earth's atmosphere under comparable conditions (speed, angle), minimizing possible systematic errors.

The field of view of CARMEN was about 5.5 times as large as the field of view of AVIS. On the other hand, its limiting magnitude was about 3 magnitudes brighter. Given a conservative low estimate of $r = 2.0$ for the population index of the Leonids at maximum, one would expect that AVIS recorded $(2^3)/5.5 \approx 1.5$ times as many Leonids as CARMEN. On the contrary, however, CARMEN recorded more than twice as many Leonids than AVIS between 1^h00^m and 3^h00^m UT:

- AVIS (field of view of 15°, lm = +9): 165 Leonids; and
- CARMEN (field of view of 35°, lm = +6): 393 Leonids.

The difference becomes even more prominent if we consider only meteors whose beginning (124 versus 373 Leonids) or end point (89 versus 325 Leonids) was inside the field of view of the camera.

On the other hand, AVIS recorded about five times as many non-Leonid meteors as CARMEN (90 versus 19), which is in very good agreement with an average value of $r = 3.0$ for those. Figure 3 shows the preliminary brightness distributions of the video meteors. In contrast to visual observers, the detection probability of video systems is almost 1 to about 3 magnitudes above the limiting magnitude. Hence, the meteor counts are almost complete for meteors up to magnitude +6 (AVIS) and +3 (CARMEN), respectively.

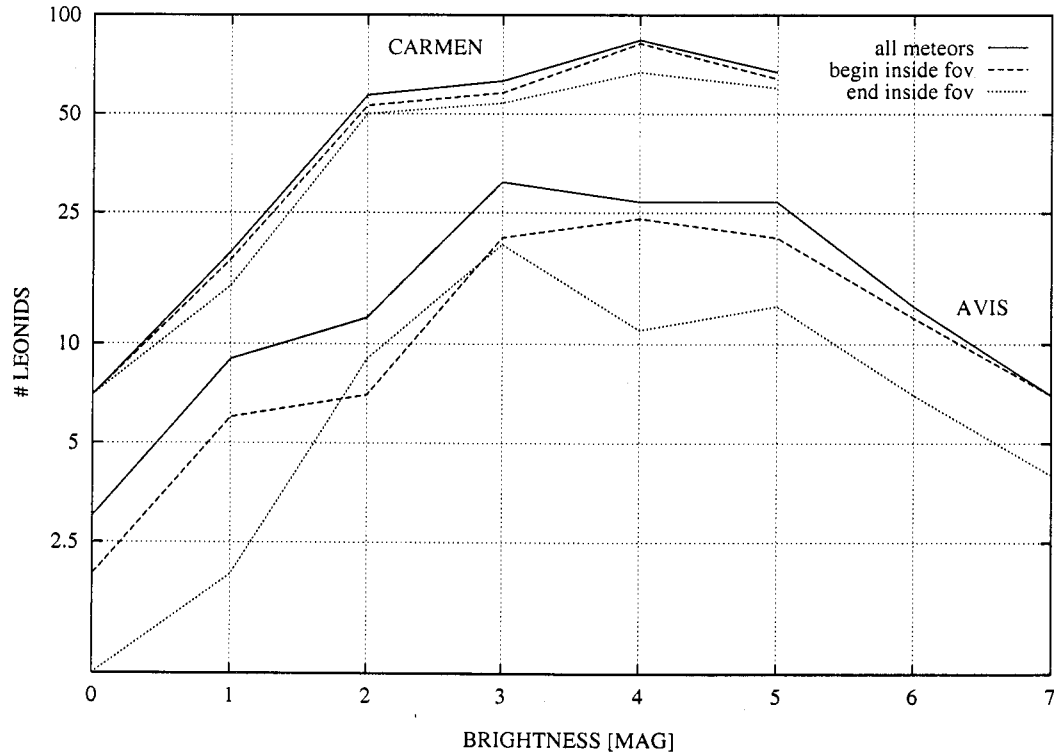

Figure 3 – Brightness distribution of video meteors observed with AVIS (lower lines) and CARMEN (upper lines) between 1^h00^m and 3^h00^m UT. The number of Leonids is decreasing significantly towards fainter magnitudes.

The derived population index is near $r = 3.0$ for bright Leonids (magnitudes 0 to +2), and decreases to values below 2.0 for Leonids around magnitude +3. Clearly, the magnitude distribution shows a turning point: the number of meteors fainter than about magnitude +5 is decreasing. The conventional population index r becomes meaningless in this situation. Our data indicate that smaller Leonid meteoroids are less abundant, and it is subject of investigation whether there is a lower mass limit for visible (luminous) Leonids.

4. Leonid activity

During the observations, it became immediately obvious that the time of the storm was very close to the predicted moment. Of course, the succession of meteors did not happen uniformly, i.e., there were instances with several meteors at the same time, as well as short pauses without meteors. Such fluctuations are expected from a Poisson distribution of randomly distributed particles and were observed in previous meteor storms and also during "normal" major-shower activity peaks. Besides these statistical fluctuations, we looked for variations at a 3-minute-scale, which may indicate fine structures within the particle stream. When data from other video systems become available, shorter time intervals may be chosen. Our video results can be compared with results from visual data as well.

Figure 4 shows the details of the Leonid counts per minute, averaged in sliding 3-minute intervals. Due to the identical field centers, the samples of the two cameras operated in southern Spain are not fully independent. Of the 554 Leonids recorded, 116 were recorded by both cameras and subsequently considered only once in the combined profile. The camera at Tenerife recorded another 72 Leonids.

Despite the overlap in the camera fields, the determined rates differ sometimes. The combined activity profile obtained from all three cameras shows a number of maxima, among which the 1^h58^m and 2^h11^m peaks are most prominent. These times are corrected for the topocentric time of the stream encounter. The time difference between Alfarnatejo and Vilaflor is of the order of 45 seconds.

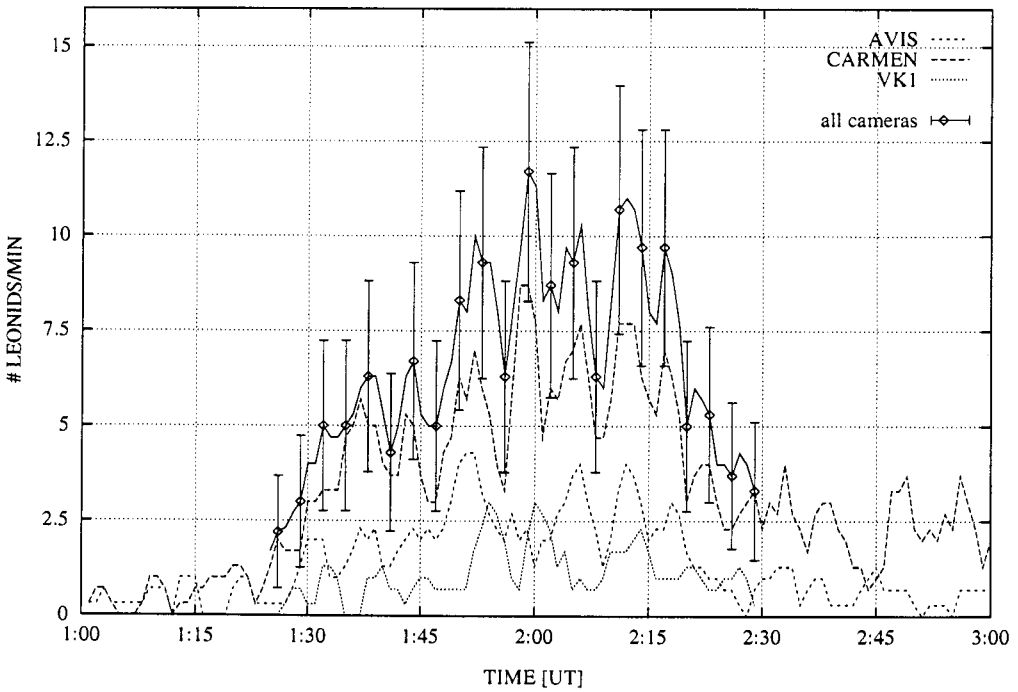

Figure 4 – Activity fluctuations during the 1999 Leonid storm derived from sliding 3-minute intervals of the three video systems. The rate is given as Leonids per minute. The most prominent peaks occur at 1^h58^m and 2^h11^m UT (topocentrically corrected). The 116 Leonids recorded by both AVIS and CARMEN were considered only once in the combined profile of all cameras.

The results are slightly different from the results of a preliminary analysis of visual counts, as presented elsewhere in this issue. These graphs show a sharp maximum at 2^h02^m UT (topocentrically corrected), with a number of sub-peaks on both sides, but "regionally" assembled profiles reveal more sub-peaks typically for that region, which may indicate very small-scale number density variations in the Leonid meteoroid stream.

Reports of visual observers demonstrated that the peak rate of the 1999 Leonids could still be managed with the "traditional" recording methods (tape recorder as well as paper roll). During most intervals, observers were even able to record meteor magnitudes. In this activity range, however, the advantages of intensified video cameras start to become obvious. As proposed earlier [9], the data obtained synchronously by different methods could help to verify the debated 1966 rates, which is one of the next steps in our analysis.

5. Conclusions

The 1999 Leonid meteor storm was a fascinating event, and it was worth every effort to apply all available observing methods. The preliminary video data show distinct activity peaks on November 18 at 1^h58^m and 2^h11^m UT. Obviously, the population index decreases from $r = 3.0$ for Leonids of magnitudes 0 to +2 to $r \leq 2.0$ for Leonids fainter than magnitude +3. Beginning at about magnitude +5 the number of Leonids even starts do decrease. As expected, the Leonid radiant is very compact.

This preliminary analysis will be refined as more data from other video systems become available. We are interested to include further data. Video observers may send even unprocessed video tapes of the Leonid storm with the reference data (start and end time, location, field of view, etc.) to Sirko Molau (address see inside back cover).

References

[1] R.H. McNaught, D. Asher, "Leonid Dust Trails and Meteor Storms", *WGN* 27, 1999, pp. 85–102.

[2] P. Brown, "Evolution of Two Periodic Meteoroid Streams: The Perseids and Leonids", Ph. D. Thesis, Univ. of Western Ontario, London, Ont., 1999, pp. 171–258.

[3] S. Molau, "The Meteor Detection Software METREC", in *Meteoroids 1998*, Tatranská Lomnica, August 1998, W.J. Baggaley and V. Porubčan, eds., Astronomical Institute of the Slovak Academy of Sciences, Bratislava, 1999, pp. 131–134.

[4] S. Molau, "Six Months of Automatic Video Meteor Observations—First Results", in *Proceedings IMC 1999*, Frasso Sabino, Italy, to appear.

[5] R. Arlt, "The Software RADIANT", *WGN* 20, 1992, pp. 62–69.

[6] M. Ueda, Y. Fujiwara, "Double-station TV Observations of the Leonids During 1991 and 1996", in *Meteoroids 1998*, Tatranská Lomnica, August 1998, W.J. Baggaley and V. Porubčan, eds., Astronomical Institute of the Slovak Academy of Sciences, Bratislava, 1999, pp. 131–134.

[7] S. Suzuki, T. Yoshida, K. Suzuki, T. Akebo, "TV Observations of the Leonid Meteor Shower 1995–1997", in *Meteoroids 1998*, Tatranská Lomnica, August 1998, W.J. Baggaley and V. Porubčan, eds., Astronomical Institute of the Slovak Academy of Sciences, Bratislava, 1999, pp. 215–218.

[8] S. Molau, "Systematic Errors of Visual Meteor Brightness Estimates", *WGN* 23, 1995, pp. 225–229.

[9] J. Rendtel, "Summary Report: Workshop on the Coming Leonid Returns", in *Proceedings IMC 1996*, Apeldoorn, the Netherlands, A. Knöfel and P. Roggemans, eds, IMO, 1997, pp. 64–67.

The 1999 Leonids from Spain

Pierre Martin

This November, I had the wonderful opportunity to join members of the *International Meteor Organization* and witness the Leonid meteor outburst from the southern coast of Spain, just north of Malaga. What an adventure! Here is a summary of what turned out to be the most dramatic display of nature's fireworks I have ever seen...

On Saturday, November 13, I left Ottawa (Ontario, Canada) for a trip to Berlin in Germany with fellow meteor observers Cathy Hall and Robert Lunsford. This was of course not a direct flight to Berlin; we had to make Toronto to Frankfurt (Germany) connections first. Flying at 11 000 meter above the Atlantic Ocean, we spotted the greenish arc of an aurora standing still in the dark night. Once we arrived at Berlin-Tegel airport in the evening of November 14, we were exhausted, but had the warm reception of almost half the Council of the *International Meteor Organization* (*IMO*). It was nice to finally meet these people, some of which I have known for several years with the Internet serving as the only means of communication. Upon our arrival in Berlin, we were quite tired of all the various airports we encountered plus the effect of different time zones, so a long night's sleep felt good. The Monday and Tuesday (November 15 and 16), we spent the daytime with sightseeing of Berlin. We first visited the Archenhold Observatory and surrounding astronomical facilities. The highlight was a gigantic refractor telescope with the longest lens in the world! This was the most unusual setup I have seen so far with a large telescope. The facility also contains a number of smaller observatories with modern telescopes and planetariums used for public programs. With clear skies, we watched some interesting groups of sunspots using a solar filter, with one of the excellent instruments. We also had a demonstration of a unique solar theater, where the Sun is projected from a series of mirrors outside all the way into a screen inside a darkened room.

Our tour continued with the visit of many beautiful historical sites across Berlin. There were certainly lots of great photographic opportunities with so many intriguing buildings and monuments. We passed by one of the few remaining sections of the "Wall," and many other interesting sights. I found it amazing to see all this history well preserved.

Figure 1 – Two days before the Leonid maximum night, we had a relaxed meeting in Marquardt, discussing *IMO* matters as well as the observing campaign. From left to right: Pierre Martin (foreground), Manuela Trenn, Robert Lunsford, Rainer Arlt, Marc Gyssens (foreground), Cathy Hall, and Sirko Molau.

On Monday, November 15, we got together to discuss matters relating to *IMO*, and also to determine the weather prospects for the November 17-18 Leonids. Judging from the best weather models, it became clear that we were seeing the worst-case scenario—most of Europe would suffer from overcast skies by Wednesday. There was only one possibility of clear sky in southern Spain (a flight to Spain would be about four hours). We decided to wait until the next morning for a more definite forecast. We had hoped to begin meteor observations one or two nights before the peak; however, the cloud cover was gradually increasing, with only the odd clear break for brief periods. Instead, we chose to check out Sirko Molau's automated video camera and software, used specifically for meteor observing. Such data as meteor counting with proper shower classifications can happen when the observer is sound asleep in bed! In the morning, the computer produces a meteor data report of the night's observations! Hey, what a good idea when one wants to monitor really low meteor rates on a $-30°$ C January night! One does not even need to step outside!

By Tuesday, November 16, it immediately became certain to us that nearly all of Europe was ready to get clouded out by Wednesday, and snow was now in the forecast. In the meantime, a large high pressure of clear blue skies was gaining strength in southern Spain. The high mountain tops of Spain would likely delay any clouds from descending there until at least Friday. So we made our decision swiftly... off we were to Malaga, southern Spain! After a restful night, our plane took off around noon of Wednesday, November 17. Once there, the eight of us gathered up at our two rental cars. It was already evening and the Sun was down. It was time to get going, stock up on some supplies and find a suitable observing site somewhere in the mountains. After some driving deep into the twisting and narrow roads of the mountains, we came up to a small road that looked quiet, and we stopped. It seemed to be an unused road and the area was free of light pollution. We gave it a try and came up to an abandoned well and old building, and decided to set up there. Almost instantly, we realized what kind of night we could expect; skies were clear but the wind was howling strongly from the east. It was about 9 p.m. when we got there, and Leonid peak time was just 5 hours away! Despite this, the Leonid radiant was not due to rise from that location until around midnight, so we had plenty of time to set up and test our equipment and cameras. The crew of the German *Arbeitskreis Meteore* (*AKM*) had a number of image-intensified cameras running, and we had several 35-mm cameras with various lenses and films. Despite the relatively mild $+5°$ C night, the persistent wind gave a much colder wind-chill factor, so the full winter gear was needed. It was a serious challenge to keep things from being blown away with the wind.

Figure 2 – Waiting for the departure to Malaga at the Berlin-Tegel airport on November 17, 1999, from left to right: Robert Lunsford, Pierre Martin, Manuela Trenn, Cathy Hall, and Sirko Molau, just 14 hours before the expected peak time.

Figure 3 – Our Leonid observing site was in the Sierra de Camolores, north of Malaga. Observers had to protect against the wind, using parts of the old building or placing behind walls or cars.

I began observing just past midnight (local time) or 23^h10^m UT. The sky was perfectly clear, just as we had expected, and the moon shone brightly over the hills. To keep the lunar glare from blinding me, I faced north-east to start. After moonset, the sky's limiting magnitude reached +6.4. It took me just 17 minutes to spot my first Leonid, and it was a memorable one. With the radiant just rising, a nice Earth-grazing Leonid shot a dramatic 70° to finally end low in the south. The first hour was slow with just 6 Leonids, among a few Taurids and sporadics seen until 0^h21^m UT. It was, however, normal to have low rates with Leo still so close to the horizon. The next 30 minutes began to show signs of increase with 15 Leonids observed. Some of those meteors were vividly colored. One 0^h19^m UT Leonid flared to magnitude −3 with a white color changing to blue before extinguishing. A few faint Leonids showed an obvious orange, a color I rarely ever see. As Leo rose higher in the east, I also switched my field of view in that direction. Meteor rates soon intensified... Between 1^h00^m and 1^h30^m UT, I was averaging 3 Leonids per minute (180 per hour). Most meteors were now of average brightness, leaving brief trains behind. Every once in a while, a brighter colorful Leonid would shoot long lengths in the sky. The brighter ones would display vivid blues, golden yellows, and more orange. The numbers were now going nowhere but up, and a sense of excitement was felt!

Near 1^h45^m UT, my Leonid rates jumped quickly to 16 per minute (960 per hour). Most meteors were now on the faint side (magnitudes +3 and +4), but a good number of magnitude +1 and +2 were also there. It was soon becoming very hard to record all the meteors, as they kept coming fast, with occasional bursts of a few Leonids following nearly simultaneously. I kept calling only the magnitudes as fast as I could with my tape recorder running continuously. At 1^h56^m, a burst of at least 8 Leonids flashed all over the sky in a single second! I was almost overwhelmed, and it was becoming too hard to record them all! At 2^h00^m–2^h10^m UT, Leonids rained down at an average rate of 39 per minute (2300 per hour)!! At this point, I only had time to "beep" into my recorder every time I would see one, and even so, it was sometimes hard to keep up! Swift moving shooting stars were all over the sky! Near the radiant, many near head-on meteors would produce foreshortened paths. A quick glance in the opposite direction from the radiant would show long Leonids plunging all the way to the horizons.

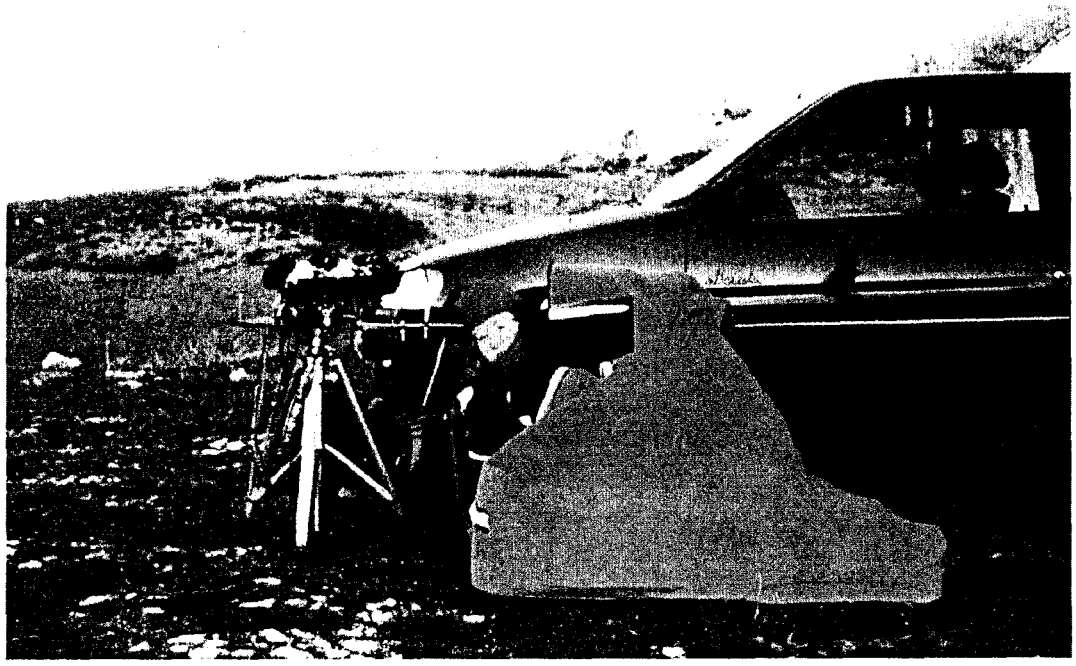

Figure 4 – Cathy Hall with her winter gear and her photographic equipment placed close to one of the rented cars.

The best single minute was between 2^h08^m and 2^h09^m UT with 69 Leonids!! It was easy to hear laughs of joy from the other observers around me! I also found it difficult to attend to my camera with all the excitement going on.

By 2^h20^m UT, the rates began to decrease to 29 per minute (1740 per hour). It became obvious that the peak had just passed, and that Leonids were already beginning to lose strength. I resumed calling Leonid magnitudes once again. Shortly after 2^h30^m UT, Leonids were already down to 18 per minute (1080 per hour). At this point, a number of brighter Leonids were seen, and displayed more colors. One blue-green fireball flashed to magnitude −5. At 3^h00^m UT, Leonids averaged 7 per minute (420 per hour). With such a sharp decline, I realized that observers in eastern America would not get to see anything of the meteor storm. By 4^h00^m UT, I was becoming very tired, but I managed to stay awake for a short period. Leonids continued to display about 2 or 3 per minute (165 per hour). I lasted until 4^h13^m when total exhaustion got to me and I finally had to sign off.

Although a huge number of meteors were seen, the display consisted mostly of faint (magnitudes +2 to +4) meteors. There were only a few fireballs, with the highlight coming at 3^h44^m UT, when a magnitude −6 Leonid lit up the southern sky with a bright blue-white terminal flash. It left a 3-minute long train that slowly drifted low in the south.

A total of 2341 meteors (2267 Leonids, 9 Taurids, 3 α-Monocerotids, and 62 sporadics) were seen during 4.65 hours of effective observing time. Table 1 shows my magnitude distribution from 1586 Leonids during November 17-18 (note that no magnitude data was obtained between 2^h02^m and 2^h22^m UT). Out of 1586 Leonids, only 19 can be considered as fireballs...

Table 1 – Magnitude distribution of the 1999 Leonids seen by Pierre Martin during the night of November 17-18.

Magnitude	−6	−5	−4	−3	−2	−1	0	+1	+2	+3	+4	+5	Tot	$\overline{m}$
Leonids	1	2	7	9	24	56	121	120	351	369	401	125	1586	+2.51

The following night (November 18-19), our group observed again to monitor meteor activity between moonset and dawn. The Leonids appeared to me at a much lower visual rate of 10–15 per hour. I also plotted weak activity from the α-Monocerotids and Taurids. Plotting was a challenge due to the strong wind we encountered again that night.

After visiting the southern coast of Spain, we flew back to Berlin on Friday November 19. We spent Saturday afternoon visiting historic parks in Potsdam. Then we had a final evening get-together with the *AKM* crew, where we were shown slides of the 1998 *AKM* Leonid expedition in Mongolia. We were also shown a segment of the 1999 storm captured by one of the intensified video cameras. The trip ended Sunday morning, and I was back to Canada by evening.

The November 17-18 Leonid maximum was brief, but the nearly overwhelming numbers of meteors left an unforgettable impression in my mind! This meteor storm was quite a bit higher than I had hoped for, even though the rates were just a fraction of what was seen by western North America in 1966. Finally, I would like to express many thanks to the following people for their very kind hospitality and for making the dream of seeing such a meteor storm a reality: Sirko Molau (and parents), Robert Lunsford, Jürgen Rendtel and Manuela Trenn, Rainer Arlt, Ina Rendtel, Cathy Hall, Marc Gyssens, and Ralf Koschack.

The 1999 Leonid Multi-Instrument Aircraft Campaign: The Storm from Altitude

Peter Jenniskens and Steve Butow, NASA/Ames Research Center

An airborne campaign was organized, sponsored by NASA and USAF, with the goal to view the Leonid meteor storm at an altitude above the clouds over the Mediterranean in November of 1999. The mission proceeded as planned and resulted in much exciting scientific data. Here is a brief first impression of the Leonid Multi-Instrument Aircraft Campaign.

The 1999 Leonid Multi-Instrument Aircraft Campaign (MAC '99) is behind us and an overwhelming success. 35 researchers of seven nationalities had a prime view of the 1999 Leonid storm onboard two aircraft, the NKC-135 "FISTA" and the EC-18 "ARIA," both operated by the USAF/452nd Flight Test Squadron (FTS). This was a follow up on NASA's first astrobiology mission in November of 1998, again aimed at studying the fate of extraterrestrial matter accreting into Earth's atmosphere and its potential role in the origin of life [1,2].

This year, the US Air Force sponsored the campaign also, with the goal of providing near-real time meteor rates to satellite operators worried about the possible impact on satellites in Earth's orbit. The mission unfolded as planned and became a nice example of an excellent collaboration between the two agencies. In addition, space agencies ESA, ISAS, and ISA and many individual institutes contributed in kind to participating researchers to make the mission an international endeavor.

The USAF/452nd FTS flew researchers, crew, and journalists safely from Edwards Air Force Base (AFB) to Israel and back for prime viewing of the meteor shower. The USAF/106th Rescue Wing, based in New York, provided a C-130 ADVON mission, which took care of advanced arrangements of logistics for a total group of 78 people.

On the flight over to Mildenhall Air Base, UK, we got a dancing aurora to practise aircraft positioning and instrument pointing for persistent trains. In the UK, we entertained school children with the how's and why's of our mission. In the flight from the UK, over Northern Spain, to Ben Gurion International Airport, Israel, we observed airglow and solved numerous small technical problems.

On mission night, we all saw a splendid meteor storm under excellent conditions while flying over Greece on our way from Israel to Lajes Air Base in the Azores. Better yet, the background component returned with numerous fireballs and persistent trains all night long. We got amazing spectra of a bright meteor afterglow at $4^h00^m29^s$ UT. The afterglow was so bright it registered on slit-less spectrographs (Figure 1). The persistent train of that meteor formed a "2" to signal the end of the second millennium. By that time, we were celebrating! The champagne had to wait until we landed at Lajes Air Base.

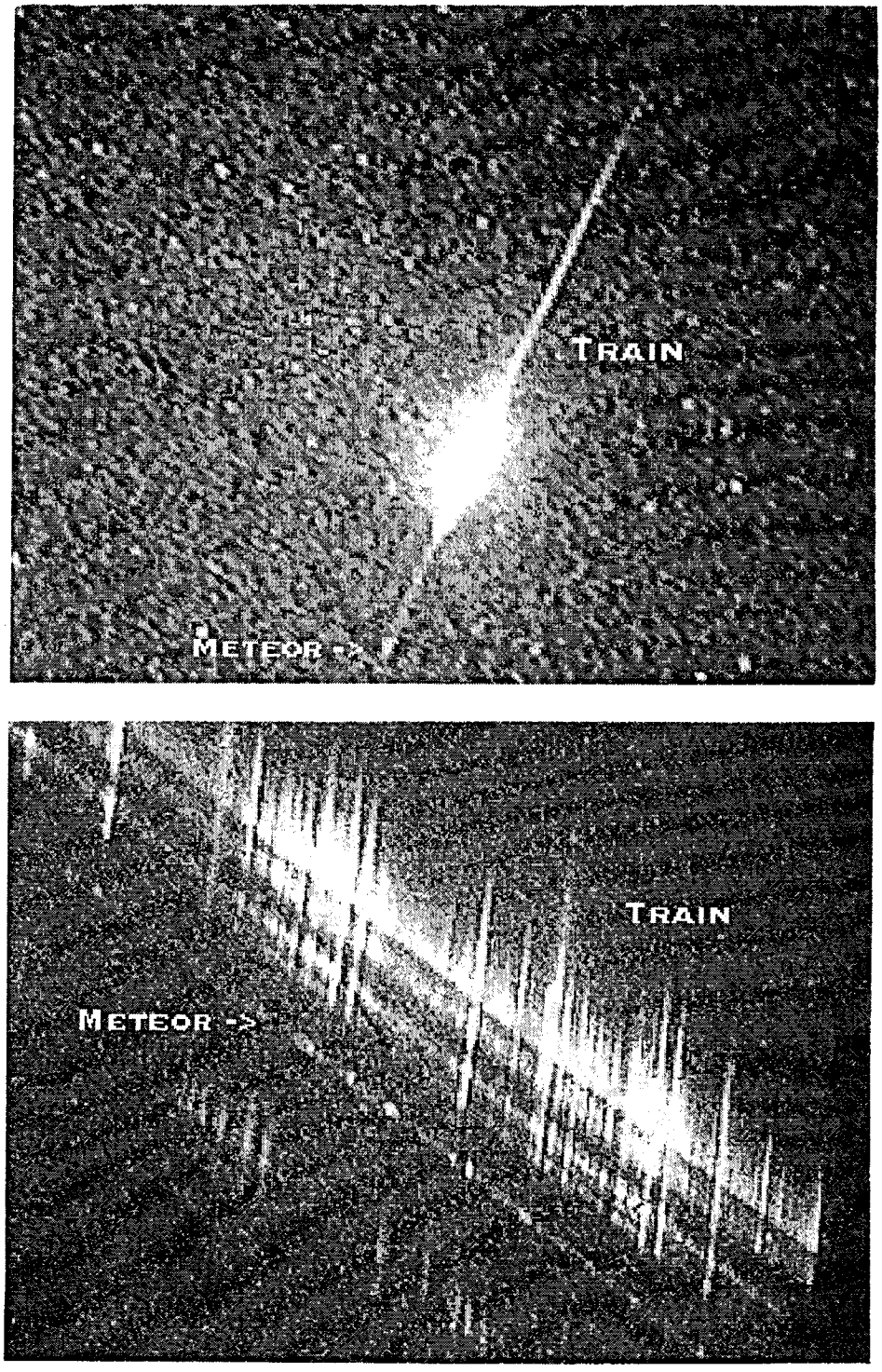

Figure 1 – *Top*: One video frame of the November 18, 1999, $4^h00^m29^s$ UT fireball as seen from ARIA. *Bottom*: The afterglow was so strong that a spectrum of it was recorded by slit-less spectrographs (*Photo P. Jenniskens/M. Wilson, FISTA*).

During the storm, we were able to use the space shuttle satellite communication network TDRSS to send a video signal down to Ames for distribution on the Internet. NHK made that meteor storm video look impressive. Those that were running Real-Player were the first to see the rates increase that night, and hear Col. (soon Brig. Gen.) Worden comment on the events live from the ARIA aircraft, *"This is impressive if you are in the space business!"*

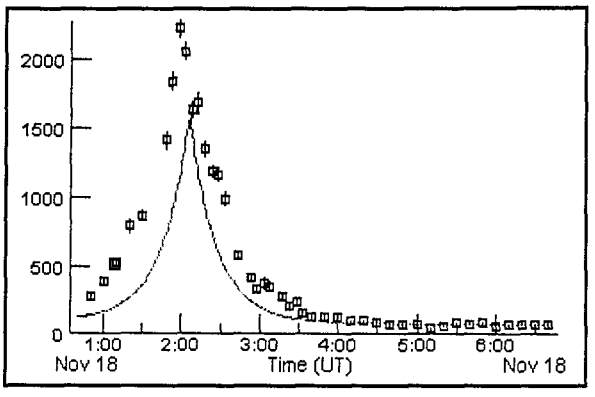

Figure 2 – Leonid rates reported in real time by the ARIA flux measurement team (cf. `http://leonid.arc.nasa.gov`).

We supplied near-real time flux measurements in 5-minute intervals to NASA/Ames, and from there on to other agencies, that nicely showed the onset of the storm and allowed us to predict the peak rate already half an hour before the maximum (Figure 2). We used a new counting computer developed by Chris Crawford. It gathered the counts of 6 visual observers, the ARIA flux measurement team, using video head displays to monitor the video cameras pointed from the side of the aircraft. The team consisted of amateur meteor observers Gary Kronk, Jane Houston, Klaas Jobse, David Holman, Kelly Beatty, and Michael Schmidhuber.

Based on our counts, in talking to Worden, we predicted the peak level of the storm more than half an hour before the peak (assuming Asher's time at 2^h08^m UT).

A unique Track II capability, using satellite communication to keep track of the aircraft positions, made the stereoscopic work a lot easier than last year. The Japanese team of Hajime reported *"Meteor, meteor, meteor!"* every time when yet another meteor was captured by HDTV from both FISTA and ARIA. All researchers were beaming afterwards. Aerospace Corporation's mid-IR spectrometers got data already in the night before the peak! They overcame many technical problems to celebrate that feat. Cars broke down, dewars leaked, instruments failed to detect signal a mere week before departure. Now, all worked the way it should!

Pilots repositioned FISTA for best observing of two long-lasting persistent trains that appeared at an ideal altitude for all instruments to observe it, just in between the low (12°) and intermediate (40°) altitude windows. After the storm, there was the surprising occurrence of sprites, with a rare opportunity to study the hypothesis that meteors trigger sprites. Researchers of the University of Utah measured airglow as never before across the Atlantic.

We continued our journey from the Azores to Patrick AFB in Florida and from there on home to Edwards AFB in California. On the last leg, FISTA did one other night time flight to secure airglow data for AFRL. We completed a number of coordinated observations with the ground, including combined observations of Leonids with an Israeli radar site, and multi-station meteor observations with ground-stations of the Dutch Meteor Society in Spain. The campaign was also a great success because we all enjoyed ourselves so much. We got great data from fine celestial surprises. We also had a good time in England, walked the Mediterranean beach in Israel, visited the islands of the Azores, and had a final dinner on the Atlantic beach in Florida. We are indebted to all that made this mission possible. We know for certain now that there are two more opportunities coming up for viewing a meteor storm, namely in 2001 and 2002, when Earth by chance goes smack through the middle of dust trails ejected in 1866 and 1833. You can read much more about this year's campaign and possible future missions at `http://leonid.arc.nasa.gov`.

References

[1] P. Jenniskens, S. Butow, "Successful Leonid Airborne Mission", *WGN* 26, 1998, pp. 249–252.

[2] P. Jenniskens, S. Butow, "The 1998 Leonid Multi-Instrument Aircraft Campaign—An Early Review", *Meteoritics and Planetary Science* 34, 1999, pp. 933–943.

Ongoing Meteor Work

A Detailed Analysis of the Geometric Shower Radiant Altitude Correction Factor

James Richardson, Florida State University

The heart of the visible meteor Zenithal Hourly Rate (ZHR) formula is the correction factor for shower radiant angular altitude (or zenith angle). This correction factor is primarily an effect of the geometry between the incident shower meteor flux vector and the oblique target area presented by the atmospheric "meniscus" visible to a single observer on the surface of the Earth. Presented in this paper is a detailed analysis of the full geometric portion of this correction factor, for apparent radiant altitudes both above and below the local horizon, and with the radiant zenith attraction effect also included. This analysis opens the way toward a better understanding of the non-geometric effects within the complete correction factor, which must currently be derived empirically.

1. Historical review

Perhaps the most important portion of the visible meteor Zenithal Hourly Rate (ZHR) formula is the shower radiant angular altitude correction factor. In fact, for many years this single factor was considered as the *primary* zenithal hourly rate equation, especially since the remaining, more modern factors could be eliminated or at least minimized by utilizing only observations made under very dark, perfectly clear skies, using an observer with normal visual meteor perception, and collecting data for a full observing time period. Given the unavoidable need to address this change in observed meteor shower flux with apparent shower radiant zenith angle (the complement of the radiant altitude), meteor astronomers who wished to study shower activity profiles began to discuss this factor in the professional literature, beginning in the 1950s. Three of the more notable derivations are outlined below.

The most basic version of this correction factor is the geometric first order (flat Earth) approximation, put forward by Öpik in 1955 [1], given as $V = V_0 \cos z_a$, where V_0 is the incident meteor flux, V the detected meteor flux, and z_a the apparent radiant zenith angle. The most commonly used radiant zenith angle correction factor used today is a variation on Öpik's equation, developed by Zvolánková in 1983 [2,3]. This version adds a derived exponent to the cosine factor, called γ, which is an empirically derived correction factor: $V = V_0 \cos^{\gamma} z_a$, with γ in the range 1.0–2.0. This equation empirically takes into account such additional factors as average magnitude extinction, average meteor path length changes, and other effects on the number of meteors observed as a function of radiant zenith angle, in addition to the geometric effect.

Note, however, that the above formulae do not take into account the curvature of the Earth and atmosphere, and thus can only be utilized for apparent shower radiant zenith angles of less than about 75°–80°. Beyond this, at low radiant altitudes, they loose their accuracy very rapidly. The best attempt to take into account the curvature of the atmosphere and extend the geometric correction factor down to low radiant altitudes was published by Kresák in 1954 [4], utilizing a piecewise function:

1. for apparent radiant zenith angle below 80°,

$$V = V_0 \cos z_a \,; \tag{1}$$

2. for apparent radiant zenith angle above 80°,

$$V = V_0 \frac{\sqrt{2rh + h^2 \cos z_a} + r(1 - \sin z_a) + h}{2\sqrt{2rh + h^2}}, \tag{2}$$

where r is the radius of the Earth (on average 6378 km) and h the meteor atmospheric altitude (between 80 km and 120 km).

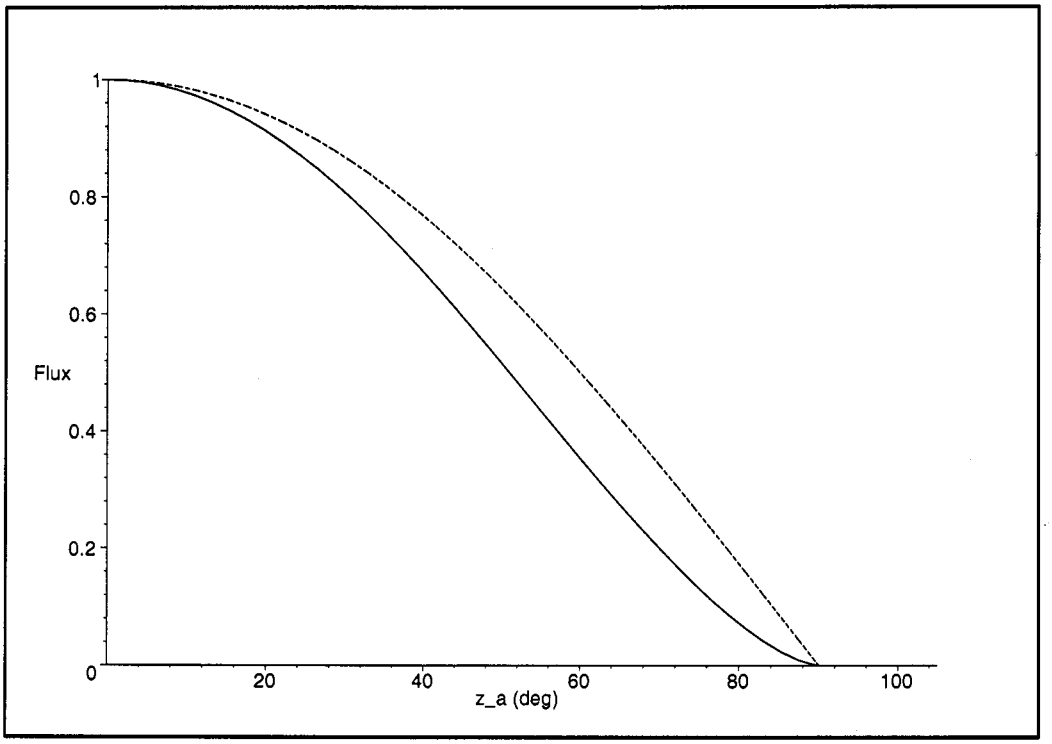

Figure 1 – Normalized shower meteor flux as a function of apparent radiant zenith angle: Zvolánková, 1983 (solid, $\gamma = 1.5$) and Öpik, 1955 (dashed).

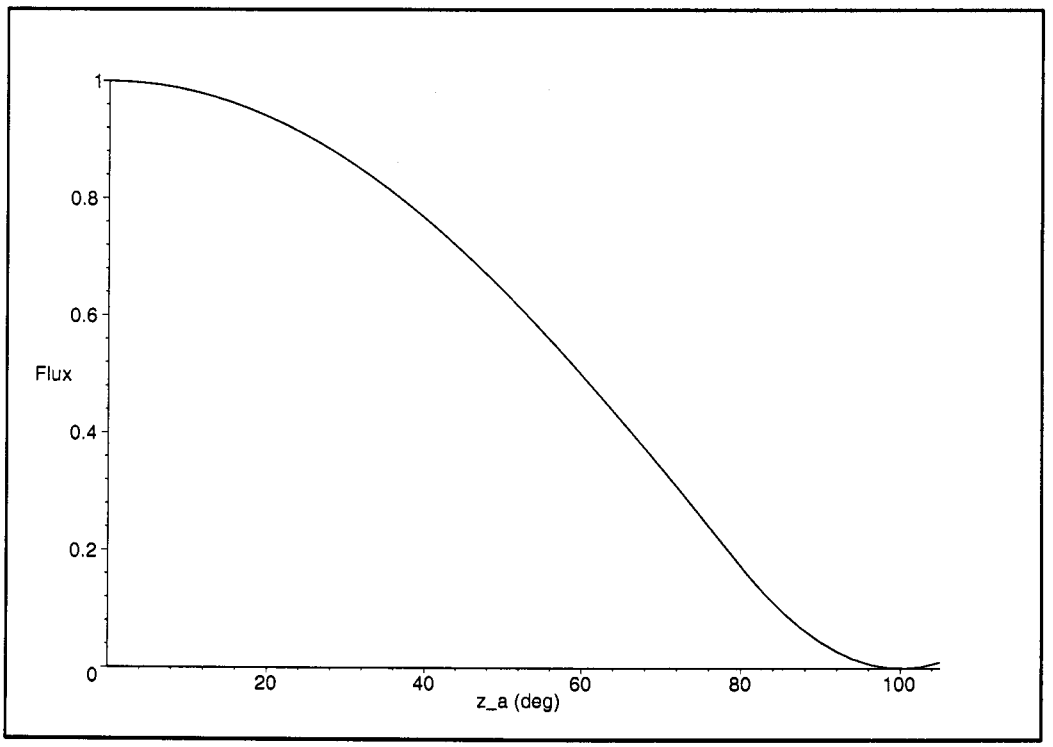

Figure 2 – Normalized shower meteor flux as a function of apparent radiant zenith angle: Kresák, 1954 ($r = 6378$ km, $h = 100$ km).

The first portion of this function—equation (1)—is the standard first-order approximation given in Öpik [1], while the second portion—equation (2)—is an approximation for the response of the curved observable atmosphere to low shower radiant altitudes. Note that Kresák's function shows the small, yet present, possibility of shower meteors from a radiant below the horizon, with the normalized flux reaching 0.0 at $z_a = 100\overset{\circ}{.}08$ (for $r = 6378$ km, $h = 100$ km).

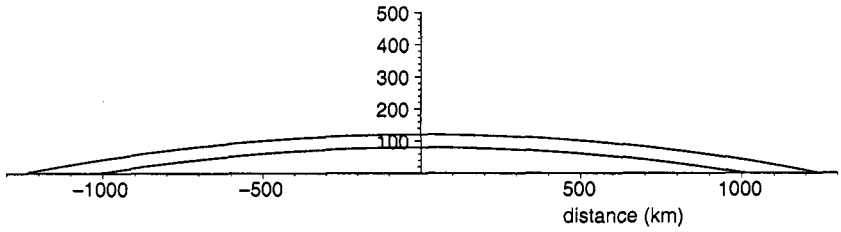

Figure 3 – Cross-sectional view of the atmospheric meteor layer visible to a single station on the surface of the Earth (located at the origin), drawn to scale and in units of km. The lower curve represents a meteor altitude of 80 km, while the upper curve represents a meteor altitude of 120 km.

All of these correction factors are good approximations, quite adequate to the task of providing a reasonable radiant zenith angle correction factor for ZHR calculations. However, an exact solution to the geometric portion of this correction factor has not yet been published (as far as this author knows), which would aid in investigating the remaining effects as well as providing an interesting theoretical discussion. Therefore, the purpose of this paper is to present an exact solution to the geometric shower radiant zenith angle correction factor, not taking into account such additional factors as magnitude extinction, and extending the analysis to apparent radiant zenith angles both above and below the horizon.

2. Model description

At the geometric level, the portion of atmosphere visible to a single observer on the surface of the Earth, exposed to a shower meteor flux, is nicely analogous to a scintillation detector exposed to a particle beam. This analogy creates a very convenient way of handling this problem, reducing it to a standard physics detector response curve analysis.

This spherical atmospheric cap or meniscus, visible to a single ground station, can be treated as a scintillation detector window, contained as part of a very large spherical housing (Earth plus atmosphere). This housing is then rotated in a broad, constant flux, single-velocity particle beam, such that the particle flux vector will pass directly through the zenith (z axis) of the detector window. The detector response is then analyzed as a function of the particle flux vector zenith angle. This is done as a piece-wise function, similar to Kresák's approach, for radiant zenith angles below and above 90°, respectively. Note also that the center of the Earth is used as the coordinate system origin, with the incident meteor flux vector seen from this geocentric frame.

The one modification which must be made to a standard detector response problem is that, in this instance, the particle paths will be bent hyperbolically by a small amount toward the center of the Earth due to gravity (zenith attraction), altering the incident flux vector. Thus, to remain accurate, the analysis must be performed using this apparent incident flux vector (in rectilinear fashion), rather than the true incident flux vector. The correction between true radiant zenith angle (z_t) and apparent radiant zenith angle (z_a) is given below, taken from Lovell [5]:

$$\begin{cases} z_a = z_t - 2\arctan(k\tan\frac{z_t}{2})\,; \\ k = \dfrac{v_\infty - v_g}{v_\infty + v_g}\,; \\ v_g = \sqrt{v_\infty^2 - 124.9}\,, \end{cases} \tag{3}$$

where v_g is the meteors' geocentric speed (km/s) and v_∞ the meteors' atmospheric entry speed (km/s).

Zenith attraction has its greatest effect upon slow meteors having heliocentric radiants near the antapex point, and has much less effect upon fast meteors originating near the apex point. A practical limit for this correction in working with very slow showers is about 17°–20° when these true radiants (z_t) are located at the observer's horizon. However, for fast- and medium-speed showers, the difference between z_t and z_a will be quite small, generally not more than a few degrees.

3. Apparent radiant zenith angle below 90°

With the apparent meteor shower radiant above the horizon, two approaches can be used toward finding an exact solution: either solving the problem as a surface integral, or analyzing the detector target area presented to each component of the incident particle flux [6]. Both approaches lead to identical solutions, providing a source of equation verification. The surface integral approach proceeds as follows, initially utilizing a Cartesian coordinate system and placing the center of the Earth at the coordinate system origin.

The incident meteor flux vector has components

$$\vec{V}_0 = -\sin z_a \, \vec{i} - \cos z_a \, \vec{k},$$

where $\vec{V}_0$ is the incident flux vector and $\vec{i}$, $\vec{j}$, and $\vec{k}$ are the unit component vectors for the axes x, y, and z, respectively. This vector $\vec{V}_0$ has negative components, pointing radially towards the Earth's center, with the zenith angle (z_a) measured from the zenith of the observer (positive z axis), and as a rotation about the y-axis.

The normal vector for the detector surface is given by

$$\vec{N} = -\frac{x}{r+h}\,\vec{i} - \frac{y}{r+h}\,\vec{j} - \frac{z}{r+h}\,\vec{k},$$

with r the radius of the Earth (6378 km) and h is the meteor zone altitude (80 km–120 km). Taking the dot product of these two vectors, converting to spherical coordinates, and applying to the surface integral formula over the right (positive x axis) half of the spherical atmospheric cap gives

$$V_1 = \int_{-\pi/2}^{+\pi/2} \int_{0}^{\delta} (r+h)^2 \sin z_a \sin^2\theta \cos\phi \, \mathrm{d}\theta \, \mathrm{d}\phi + \int_{-\pi/2}^{+\pi/2} \int_{0}^{\delta} (r+h)^2 \cos z_a \sin\theta \cos\theta \, \mathrm{d}\theta \, \mathrm{d}\phi.$$

Solving gives

$$V_1 = +[\delta(r+h)^2 - rd] \sin z_a + \frac{\pi d^2}{2} \cos z_a,$$

with d the distance from the observer to a meteor at the horizon and δ the angle opposite d (from the Earth's center). The left hand (negative x axis) side of the spherical cap is integrated in a similar fashion, to give

$$V_1 = -[\delta(r+h)^2 - rd] \sin z_a + \frac{\pi d^2}{2} \cos z_a.$$

Note that, in this case, the sine term is now negative, and that summing the response from the two halves of the detector ($V_1 + V_2$) would result in simply getting back the old first-order approximation after normalizing. This is because the negative sine term in the second equation physically represents flux lines exiting the detector from the *inside*—something which

cannot occur in reality, since the particles are stopped at the outside detector surface (upper atmosphere). That is, the surface integral, as a mathematical tool, is set up for continuous flux lines which can pass through a hypothetical surface in both a positive and negative direction without being stopped. In this application, however, the particle flux can reach the detector surface only from the positive direction (outside), allowing us to neglect the negative flux terms produced by the integration.

After summing the solutions for the two halves of the detector and neglecting the negative sine term, the equation is then normalized to the flux present when $z_a = 0$. The final equation for radiant zenith angle below 90° is thus given by

$$V = V_0(\cos z_a + \frac{\delta(r+h)^2 - rd}{\pi d^2} \sin z_a), \quad (4)$$

with

$$\delta = \arcsin\left(\frac{d}{r+h}\right) = \arccos\left(\frac{r}{r+h}\right)$$

and

$$d = \sqrt{2rh + h^2}\,.$$

As expected, this equation is quite similar to the old first-order approximation, but with a smaller sine term added. The cosine term represents the contribution of the vertical component of the incident meteor flux, while the sine term represents the contribution of the horizontal component of the incident meteor flux. The fraction coefficient for the sine term also has a physical meaning as a ratio: the vertical cross-sectional area of the atmospheric cap (shown in Figure 3) over the horizontal cross-sectional area of the atmospheric cap (which is a disk having radius d). In other words, the normalized coefficient for the sine term is the ratio of the detector target area presented to the horizontal component of the meteor flux to the detector target area presented to the vertical component of the meteor flux. This will be a useful technique in the next portion of the analysis ($z_a > 90°$), where the surface integral approach cannot be utilized.

In order to give an idea as to the effect of this second term on the overall equation, some numerical examples of this first solution are given below. The coefficient for the sine term in equation (4) is expressed here as a function of meteor height (h), with the Earth radius (r) held constant. This function is called mdr(h) (from "meniscus/disk ratio"):

$$V = V_0[\cos z_a + \mathrm{mdr}(h) \sin z_a].$$

We have

$$\begin{aligned}
\mathrm{mdr}(\ 80\ \mathrm{km}) &= 0.03355;\\
\mathrm{mdr}(\ 90\ \mathrm{km}) &= 0.03557;\\
\mathrm{mdr}(100\ \mathrm{km}) &= 0.03749;\\
\mathrm{mdr}(110\ \mathrm{km}) &= 0.03931;\\
\mathrm{mdr}(120\ \mathrm{km}) &= 0.04104.
\end{aligned}$$

This additional sine component is rather small, reaching only 3–4% of the maximum cosine term value as the radiant approaches 90° of zenith angle. A simple analogy for visualizing the relationship between these two terms (cosine and sine) is to imagine a very large cloud of locusts flying toward a small, square wheat field having sides facing the cardinal directions. If the locusts initially approach the field directly from the north, all of the locust flux (number of locusts per hour) will be seen on the north side of the field, with the entry rate of locusts being proportional to their southerly flight velocity (holding their density constant). Rotating the flight direction of the locusts around the compass, such that they are now coming from the north-east, will cause the north side of the field to see a decrease in flux, because the locust velocity now has two components: southerly and westerly. That is, the north side of the field will "see" the southerly

component of the locust velocity vector, which will change as a function of the *cosine* of the compass direction from which the locusts are coming. By the same token, the east side of the field will see a corresponding increase in flux as the locust direction is rotated toward the east, beginning at zero when the locusts come from due north, and changing as a function of the *sine* of the compass direction from which the locusts are coming. If this direction is rotated fully around to the east, the field north side flux will decrease to zero (as the locusts fly parallel to it), while the field east side will see the full locust flux. With a perfectly square wheat field, neither north nor east side flux terms dominate the combined equation, each being weighted equally. However, in the atmospheric-cap application being examined here, the analogous "field" is a very skinny rectangle, having a north side which is about 25 times longer than its east side. This will cause the flux seen by the north side of the field to become a very dominant cosine term in the overall flux determination of equation (4), with the flux seen by the east side of the field becoming a minor sine term.

4. Apparent radiant zenith angle above 90°

Once the shower radiant drops below the horizon, two important effects come into play: (*i*) only the horizontal component of the shower meteor flux will be present, since the vertical component has switched signs and will be coming from directly underneath the detector (obviously impossible), and (*ii*) the vertical target area now presented to the remaining horizontal component of the meteor flux will change dynamically as a function of the radiant zenith angle (previously, it was static). This can be visualized by imagining the shower flux as a broad light beam illuminating a sphere—with half of the sphere in the light and the other half in darkness. When the shower radiant is at the horizon, the limbus dividing light from dark on the surface of the sphere will neatly split the detector into two halves, one half lit and the other half in shadow. At this moment, the horizontal component of the meteor flux is maximized, the vertical component is at zero, and the target area presented by the atmospheric cap is given by

$$A_v = \delta(r+h)^2 - rd, \tag{5}$$

with A_v the atmospheric cap vertical target area. As the radiant continues to drop, less and less of the detector will be illuminated, presenting a shrinking vertical target area to the now decreasing horizontal component of the meteor flux. When the apparent shower radiant reaches a critical angle, given by $(\delta + 90°)$, the flux seen by the detector will reach zero.

The key to solving for the vertical dynamic target area of the detector with $z_a > 90°$ is realizing that the problem can be approached from either the "front" or the "back"—either finding the vertical area of a piece of a spherical cap, or finding the vertical area of the small piece of disk slicing through it (shaded in gray in Figure 4). These two surfaces have the same vertical target area (silhouette), and the second approach is obviously easier.

Utilizing some standard and spherical trigonometry for angles α, β, and δ (shown in the figure), the following vertical surface area is obtained for the atmospheric cap (detector) as a function of radiant zenith angle ($z_a > 90°$):

$$\begin{cases} A_v = \left[\beta(r+h)^2 - \dfrac{r}{\sin z_a} \sqrt{(r+h)^2 - \dfrac{r^2}{\sin^2 z_a}} \right] \sin z_a; \\ \beta = \arccos \left[\dfrac{r}{(r+h)\sin z_a} \right], \end{cases} \tag{6}$$

where $\alpha = z_a - 90°$ is the limbus tilt angle, β is half of the target area width angle (from the center of the Earth), and δ is the cap radius angle (from the center of the Earth).

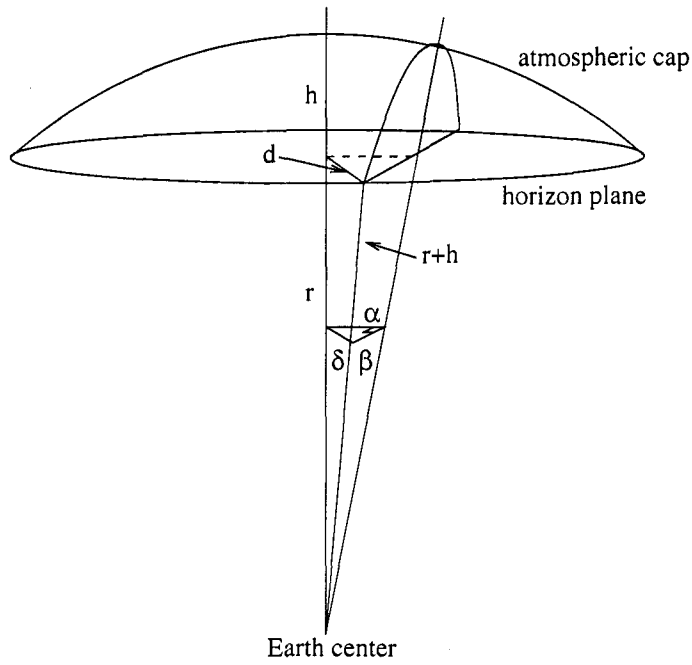

Figure 4 – Geometry utilized for obtaining the vertical target area of the atmospheric cap for $z_a > 90°$ (not drawn to scale).

Note that, when $z_a = 90°$, this target area—equation (6)—properly reduces to equation (5), and, when $z_a = \delta + 90°$, it properly reduces to zero. Combining this target area with the remaining horizontal component of the shower meteor flux and normalizing to the flux present when $z_a = 0$ gives

$$\begin{cases} V = V_0 \left[\beta(r+h)^2 - \dfrac{r}{\sin z_a} \sqrt{(r+h)^2 - \dfrac{r^2}{\sin^2 z_a}} \right] \dfrac{\sin^2 z_a}{\pi d^2}\,; \\ \beta = \arccos \left[\dfrac{r}{(r+h)\sin z_a} \right], \end{cases} \tag{7}$$

Utilizing equations (3), (4), and (7) for $z_a < 90°$ and $z_a > 90°$, the full geometric shower radiant altitude correction factor can be plotted as shown in Figure 5.

Figure 5 shows this correction factor as a function of the true radiant zenith angle for three shower meteor velocities: Leonids at $v_\infty = 70.7$ km/s, Geminids at $v_\infty = 34.4$ km/s, and October Draconids at $v_\infty = 20.4$ km/s (from [2]).

Note that the difference in this correction factor between the very fast and medium-speed showers is quite small, while the effect on a very slow shower is much more severe. This curve also shows the higher probability (although still quite small) of meteors occurring from a very slow shower whose true radiant is below the horizon, as compared to a faster shower. For the Leonids, the critical (cut-off) true radiant zenith angle is 101°.0, while for the Draconids, this critical true radiant zenith angle is 116°.4. Both of these values correspond to an apparent radiant zenith angle of 100°.1, and all angular values here assume $r = 6378$ km and $h = 100$ km.

Also, note the sharp inflection point in the curve at $z_a = 90°$, followed by the gradually decreasing "toe" of activity until a flux of 0.0 is reached at $z_a = 100°.1$. This flattened 90°–100° portion of the profile is analogous to a curve for sunlight levels before sunrise or after sunset (twilight), with a corresponding very rapid rise in light levels the instant that the sun breaks over the horizon.

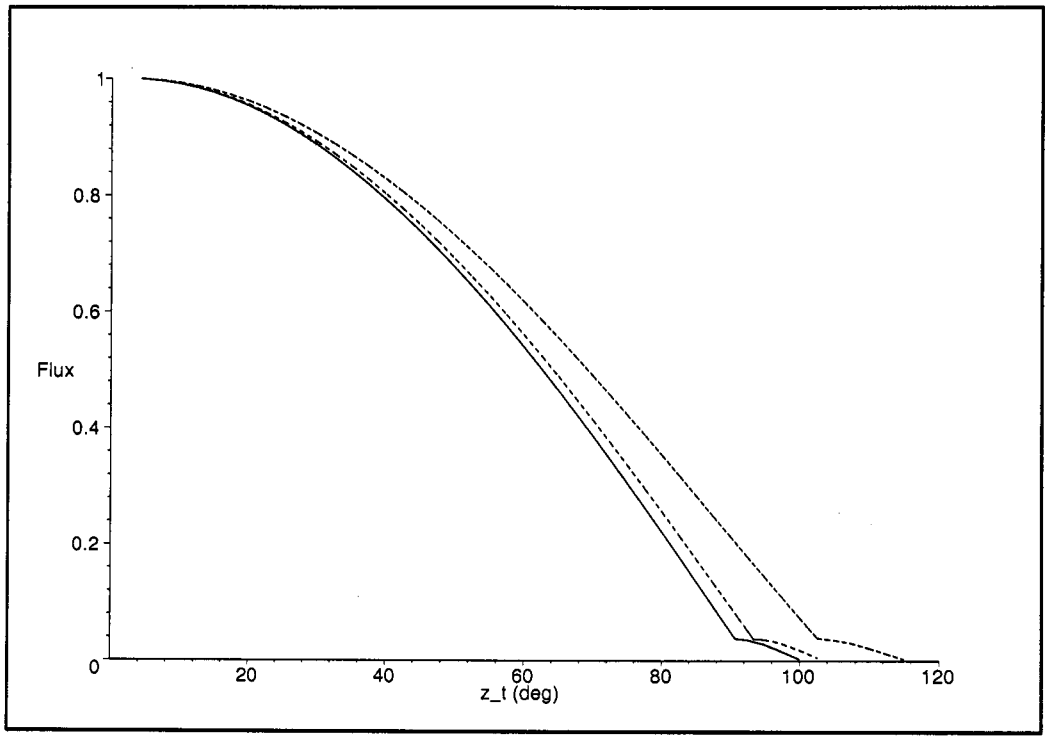

Figure 5 – Normalized shower meteor flux as a function of true radiant zenith angle: exact geometric solution (r = 6378 km, h = 100 km). Shown (*from left to right*) are the solutions for the Leonids (solid), Geminids (dotted), and October Draconids (dashed).

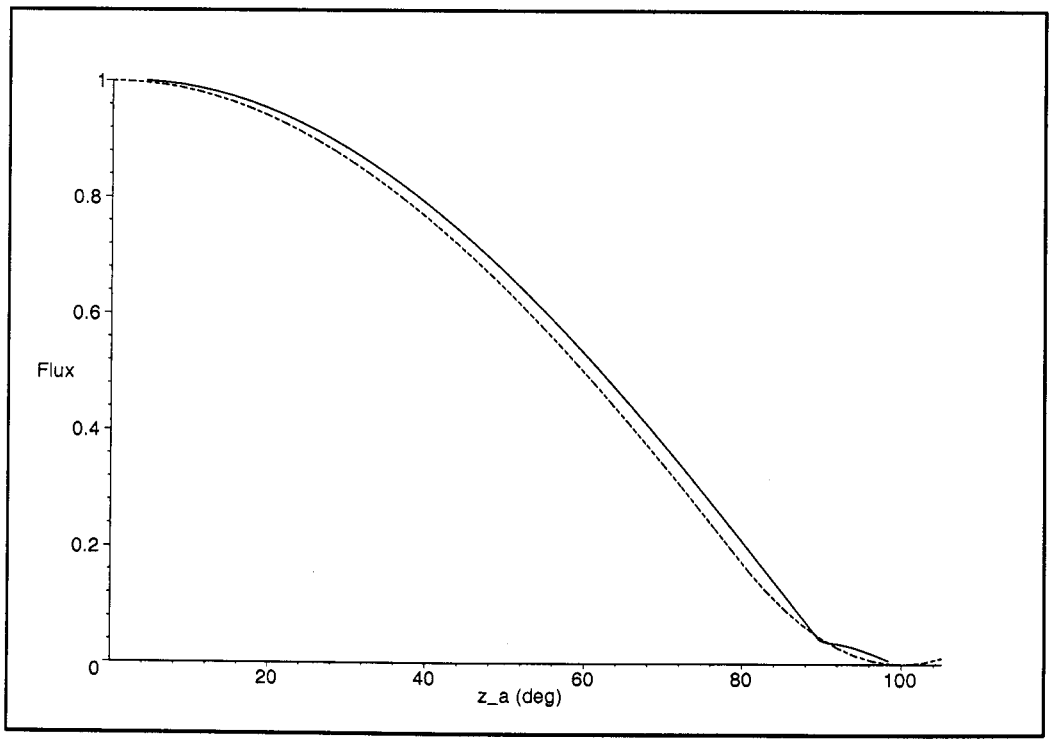

Figure 6 – Normalized shower meteor flux as a function of apparent radiant zenith angle (z_a = 0°–105°): Richardson (solid) and Kresák (dashed).

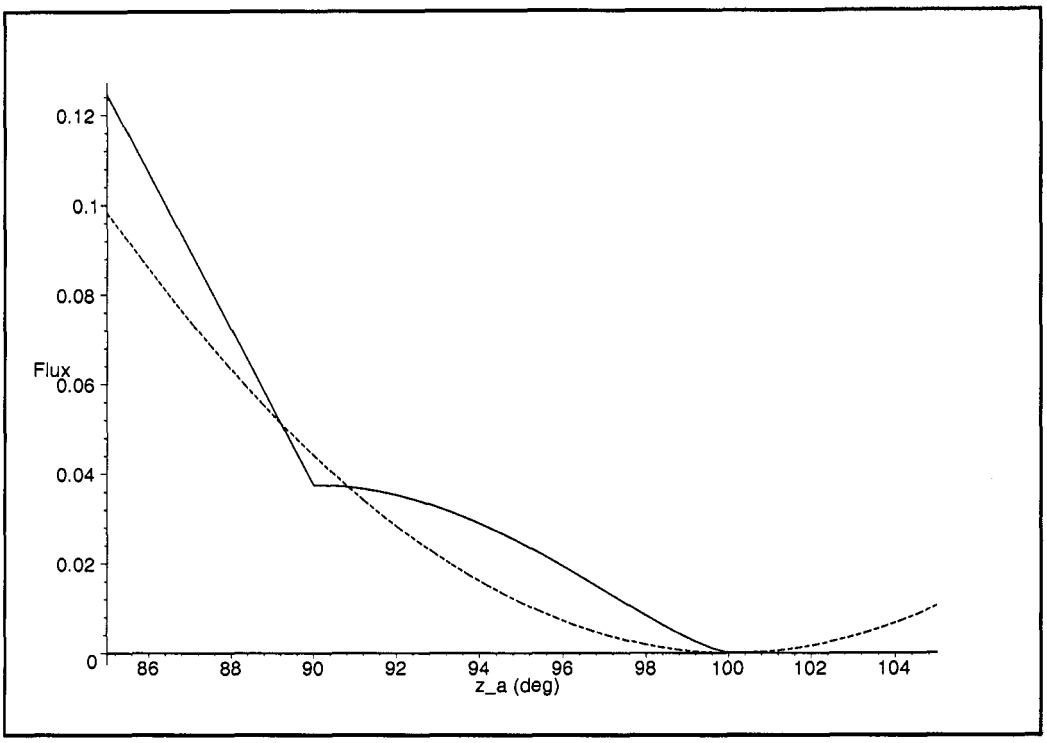

Figure 7 – Normalized shower meteor flux as a function of apparent radiant zenith angle ($z_a = 85°$–$105°$): Richardson (solid) and Kresák (dashed).

Table 1 – Normalized shower meteor flux as a function of apparent radiant zenith angle—geometric factor numerical comparisons.

z_a	Öpik (1955)	Kresák (1954)	Richardson
0°.0	1.00	1.00	1.00
5°.0	0.996	0.996	0.999
10°.0	0.985	0.985	0.991
15°.0	0.966	0.966	0.976
20°.0	0.940	0.940	0.953
25°.0	0.906	0.906	0.922
30°.0	0.866	0.866	0.885
35°.0	0.819	0.819	0.841
40°.0	0.766	0.766	0.790
45°.0	0.707	0.707	0.734
50°.0	0.643	0.643	0.672
55°.0	0.574	0.574	0.604
60°.0	0.500	0.500	0.532
65°.0	0.423	0.423	0.457
70°.0	0.342	0.342	0.377
75°.0	0.259	0.259	0.295
80°.0	0.174	0.174	0.211
85°.0	0.0872	0.0984	0.125
87°.5	0.0436	0.0686	0.0811
90°.0	0.00	0.0441	0.0375
92°.5	–	0.0250	0.0341
95°.0	–	0.0112	0.0245
97°.5	–	0.00290	0.0111
100°.0	–	0.00000281	0.0000743
100°.1	–	0.00	0.00

5. Comparison with previous results

Figures 6 and 7 show a comparison of the exact solution presented in this paper with that obtained by Kresák [4].

Figure 6 shows this comparison over the full range of zenith angles, while Figure 7 shows the two curves over the narrower range of $z_a = 85°$ to $z_a = 105°$. Note the very good agreement over the entire range, although the two curves are quite different in basic shape over the final $z_a = 85°$–$105°$ portion.

Table 1 presents a numerical comparison of the exact solution presented in this paper with the Öpik [1] flat atmosphere approximation, as well as with the Kresák [4] curved atmosphere approximation.

6. Conclusion

It is important to keep in mind that the exact solution presented here represents only the geometric correction factor—treating the entire atmospheric cap as a detector in a particle flux and obtaining a theoretical response curve as a function of particle beam apparent zenith angle.

There are several other important factors which effect how *real* observers view the meteors occurring in this atmospheric cap, including the following:

- average meteor magnitude extinction change with z_a;
- average meteor trail angular length change with z_a;
- average meteor brightness change with z_a (incident angle with atmosphere); and
- shifting direction, less than full sky field of view for observer.

All of these effects seriously undermine any potential gain in accuracy from utilizing the complex, exact solutions presented in this paper.

Therefore, care should be taken not to imply too much from this work, with the equations given here being more of academic interest than actual practical value. To date, the Zvolánková [3] equation still provides the singular means of including all effects, if only at the empirical level.

Nonetheless, the solutions presented here do clear the way for a greater understanding of how these additional factors affect real meteor observations, by providing an answer for the most fundamental, geometric effect, especially for low shower radiant altitudes.

References

[1] E. Öpik, "The Distribution of Meteor Stream Intensity over the Celestial Sphere", *Contr. from the Armagh Obs.* 15, 1955, pp. 147–173.

[2] P. Roggemans (ed.), "IMO Handbook for Visual Meteor Observations", Sky Publishing Co., 1989.

[3] J. Zvolánková, "Dependence of the Observed Rate of Meteors on the Zenith Distance of the Radiant", *Bull. Astron. Inst. Czechoslov.* 34, 1983, pp. 122–128.

[4] L. Kresák, "A Nomogram for Computing the Zenith Hourly Rates of Meteor Showers", *Bull. Astron. Inst. Czechoslov.* 6, 1954, pp. 120.

[5] A.C.B. Lovell, "Meteor Astronomy", Oxford University Press, New York, 1954.

[6] R. Shankar, "Basic Training in Mathematics: A Fitness Program for Science Students", Plenum Press, New York, 1995.

Radio Meteors—On Your PC!

William H. Black

The ICOM IC-PCR1000 is presented as a very suitable radio for radio meteor observers.

In the last few years, innovative electronics has taken markets to the point where it is difficult to differentiate the toys from the functional items. One such item is presented in this article as a wonderfully versatile, comprehensive, and powerful instrument that merits consideration by anyone casually or seriously interested in meteor astronomy.

The radio I am referring to is the ICOM IC-PCR1000, available on the American market. (For commercial information on this radio, refer to `http://www.icomamerica.com`.) The radio offers all modes (AM/FM/WFM/SSB/CW) on almost all frequencies between 500 kHz and 1300 MHz. This offers the possibility of monitoring *any* frequency and *mode* used to monitor radio meteor activity using your PC as the radio dial and a radio that is not much larger than a zip drive. The receiver does not cover the cellular phone frequency ranges. I have had one of these radios for the past several months, and am continually amazed by its performance and versatility. It is easy to install, and offers a huge spectrum coverage for only 400 USD. I have at times in the past spent almost that much just to get a converter to monitor a single frequency.

The antenna that comes with the radio is useless, except for local FM. For radio meteor monitoring, I use a three element Yagi for TV Channel 4, or for other frequencies, a doublet antenna cut to the appropriate half wavelength. A seven-foot doublet will work very well on all the low TV channels (2–5). The antenna connects to the radio through a BNC connector. The instruction manual emphasizes that a resonant antenna is the best way to maximize performance on specific frequencies. The radio requires a dedicated RS-232 port on a PC. Port options are available in the installation process. The addition of a converter to change from a DB9 to a DB25 RS-232 plug-in may be required. By using an external speaker, it is possible to connect a detector to the speaker coil to input the audio into another computing or counting device. My computer is a 133 MHz Pentium, and only runs one program at a time, but some of the more recent and faster PCs that run partition supervisor, dual screen, and/or background would allow the radio to be operated concurrently with other programs.

The active visual observer could use this radio to monitor for the onset of meteor activity, a scenario that is played out regularly by HAM radio operators who use periods of enhanced meteor activity to try for radio contacts via meteor trails. Several radios that offer similar frequency coverage capabilities are available from about 1500 USD up to several thousands of dollars. At 400 USD, this unit is an affordable and functional addition to your meteor monitoring activities.

Meteors, Comets, and Millennialism

Alastair McBeath

An overview of meteoric and cometary activity between circa 250 BC and circa 1600 AD is discussed with especial regard to the inclusion of meteoric imagery in Christian religious texts. Evidence is presented to suggest meteoric images played a leading role in the creation of millennial fears among adherents of the early medieval Church in Europe, which fears still persist into modern times, but which may have their origins in Mesopotamia circa 2200 BC. An extended discussion of meteoric imagery in Christian writings is also presented.

1. Introduction

In 1990, Rasmussen published details on a statistical examination of meteor shower, fireball, and meteorite data between 700 BC and 1850 AD [1]. He found evidence for a circa 1050-year periodicity in increased meteoric activity seen from Earth within that interval, and lesser

evidence for a circa 325-year subsidiary (possibly harmonic) periodicity. It could be argued that the longer-term implications of his findings are uncertain, due to the examined interval being just under 2.5 times the circa 1050-year periodicity's length. However, it is intriguing that, within this interval, and especially in the last 1300 years of it, millennialism among the world's Christian community featuring strong celestial imagery, has apparently risen from nowhere to have now become a prominent feature near the end of each century, possessed of a particular underlying dominance in the Western world's media as millennium's end in 2000-2001 approaches.

2. Millennialism

Millennialism is the belief that the end of the world is imminent, thought to be foretold by events on Earth such as wars, famines, diseases, and earthquakes, and astronomical signs in the sky like eclipses and stars falling from the heavens. It is a peculiarly Christian phenomenon which was encouraged by the medieval Church to deter recalcitrance among the populace in many Christian countries, with elements of it also used for political ends. An example of this latter was the meteor storm of April 3, 1095, which was coupled with other events interpreted as signs in November 1095 when Pope Urban II authorized the First Crusade [2, pp. 112–113 and references therein].

The importance of the 1000-year period to Christians seems to be most obviously stated in the biblical *Book of Revelation* (*Rev.*). For instance, in *Rev.* 20–21, after signs and events presaging the end-times, there is a passage describing how an angel descends from heaven and overpowers Satan in the form of a huge dragon, casting him into the Abyss, to be chained and sealed-in for 1000 years. Christ and his risen believers reign on Earth for this millennium, and then the rest of the dead are revived and Satan released prior to the Last Judgment, the end of the world, and the appearance of a new one. All this makes clear why Christians should have associated the end of the world with millennium's end and sought signs giving advance warning of it.

The dating of the Christian millennia is attributable to Dionysius Exiguus ("Little Dennis," circa 500–560 AD [3]), an abbot acclaimed as a brilliant scholar, mathematician, and astronomer. In 525, Pope John I tasked him with foretelling the date for Easter. At the time, this was an esoteric matter which few were thought capable of, but using known lunar cycles—a method he had to conceal by mystical language—Little Dennis ultimately produced and published an Easter date-list for 95 years from 532 to 627. His listing included the new dating notation "Anno Domini" (AD) to replace the then-existing "Anno Diocletiani," as this celebrated the Roman Emperor noted for persecuting Christians.

For a now unknown reason, Dennis chose the year 531 years before his own time for his "Year 1," as the year of Christ's birth. Recent scholars have suggested dates from circa 7 BC to circa 7 AD as Christ's birth-year, so that 2001 $\pm$ 7 years will see, or has already seen, the start of the third Christian millennium. Those who wish to could thus celebrate the coming millennium in 2001 as a reaffirmation of our humanity, as its date results from human error!

3. Meteor and comet activity

Drawing on various ancient and medieval sources, it is possible to construct at least a qualitative time line of cometary and meteoric activity for the period before and during which millennialism first appeared and developed, as Table 1 demonstrates. From the 15th and 16th centuries onwards, there are problems in interpreting the data, because of the rapidly increasing global population, and a consequent rise in the number of astronomical observations being made, although most of the data used in Table 1, especially for meteoric activity, was roughly corrected for such population shifts in the references used. Information after circa 1500 AD is of lesser interest in considering the origins of millennialism anyway.

Several points are worth further comment. Firstly, except for the earliest period in Table 1, prior to which the available records are often not sufficiently detailed or extensive enough to definitely indicate specific comet or meteor fluxes, an increased comet flux was registered about

1–2 centuries before an over 1–2 century-long increase in meteoric activity. The limited number of such events cannot be seen as conclusive, and could simply be coincidental, but the time delay would easily accommodate typical loop-formation times for meteor streams visible from Earth and associated with average short-period comets, as well as being similar to the largest short-period comet orbital periods.

Table 1 – A qualitative time line showing periods of enhanced meteoric and cometary activity, from circa 250 BC to circa 1600 AD, compiled from data in [1,2,4].

Dates	Events
ca. 250 BC– ca. 50 AD	*Bright meteors*: Increased flux from ca. 250 BC to early decades AD, with peak ca. 150 BC. *Meteors and meteor showers*: Enhanced activity from ca. 200 BC to ca. 50 AD.
ca. 100 AD	*Meteors and meteor showers*: Possible enhanced activity.
200–300	*Comets*: Increased flux.
400–500	*Meteors and meteor showers*: Enhanced activity.
ca. 600–ca. 650 ca. 750–ca. 1400	*Meteors and meteor showers*: Strongly enhanced activity? *Comets*: Increased flux 8th–11th C. and again 13th–14th C. *Bright meteors*: Increased activity 9th–13th C., with huge peak in 11th C. *Meteors and meteor showers*: Enhanced activity ca. 750–ca. 1250, with peaks ca. 850–ca. 950 and in 11th C.
1400–1600	*Comets*: Increased flux. *Meteors and meteor showers*: Enhanced activity, becoming greatly enhanced during 17th C.

Secondly, significant peaks in bright meteor activity coupled with extensive enhancements in meteoric activity generally (showers and storms) coincided with both the BC/AD boundary period and around the end of the 1st millennium AD, with lesser, though still more obvious, activity bracketing these times by 100–200 years. These might be just by-chance coincidences again, but the second was clearly most serendipitous for Church purposes if so. Evidence to be examined later supports the idea that the BC/AD boundary enhancement resulted in the inclusion of meteor storm imagery in biblical and early extra-biblical Christian literature for the first time as well.

The shortest enhancements in meteoric events within the 1st millennium, ca. 100 and ca. 600–650, are more suspected than well-attested, but the longer 5th century peak can be traced rather better, and immediately preceded Little Dennis's calendrical work. There are also surviving fresh Christian texts from around the 5th and 8th–10th centuries which use meteoric imagery, but the dating of these works is often uncertain, and it would be unwise to use them, or the AD dating revision, to draw conclusions from. It is clearer that upswings in meteoric and cometary activities were often used by the Church authorities to reaffirm the principles of millennialism, however.

4. Meteoric imagery in Christian sources

Generally speaking, the Old Testament (OT) biblical sources are believed to have been written during the last millennium BC, while the New Testament (NT) texts belong unsurprisingly to the opening centuries AD. A further class of Christian texts, sometimes called "The Apocrypha" (with a meaning of "secret" or "hidden," though in especially protestant Christian terms, these works are often treated as false, which has led to the modern English word "apocryphal" having the meaning "dubious, false"), span the late centuries BC into the early medieval AD period. Here, I have preferred the term "extra-biblical" to "apocryphal," since later attempts to discredit them conceal the fact that such works were hugely influential on medieval Christian beliefs, especially as many were often available in local languages. For example, the detailed Christian

concepts of heaven and particularly hell, which reach their pinnacle of expression in Dante Alighieri's "The Divine Comedy" (completed 1321), can be traced chiefly through extra-biblical sources written during the 1st millennium AD.

The OT books show a singular lack of reference to falling stars. The sole unequivocal mention is in *Isaiah* 14:12, where "Daystar, son of Dawn" (a title of Satan's as Lucifer, "Light-bringer," the morning star, often taken to be the planet Venus) falls to the ground from the heavens. *Isaiah* 14:15 varies this by having Daystar flung into Sheol, the Abyss, instead, though here "Daystar" refers to the King of Babylon, not Satan. *Isaiah* is thought to have been written around the 6th century BC.

Numerous OT references are to effects which could be reinterpreted as meteors or meteorite impacts, but which are actually stated as being fire falling from heaven, lightning strikes, or hailstones instead. Falls of fire from heaven are among the most frequent of these in biblical sources, beginning with the destruction of the cities Sodom and Gomorrah, the plain around them, and all living things on it by a rain of fire and brimstone (modernly regarded as burning sulphur) from heaven in *Genesis* 19:24–26. Such fire is re-used in this blanket way in for instance, *Psalms* 11 and 18, *Wisdom* 16:16–17, as well as in the NT *Luke* 17:29 (repeating the Sodom and Gomorrah story) and *Rev.* 13:11–13. This last is an apocalyptic usage which recurs reworked in extra-biblical sources such as the ca. 2nd century AD *Syriac Apocalypse of Baruch* 27:10 [6, p. 855], or a late 12th century German poem listing the signs before Doomsday [7, p. 120], where the 15th and final sign is God's fire shooting 40 fathoms into the Earth, destroying both it and heaven. In the ca. 2nd–3rd century AD *Sibylline Oracles* 2 [8, pp. 613–614], this is converted into a river of fire and brimstone which pours down from heaven.

Such fire can also be targeted more precisely, however. In *Numbers* 16:35, fire shoots from the god Yahweh and consumes a group of 250 men making incense offerings, while in *1 Kings* 18:38 (written ca. 7th century BC), this same fire consumes only a burnt offering, the wood it was burnt on, and some water in a trench around the altar. Later, this accuracy improves still more. In the *Testament of Abraham* 10:13–14 [9, p. 408], written in the early centuries AD, Abraham has the archangel Michael have fire descend from heaven to destroy just two burglars!

Lightning is a phenomenon often linked popularly or in folklore to meteors. The similarities—swift, bright, unexpected, linear (though in lightning's case only roughly)—make such a colloquial connection unavoidable. Lightning also frequently strikes the Earth and is followed by the loud rumbling of thunder. For a casual witness, the difference between this and the events of a meteorite impact is nonexistent. Medieval woodcuts of meteoritic events commonly show lightning in association, and meteorites can be folklorically named "thunderstones." Lightning can start fires too, and in Jewish and Christian literature is typically perceived as an agent of divine retribution. Some of the descriptions of fire descending from heaven are tied in with lightning imagery, so lightning strikes causing fires may well be intended in these instances. We should recall that popularly, even today, small meteorites are thought to be hot enough to start fires on landing (cf. the media reports discussed by Korlević [10], following a brilliant meteor being linked to a house fire on the opposite side of the Adriatic Sea in January 1993), however generally incorrect such a belief may be.

In the OT, lightning is commonly described as either like, or the same as, divine arrows used against transgressors and enemies, as seen in *2 Samuel* 22:8–15, where the fire-breathing god Yahweh rocks Earth and the heavens in his descent, wrapped in dark clouds, throwing down hail, fire and shooting lightning arrows before him. As *Job* 36:29–33 (probably written in the early 5th century BC) makes clear, the "Tent of Yahweh" is a dark, threatening thundercloud, imagery reinforced in *Psalms* 18 and 77, while 76 and 144 support the lightning-arrows concept. Lightning used as a punishment for sinners recurs in the late 1st century BC biblical *Book of Wisdom* (5:21–22) and the extra-biblical *Apocalypse of Abraham* 8:1–7 ([11, p.375] dated vaguely between ca. 70 AD and the mid-4th century), where Abraham's father is killed and his house destroyed when God hurls a thunderbolt at it, which sets it alight.

An important extra-biblical text dealing with large amounts of Jewish astronomical lore, and which also contains some fascinating vision-imagery, highly influential on that later used in *Revelation*, is the circa late 3rd to early 2nd century BC *Book of Enoch* (now normally called *1 Enoch*; [12, 13]). In his second vision (*1 Enoch* 43–44 [12, p.226]) the patriarch Enoch describes seeing the "other lightnings," which are different to the ordinary thunder and lightning he had seen in an earlier vision. These "others" are with the stars of heaven, and he sees how the stars' revolution produces them. He goes on to discuss how some stars arise and become lightnings, but then cannot part with their new forms. This is a feasible lay-description of meteors which also invokes Aristotle's theory that meteors occurred when vapors rose from the Earth and became ignited by the friction of the rotating celestial spheres, or the change in pressure due to cold higher in the atmosphere, described in *Meteorologica* Book I, Chapter 4)[14, pp. 28–35]; written circa the mid-4th century BC). It also shows an understanding that "shooting stars" were neither the same as "ordinary" lightning, nor the fixed stars, while implying a loose connection to both phenomena.

Hail is used much as fire and lightning in Jewish and Christian texts, as a punishment, with most references to it being typical for a heavy meteorological hailstorm, as in *Job* 20:23 (coupled with God's burning wrath and (lightning?) arrows), or *Wisdom* 16:16–17 (with torrential rain and fire). However, *Wisdom* 5:22 with its furious hailstones being hurled from a catapult, suggests a more directly-targeted use which could hint at a more meteoritic source. Further variants creep into the later extra-biblical material, for example "great hailstones of severe fire" which will fall on the Last Day, according to the late 2nd century AD *Epistle of the Apostles* 34 [8, p. 578]. A particularly interesting event occurs in the *Acts of Paul* 7 ([8, p. 379]; from the end of the 2nd century AD), where *"a violent and exceedingly heavy hail-storm fell from heaven, although the sky was clear"* to save Paul and a baptized lion from being killed by an armed crowd. The description is of a severe natural event, but the clear sky could infer a combined meteoritic and hailstorm explanation.

Many of the fire-lightning-hail events could also be visualized as pyroclastic bombs hurled from a distant volcano, but none of this should be taken to imply that the ancient authors were describing single, specific events they had witnessed. While this may seem self-evident, many scientific authors over the years have made exactly this mistake. A classic example is to see a particular volcanic eruption (e.g., Santorini, ca. 1604 BC) or comet (e.g., Halley, ca. 1404 BC) in the *Exodus* 13:21–22 imagery of the pillar of cloud-by-day and fire-by-night which leads the Israelites out of Egypt. This pillar is the god Yahweh, and as we have seen already, he always appears in OT descriptions as a cloudy and/or fiery presence, a theological fact which is generally overlooked in scientific treatments. Non-theological discussions also usually fail to note the many unknowns about the biblical Israelite exodus, including when it occurred, where it started from, which directions the Israelites traveled in, or where the two critical places *en route* (the Sea of Reeds—often mistranslated as the Red Sea—and Mount Sinai) were, as well as the fact that at least two distinct migration tales have been drawn on in constructing the biblical exodus story!

In all of this imagery found in Jewish and Christian texts from OT times forwards, apart from *Isaiah*'s falling Daystar, the closest we come to true meteors can perhaps be found in the objects like burning coals or torches that dart to and fro between four, winged composite creatures (which themselves vanish and reappear like lightning flashes) in the midst of Yahweh's brilliant, fiery chariot in the prophet Ezekiel's vision *Ezekiel* 1:1–28, especially 13–14). *Ezekiel*'s dating is uncertain, but the prophet flourished ca. 593–571 BC. Like the *Book of Enoch*, *Ezekiel*'s visionary images were highly influential on those used in *Revelation*. In a later vision (*Ezekiel* 10:1–17), Ezekiel sees an angel instructed to take some of these darting, fiery coals and scatter them over the city of Jerusalem to destroy it, following the slaughter of sinners there. Such use of specifically burning coals against transgressors is apparent again in *Psalms* 11 and 140, for instance.

Clear references to falling stars only commence with the apocalyptic biblical and extra-biblical material which flourished especially between the circa 2nd century BC and the circa 1st century AD. The ending of this period is less easy to define, but most texts using typical apocalyptic imagery later than the circa 3rd century AD seem to offer simply variants on earlier ideas, and no longer appear as original (on Jewish and Christian apocalyptic written between ca. 300 BC and ca. 300 AD, see [15]).

Such reworking of material helped carry apocalyptic traditions and beliefs through as common knowledge well into the medieval period in forms including the circa 6th/8th century *Saltair Na Rann*, and the medieval *Evernew Tongue*, and they continued to recur in official and unofficial Church teachings until relatively modern times. These texts have survived especially well from early Christian Ireland, a peripherally-placed island on Europe's border initially beyond the doctrinal control of the Church of Rome.

1 Enoch dates to the start of the flowering of apocalyptic literature. There, along with the "other lightnings" already discussed, we find another vision (*1 Enoch* 86:1–3 [12, p. 277]) where Enoch sees one star followed by many more fall to Earth to become oxen. The later punishment of these fallen stars (*1 Enoch* 88 [12, p. 278]) makes it clear this is an earlier variant of the war in heaven described in *Rev.* 12:7–9 where Michael and his angels cast down Satan, in the form of a great dragon, and his angels from heaven onto the Earth. This concept of angels becoming falling stars persists into quite modern folklore in parts of Christian Europe, for example. As agents of the fiery, stormy god Yahweh, this is not surprising, and frequent references to the glowing nature or brilliance of the angels can be seen in both OT and NT sources. In the extra-biblical *2 Esdras* 8:21–22 [16, p. 219], we are explicitly told that, at God's command, the angels are changed to wind and fire. The composite text of *2 Esdras* dates from between the 2nd century BC to the 2nd century AD. One version of the *Syriac Narrative of the Assumption of the Virgin Mary* 1, Book III [17, p. 220] contains a description of fiery angels who descend from heaven to defend Mary's house when a mob rises up to attack it. This was probably written in or after the 5th century AD.

In the early 2nd century AD *Apocalypse of Peter*, Ethiopic text 5 [8, p. 602], the spirits of the dead are turned into lightning and fire at God's command on the Day of Judgment, while, in the *Apocalypse of Abraham* 15:7 [11, pp. 379–380], many fiery men running in all directions in heaven, and constantly changing their appearance, are seen by Abraham in the company of an angel. The 3rd/4th century AD *Testament of Solomon* 20:12–17 [18, p. 747] has a description by the demon Ornias of how the demons ascend to heaven and fly among the stars, but on growing exhausted, they *"fall away like leaves from trees, and the men that see* it *think stars are falling from heaven."* Ornias continues that the demons fall because of their weakness: *"we fall down like lightnings upon the earth, and burn up cities, and set fields on fire,"* and concludes that they are not the same as the fixed stars which remain secure in the vault of heaven. Something of this notion still survived into medieval times, as a 12th century Anglo-Norman poem listing the fifteen signs before Doomsday attests [7, pp. 28–29]. The second sign in this has the stars fall from heaven and run about the Earth like lightning, in tears and hiding beneath the mountains, until they turn black and plunge into the Abyss.

If *1 Enoch* is near the beginnings of mainstream, original, apocalyptic literature, *Revelation* (dated to ca. 68–70 AD, possibly as late as ca. 95 AD) is towards its end. Although drawing on earlier texts, it represents a culmination of such works and possesses some of the most striking visual imagery in all of biblical literature. One of the most frequently-used of these images in *Revelation* as virtually unique in the Bible is the falling of stars from heaven. In *Rev.* Chapter 6, the breaking of five of seven seals by the Lamb of God brings forth first four apocalyptic riders and then an altar to the martyred dead, before the sixth seal's breaking causes a variety of astronomical and geological events (*Rev.* 6:12–14). These include the falling of stars to Earth like figs shaken from their trees in a high wind, a depiction which re-echoes in dozens of later extra-biblical texts well into medieval times, and which is also found in the biblical gospels of

Matthew (24:29–31) and Mark (13:24–26). In a passage reminiscent of *Ezekiel* 10:1–17, *Rev.* 8:5 records an angel taking live coals from an incense-altar before God's throne and hurling them to Earth, complete with thunder, lightning and an earthquake.

The sounding of the first trumpet of seven (*Rev.* 8:7) brings a fall of hail, fire and blood to burn the Earth, a throwback to the OT, but trumpet 2 (*Rev.* 8:8–9) heralds a new image, a great blazing mountain cast into the sea. The third trumpet (*Rev.* 8:10–11) sees a huge burning star called Wormwood fall on and poison the rivers and springs, while trumpet 5 (*Rev.* 9:1–6) causes a star later described as an angel to fall to Earth, unlock the shaft to the Abyss, and release smoke which rises to darken the sky. From this smoke drop horrific gigantic armored beasts, part-locust, part-scorpion, to attack those not chosen by God. Here we have another definite link between shooting stars and angels. The final chief mention of falling stars is in *Rev.* 12:1–6, where a huge, red, seven-headed dragon sweeps one-third of the stars from the sky with its tail, a prelude to the casting down of Satan's angels in the heavenly war already referred to. Meteors and dragons are also linked together in the popular mind [19].

Later Christian works associate stars or falling stars with fire. In the Ethiopic *Apocalypse of Peter* 5 [17, p. 513], we find, *"the stars shall fly in pieces by flames of fire,"* though a more recent translation [8, p. 602] gives, *"the stars shall be melted by flames of fire"* instead. The early medieval list of signs preceding Doomsday by Peter Damien [7, pp. 27–28] has on the seventh day, *"the planets and stars will spray out fiery tails such as appear in comets, to the Earth and its inhabitants,"* while a comparably-dated Welsh poem *Arwyddion cyn Dydd Brawd* sign 7 [7, p. 116] dealing with the ninth day before the end has *"Sulphurous flames in sparks, A tumult falling from the stars."* The early Irish medieval tale *The Magi*, which preserves an earlier text now lost, describes the star seen by the magi at the birth of Christ in meteoric terms [20, pp. 40-41]: *"On the calends of January ... we suddenly saw the sign which had been recounted to us, a great star, trailing fire, between us and heaven. We were pleased at this, and moreover, nobody else saw it but ourselves."* This is a very apt word-picture of a typical fireball observation, but the details are then inflated (as also often happens in casual fireball reports, though here to a far greater extreme) to have the star's radiance fill all heaven and Earth, and to continue to lead the magi for twelve days from India to Judea, riding magically-swift horses, but still without anyone else spotting it!

One final extra-biblical text to note is the 10th century Irish *Evernew Tongue* 6–7 [20, p. 110], which appears to contain the description of an early electrophonic fireball, witnessed by a large outdoor religious assembly: *"Suddenly, at the end of the eve of Easter, there was heard in the clouds a noise like thunder, or like the crackle of fire. There was a thunderous blast meanwhile, whereby suddenly a solar mass, like a bright sun, was seen in the midst of the tumult. That radiant solar mass ... was seven times brighter than the Sun ... the eyes of the host awaited the crash, for they thought that it was a sign of Doomsday."* The meteor goes on to speak to the assembly in an angelic voice; it is the Evernew Tongue itself, alias the apostle Philip.

5. Discussion

From the above, it is clear that the appearance of apocalyptic Christian literature including the first widespread use of falling-star iconography resembling strong meteor showers or storms coincides with the period of increased meteoric activity in the closing centuries BC and the 1st century AD. As other Christian texts draw on commonly-known images, it seems highly likely that because meteor storms and bright meteor showers happened relatively frequently during this time, they were drafted-in to the repertoire of portents, and perhaps even fueled the desire to create fresh apocalyptic literature in the first place.

We know that signs and portents were looked-for in the last few centuries BC, because a Messiah was expected to arrive imminently, and such increased astronomical searching could well have led the religious authors to discover the heightened meteor activity of their day. The Babylonians—an astronomically-experienced people Jewish and proto-Christian scholars would at least have

known of, and most likely had contacts with—recorded much of the information we have on this increased meteoric flux, along with, e.g., the Chinese. One wonders if an extant, if perhaps rudimentary and apparently unstated, knowledge of the ca. 1050-year periodicity in meteoric activity found by Rasmussen helped lead to the expectation of a coming Messiah at this time.

One curiosity is that comets do not obviously feature in early Christian writings at all, which is odd considering how often they were later used as signs to help bend the will of the church-going masses by the clergy. Comets perceived as ill-omens can be traced back to ancient Mesopotamia in the Western tradition, probably to the 2nd millennium BC, if not before, with Greek and Roman authors helping to perpetuate the concept in their writings through to medieval and even modern times. Occasionally, comets were seen as more positive, such as Giotto's use of a comet as the Star of Bethlehem in his ca. 1309 fresco of Christ's nativity at Padua in Italy, but this was uncommon. Comet-fear certainly played a significant role around the end of the 1st millennium AD and has continued as a key facet of millennialism's signs and portents ever since. I have examined these beliefs in comets in more detail elsewhere [21].

6. Conclusion

We will probably never know when the idea that sky portents reflected earthly events began. The earliest connection between strong meteor shower activity and human disasters I have found concerns the collapse of the important and highly influential Akkadian Dynasty in ancient Mesopotamia, and the utter destruction of its capital city Agade, ca. 2200 BC. This date is essentially three ca. 1050-year periods before the 11th century meteoric activity peak, and two such periods before the ca. 150 BC meteoric maximum, which may be nothing other than coincidental, but is intriguing nonetheless.

A text compiling prodigies supposedly predicting the end of the Akkadian Dynasty includes the line *"stars fell repeatedly from the sky"* [22, p. 283], though the text's dating is not clear. One notable and unique poem *The Curse of Agade* (discussed and translated in [23]), probably written within ca. 150 years of Agade's destruction, makes no mention of falling-star portents, so this may be a later—or merely separate—association. Falling stars were generally viewed as ill-omens in ancient Mesopotamia as Oppenheim's commentary in [22] discusses. Another text he quotes with the Agade prodigy runs, *"end of the dynasty, a great star will fall,"* for instance.

The events at, and for about eighty years after, the end of the Akkadian Dynasty were uniquely catastrophic and chaotic in ancient Mesopotamia certainly. *The Curse of Agade* condemns the city to perpetual future obscurity, highly fitting as archaeological investigations since 1761 have so far failed to locate Agade's ruins, despite the fact that the Akkadian language was the *lingua franca* of the region through until the 8th century BC.

Recent evidence has been found suggesting an abrupt climatic change ca. 2000 BC, coupled with distinctive meteoritic impact trace-products in the appropriate archaeological horizons across the Near East, according to Courty [24]. Later in her report to the December 1998 Royal Astronomical Society's London meeting, Courty discussed evidence for an ice-lens micro-structure found in some sampled horizons, which she indicated showed the impact ejecta had been frozen rapidly at high altitude. On re-entering the lower atmosphere, she noted, these ejecta would accumulate as hailstones, a fascinating thought when coupled with the possibly meteoritic hail in biblical and extra-biblical Christian sources. If this all proves correct, perhaps the "Agade event" was the beginning of meteoric activity being associated with end-times scenarios.

General notes

I have preferentially used Wansbrough [25] as my main source of biblical translations and dating, primarily because of its annotated and recent nature. It also includes most of the accepted so-called OT apocrypha as integral parts of the OT (to identify these, see Kee [16]). Other translations of the Bible may vary compared to what I have discussed here. The dating of the extra-biblical materials was derived from the individual reference sources cited. Dates too uncertain or unknown (for instance the first five books of the Bible, or Pentateuch, are commonly stated as being written sometime between the 10th and 4th centuries BC, but were based on earlier, probably oral, traditions) have been omitted here.

References and notes

[1] K.L. Rasmussen, "Historical Accretionary Events from 700 BC to AD 1850—a 1050-year Periodicity?", *Quarterly Journal of the Royal Astronomical Society* 31:1, 1990, pp. 95–108.

[2] V. Clube, B. Napier, "The Cosmic Winter", Basil Blackwell, 1990.

[3] D.E. Duncan, "The Calendar", Fourth Estate, 1009, pp. 96–102.

[4] M.E. Bailey, S.V.M. Clube, W.M. Napier, "The Origin of Comets", Pergamon Press, 1990.

[5] H.F.D. Sparks (ed.), "The Apocryphal Old Testament", Clarendon Press, 1984.

[6] R.H. Charles (translator; revised by L.H. Brockington), "The Syriac Apocalypse of Baruch", in [5], pp. 835 a.f.

[7] W.W. Heist, "The Fifteen Signs Before Doomsday", Michigan State University Press, 1952.

[8] J.K. Elliott, "The Apocryphal New Testament: A Collection of Apocryphal Christian Literature in an English Translation", Clarendon Press, 1993.

[9] N. Turner (translator), "The Testament of Abraham", in [5], pp. 393 a.f.

[10] K. Korlević, "Exploding Fireball over the Emilia Region, Italy, January 19, 1993, $0^h33^m20^s$ UT", *WGN* 21:2, April 1993, pp. 74–76.

[11] A. Pennington (translator), "The Apocalypse of Abraham", in [5], pp. 363 a.f.

[12] M.A. Knibb (translator), "1 Enoch", in [5], pp. 169 a.f.

[13] R.H. Charles (translator), "The Book of Enoch", SPCK, 1917. Although Knibb's translation [12] is now to be preferred, Charles's translation remains a useful separate-volume edition, with much remaining unaltered in the more recent version.

[14] H.D.P. Lee (translator), "Aristotle VII: Meteorologica", Harvard University Press and William Heinemann Ltd. (Loeb Classical Library imprint), 1952.

[15] C. Rowland, "The Open Heaven: A Study of Apocalyptic in Judaism and Early Christianity", SPCK, 1982.

[16] H.C. Kee, "The Cambridge Annotated Study Apocrypha: New Revised Standard Edition", Cambridge University Press, 1994. The naming and numbering of the various "Books of Esdras" (including the biblical *Ezra* and *Nehemiah*) is very confusing. *2 Esdras* here is quite separate to the biblical works.

[17] M.R. James, "The Apocryphal New Testament (Corrected edition)", Clarendon Press, 1953. Though to an extent now superseded by Elliott's work [8], Elliott draws heavily on James's details, and quite often republishes material unaltered from this text. Some works remain uniquely, or more fully, translated only by James.

[18] M. Whittaker (translator), "The Testament of Solomon", in [5], pp. 733 a.f.

[19] A. McBeath, "Meteoric Dragons", *WGN* 25:1, February 1997, pp. 34–36.

[20] M. Herbert, M. McNamara (eds.), "Irish Biblical Apocrypha: Selected Texts in Translation", T. and T. Clark, 1989.

[21] A. McBeath, "Comet Myths Ancient and Modern", *3rd Stone* 31, 1998, pp. 13–16.

[22] A.L. Oppenheim, "The Interpretation of Dreams in the Ancient Near East, with a Translation of an Assyrian Dream-Book", *Transactions of the American Philosophical Society* (New Series) 46:3, 1956, pp. 179–373.

[23] J.S. Cooper, "The Curse of Agade", Johns Hopkins University Press, 1983.

[24] M.A. Courty, "The 4 kyr BP Impact Event: the Birth of a Scientific Hypothesis", *The Observatory* 119:1151, 1999, pp. 168–171 (in meeting report). In a personal communication (August 1999), Dr. Courty commented that the evidence for an impact ca. 4 kyr BP remains under investigation, and is not yet conclusive. She noted that the present dating for it is ca. 2350 BC, which would put it around the start of the Akkadian Dynasty according to the present convention of using the so-called Middle Chronology for ancient Mesopotamian dates. It should be noted that the 95% confidence interval in the radiometric dating of the possible impact horizons used in Dr. Courty's report referred to here spans the years ca. 2500–2100 BC, however, and that ice-core evidence for extra-terrestrial amino acids (GISP II) near this period has an error margin covering ca. 2440–2270 BC. Astronomical evidence based on the known cycles of the visibility of Venus (which are used to date the start of the reign of the Babylonian king Ammisaduqa to either 1702, 1646, or 1582 BC) suggests the Mesopotamian Middle Chronology is incorrect, and that all regnal dates prior to this time down to the start of the Akkadian Dynasty should be set back by ca. 64 years. This would alter the approximate dates of the Akkadian Dynasty to ca. 2415 to ca. 2265 BC, though the exact ending of the Dynasty is unclear anyway. The last claimed Akkadian king died ca. 2154 BC (Middle Chronology; 2218 in the later dating convention). On the problems of Mesopotamian dating, see C.B.F. Walker, "Mesopotamian Chronology," in Collon, D., 1995, *Ancient Near Eastern Art*, C. Collon, ed., British Museum Press, 1995, pp. 230–238.

[25] H. Wansbrough (general editor), "*The New Jerusalem Bible* (Study Edition)", Darton, Longman, and Todd, 1994.

Observational Results

SPA Meteor Section Results: November–December 1998

Alastair McBeath

Observations and news from data presented to the *SPA Meteor Section* for November and December 1998 are given. Moonlight and unhelpful weather conditions hampered coverage during both months, but the Leonid fireball peak of November 16-17 was well-seen from Europe and North America. Some useful Geminid results were obtained too, and another bright fireball was reported from two UK locations around 22^h28^m UT on December 25.

1. Introduction

Observations in both months clustered around the expected major shower peaks of the Leonids in November, and the Geminids and Ursids in December. The vast majority of observers were active chiefly during the Leonid epoch, most notably on November 16-17 and 17-18. The Full Moon affected the Taurid maximum phase in November, plus the early Geminid stages in December, while the northern hemisphere's winter weather did little to assist in either month. Table 1 gives the observing totals achieved. At least 35 of the photographed trails in November were Leonids.

Table 1 – Visual, photographic, and radio hours' totals, plus visual and photographed meteor numbers, recorded in each month, including a partial breakdown of visual meteor types.

Month	Visual	STA	NTA	LEO	Meteors	Photo	Trails	Radio
November	261^h	142	218	10133	12467	$149^h.8$	39	4273^h
		GEM	URS	COM				
December	84^h	1453	40	33	2010	$232^h.2$	0	5727^h

A very large number of observers contributed results, thoughts, and comments during this period, who for simplicity are given below in a single listing, but with their observing method(s) indicated by the following abbreviations: P, photographic or video; R, radio; V, visual. Where not stated, visual reports only were received. Grateful thanks are extended to everyone who contacted the *Section*. Thanks go too to Chris Steyaert for providing copies of *Radio Meteor Observation Bulletins* (*RMOBs*) 64–66, December 1998 to February 1999, inclusive, and Ina Rendtel for submitting copies of the German and Mongolian data in the form of the *Arbeitskreis Meteore* journal *Meteoros* (*AKM*) 1:12 (1998) and 2:1 (1999). All the radio data, except that by Alan Heath, R.B. Minton and Robert S. White came from the *RMOBs*. The full list of contributors is as follows:

Enric Fraile Algeciras (R, Spain), Rainer Arlt (Germany), David Asher (Northern Ireland), Pierre Bader (*AKM*; Maldive Islands), Neil Bone (England), Mike Boschat (R, Canada), Franziska Böttcher (Germany), Keith Bowley (England), Jay Brausch (North Dakota, USA), Eisse Pieter Bus (R, China), Ovidiu Cioroianu (Romania), John Coates (England), Heather Couper (England), Andrea Csiki (Romania), Maggie Daly (England), John Davies (England), Norman Davis (R, California, USA), Zoltan Deak (P, Romania), Maurice de Meyere (R, Belgium), Ade Dimmick (England), Carol Downs (England), Frank Enzlein (Germany), Steve Foggo (England), Doug Fox (England), Dave Gavine (P and V, Scotland), Christoph Gerber (Germany), Ghent University (R, Belgium), Andrei Dorian Gheorghe (Romania), Bob Gilmour (Scotland), Shelagh Godwin (England), Valentin Grigore (Romania), Mathias Growe (Germany), Alan Heath (R and V, England), Mark K. Herbert (Alabama, USA), Kath Hodges (England), Terry Holmes (England), Simon Jenner (England), Ou Yang Tian Jing (R, China), Will Kelsey (R, California, USA), Daniel Köhn (Germany), André Knöfel (Mongolia), Werfried Kuneth (R, Austria), Sylvio Lachmann (Germany), John Lambert (England), Trevor Law (Western Australia), Alan Longstaff (England), Bob Lunsford (California, USA), Hartwig Lüthen

(Mongolia), Andrew Mark (Scotland), Tony Markham (England), Alastair McBeath (England), Peter McBeath (P and V, England), Tom McEwan (Scotland), Kieron McGrath (England), John Meyer (R, Arizona, USA), R.B. Minton (P, R, and V, New Mexico, USA), Jacqueline Mitton (in-flight over the Atlantic Ocean between Florida, USA, and England), Sirko Molau (Mongolia), Neil Mortimer (England), Sven Näther (Germany), Sadao Okamoto (Japan), Guy Ottewell (South Carolina, USA), Edward Polehampton (England), Ingo Reimann (R, Germany), Ina Rendtel (P and V, Germany), Jürgen Rendtel (P and V, Germany and Mongolia), Petra Rendtel (Mongolia), Tony Rickwood (England), Ian Rigney (England), Joan Robinson (England), Maurice Robinson (England), Vanya Rodiger (Croatia), Paul Roggemans (Belgium), Andy Salmon (England), Fred Schaaf (New York, USA), Ton Schoenmaker (R, Netherlands), Thomas Schreyer (Germany), Amanda Scott (England), Harald Seifert (Germany), Jonathan Shanklin (in-flight over the Atlantic Ocean between England and Ascension Island), Dierdra Shepherd (Western Australia), Jamie Shepherd (Western Australia), Chikara Shimoda (R, Japan), Hendrik Sielaff (Mongolia), Adrian Şonka (P and V, Romania), George Spalding (England), Ulrich Sperberg (*AKM*; Cyprus), Jörg Strunk (P, Germany), Paul Sutherland (France), Melvyn Taylor (Cyprus), Pierre Terrier (R, France), Axel Thomas (Germany), Anda Tiţa (Romania), David Todd (England), Manuela Trenn (Germany), Mihaela Triglav (P and V, Slovenia), Valeriu-Mihai Tudose (P and V, Romania), James Vanderpool (England), Björn Voss (Mongolia), Andrew Walker (Scotland), Peter Ward (England), David Weldrake (England), Robert S. White (R, England), Ilkka Yrjölä (R, Finland), Wim T. Zanstra (R, the Netherlands), and Florian Zschage (Mongolia).

2. November

Very little of the Taurids' extended maximum period in the first half of November could be observed, unfortunately, following the somewhat enhanced activity found in late October, as discussed previously [1]. The radio results suggest nothing unusual occurred then at least, beyond what had been established earlier [2] around $\lambda_\odot = 221°$–$223°$ (November 4–6; the start of the extended $\lambda_\odot = 224°$ period).

Figure 1, chosen as being generally representative of the available radio data, illustrates this, along with weakly increased activity around $\lambda_\odot = 219°$–$220°$ (November 2–3), also noted before. Indeed, of all the radio echo-count peaks detected during November before, only that at $\lambda_\odot = 229°$ (November 12) failed to appear in most results, which also happened in 1997. However, the $\lambda_\odot = 230°$–$231°$ time (November 13–14) again produced a small spike in several data sets, repeating the same effect seen in 1997. This may suggest this $\lambda_\odot = 229°$ peak has shifted slightly, although it was only very weakly noted in the original analysis.

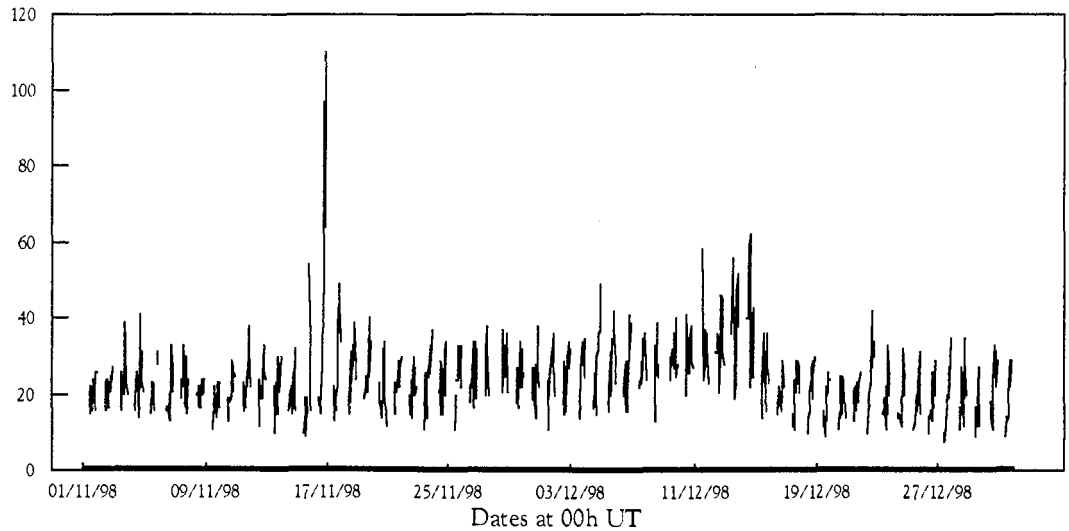

Figure 1 – Raw hourly radio meteor echo counts from November and December 1998, from data collected by Chikara Shimoda. Chikara operated his equipment usually for 12 hours a day, between 11^h and 22^h UT, with a few minor gaps. The Leonid peak is exceptionally obvious in November, though lesser peaks for the Geminids and Ursids can also be seen.

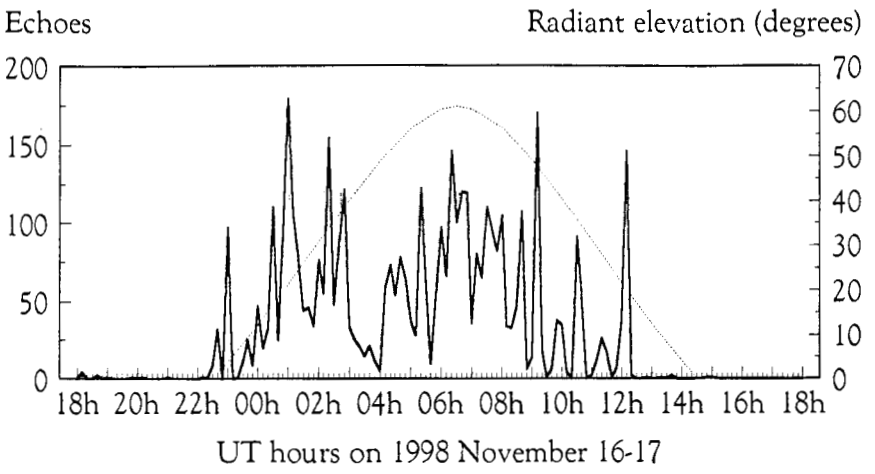

Figure 2 – Raw ten-minute radio meteor echo counts from November 16-17, 1998, recorded by Robert S. White. A graph showing the elevation of the Leonid radiant for Robert's site (around latitude 51° N) has been superimposed, as the fine-line curve. The skew of the echo counts compared to the radiant elevation is partly a result of the antenna's direction, but part results from most of the transmitting stations being east of Robert's site, hence the rapid fall-off in echo counts about two hours before the Leonid radiant set. This is a problem seen at other European radio meteor locations. It is clear most of the detected echo counts shown resulted from Leonid meteors. The echo-count profile's dip during the highest radiant elevation period is not unexpected from radio meteor theory, and the lowest echo counts near 4^h UT are purely a radio artifact, since visual observers continued to record undiminished fireball activity at this time across Europe.

The huge spike due to the Leonids is very obvious in all the radio results made during the shower's most active phases, and, as Figure 1 indicates, most observers found the peak count was about twice that during the Geminids, though it is probably best to keep such direct comparisons to a minimum. The Leonids were one of the (if not the) most significant radio meteor events in 1998. Most radio observers, regardless of their location, enjoyed large numbers of echo counts for the majority of the radio-visible period for the Leonid radiant at their site on November 16-17 especially, as Figure 2 shows. Radio coverage of the shower's profile in 1998 was insufficient to confirm specific features found in the visual profile [3], regrettably, apart from the highest counts occurring in perfect time to the extended visual fireball event of November 16-17.

It is needless to repeat what has already been said concerning visual observations of the Leonid maximum in 1998. Reference [3] provided the most detailed scientific analysis (*but see its update in the present issue*, ed.), and [4] was specifically concerned with observers' comments sent to the *SPAMS*, which along with numerous local reports that have featured in *WGN* recently provide ample information on what happened and how the observers reacted. Here, we present a single graph showing the clear difference between Leonid meteor magnitudes seen on November 16-17 and those from other times during the shower's activity (Figure 3).

Some attempts were also made to analyze the Leonid train population, but these met with little success, as many observers commented on the probable inaccuracy of their train timings from November 16-17—simply because there were so many trained meteors about—and some, including the author, found they were unable to even record accurately which meteors left trains in all but about half to two-thirds of all cases. The figures available suggest around 40% of the Leonids left trains, but this is undoubtedly an underestimate; the true figure is more likely to be 60–80%, especially during the fireball maximum. Despite this, some superb long-lasting trains were sketched, photographed, and videoed, a valuable record of such relatively rare events.

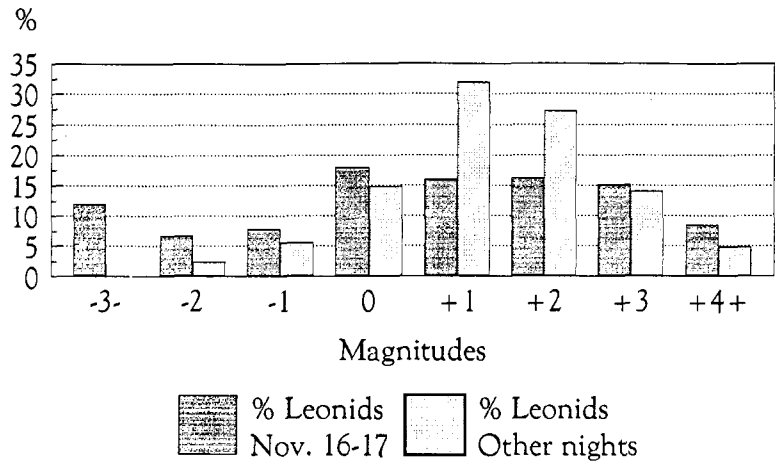

Figure 3 – Percentage magnitude distributions for 615 Leonids from November 16-17 compared with those from 125 Leonids seen on other nights. The fireball bin for November 16-17 is exaggerated due to fireball numbers extending continuously up to magnitude −12 to −13. The difference in the two distributions is very clear, despite the relatively small number of Leonids available away from the fireball maximum. The corrected mean magnitude for the Leonids on November 16-17 was +1.3, compared to +2.7 on the other nights. The November sporadics' value (from 214 meteors) was +3.7, by contrast.

Later in the month, a small radio peak was seen around the predicted α-Monocerotid maximum, $\lambda_\odot \approx 239°$ (November 21-22), suggesting nothing unexpected occurred from the shower during its radio visibility by our observers in 1998. A few shower meteors were seen visually too, but no marked rates were noted. The gradual radio rate increase towards late November and early December was again found, much as normal.

3. December

With most visual observations taking place around the predicted Geminid and Ursid maxima, due to a combination of bright moonlight during the earlier and later days, and some typically poor northern hemisphere winter weather, we must rely on radio observations for information at these times. All of the pre-Geminid radio peaks found in [2] were recorded again, though as in 1997, the $\lambda_\odot \approx 256°$ (December 8) peak shows up in only half the available results. In addition, the $\lambda_\odot \approx 252°$ (December 4) peak first detected in 1997 was visible at least weakly in most datasets, as can be seen in Figure 1. This spike was at its most noticeable in longer-duration echoes reported by Werfried Kuneth (duration larger than 6.5 s; not shown here), but did not recur in similar data from Sadao Okamoto (duration larger than 5 s).

Chief event of the month was naturally the Geminids, although many European visual and photographic observers wrote complaining about the poor skies they had to endure during the shower's best. Despite such problems, it has been possible to construct a basic ZHR graph from December 10-11 to 14-15, as shown in Figure 4. The mean ZHR on December 13-14 was 70 ± 4, but looking at the sub-dataset available from near the expected maximum time shows ZHRs were 110 ± 15 around 6^h–8^h UT on December 14 ($\lambda_\odot = 262°.05$–$261°.14$). European radio data confirms a probable peak timing around 6^h–7^h UT on December 14, with the Geminid maximum spike showing up better in the European and North-American data than the Japanese, unsurprising considering the peak's timing. This is marginally later than, but still in-line with, the expected maximum time of approximately 5^h UT [5], as was generally confirmed by the preliminary *IMO* results for the shower (cf. [6]).

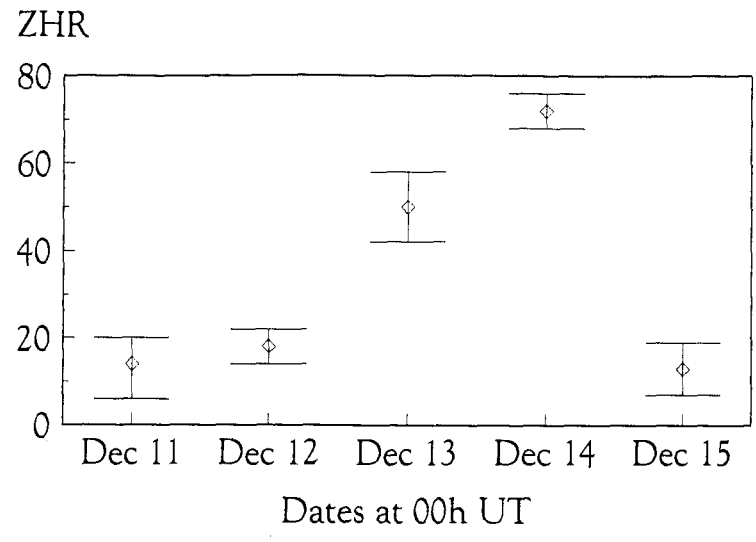

Figure 4 – Near-peak mean Geminid ZHRs from the *SPAMS* data. Each night's results have been averaged into a single data point, as most results were from European sites, except on December 13-14, when more were from North America. Standard error bars are also appended, and the ZHRs were computed using $r = 2.6$.

It has also been possible to construct a global magnitude distribution for the shower and the December sporadics, given in Table 2. There was a paucity of fireball-class Geminids reported this year, with most that were seen occurring over North America, the sites best-placed to catch the maximum and immediate post-maximum stages visually. Several correspondents commented that this aspect compared very unfavorably to the wonderful fireball night the Leonids had produced barely a month earlier! Too few Geminid trains were noted to allow a proper analysis, but around 6% of both Geminids and December sporadics left persistent trains, not atypical values from recent years.

Table 2 – Global magnitude distributions, including mean limiting magnitude and corrected mean magnitudes for the Geminids and December sporadics seen under good sky conditions.

Shower	-3^-	-2	-1	0	$+1$	$+2$	$+3$	$+4$	5^+	Tot	Lm	$\overline{m}_{6.5}$
Geminids	3	7	18.5	58	104	164.5	136.5	63	0.5	555	5.63	2.77
Sporadics		3	0.5	5	19	28.5	24.5	18	6	104.5	5.72	3.12

After the Geminids, all the usual radio maxima were spotted by the majority of active systems, and nothing unexpected was seen. The decline in overall radio rates during the second half of December is well-shown by Chikara Shimoda's results in Figure 1, with a slight upturn due to the beginnings of the Quadrantids right at the year's end.

The Ursids produced a small but noticeable spike in all the available results around $\lambda_\odot = 270°$–$271°$ (December 22–23), much as expected, but neither the radio data, nor the few visual results then suggest any unusual outburst from the shower in 1998. The small amount of visual data is not conclusive, however.

Although a sprinkling of Coma Berenicids was seen, no clear visual maximum was apparent for them.

One bright fireball was reported to us on December 25 around 22^h27^m–22^h28^m UT, seen from two sites in central-southern England. From the approximate plots, the meteor seems to have been moving roughly south to north (perhaps south-south-west to north-north-east), and a very rough estimate suggests it may have passed near or directly over Peterborough in Cambridgeshire. Both

observers reported the object as being bright white or blue-white, with a fiery red crescent of color either immediately preceding or following the head. The fireball was probably around magnitude −6 to −8.

Acknowledgments

It is as ever a pleasure to gratefully thank all our observers and contributors who made this report possible. Good luck and clear skies for your next observing!

References

[1] A. McBeath, "SPA Meteor Section Results: September-October 1998", *WGN* 27:3/4, June-August 1999, pp. 209–214.

[2] A. McBeath, "The Forward Scatter Meteor Year", in *Proceedings 1997 IMC*, Petnica, Yugoslavia, A. Knöfel, A. McBeath (eds.), IMO, 1998, pp. 39–54.

[3] R. Arlt, "Bulletin 13 of the International Leonid Watch: The 1998 Leonid Meteor Shower", *WGN* 26:6, December 1998, pp. 239–248.

[4] A. McBeath, "SPA Meteor Section Results: Personal Recollections of the 1998 Leonids", *WGN* 27:1, February 1999, pp. 33–37.

[5] A. McBeath (comp.), "Meteor Shower Calendar: October 1998–March 1999", *WGN* 26:4, August 1998, pp. 147–153.

[6] J. Rendtel, "Geminiden 1998", *Meteoros* 2:1, 1999, pp. 3–4.

Erratum on
Activities of the Spanish Photographic Network in 1998

Josep M. Trigo-Rodriguez, Julio Castellano-Roig, and Alberto Castro-Tirado, University of Valencia and LAEFF-INTA

The following table has been accidentally omitted in the previous issue of WGN. *Please accept our apologies.* (Ed.)

Table 1 – Different nights observed by the *SPMN* team. Five meteors have been photographed simultaneously, including two Geminids. Another 20 meteors have been obtained from a single station.

Month	Nights	Number of stations/observers	Double-station (hours)
July	1	3/ 5	4
August	2	4/ 6	6
September	2	3/ 3	5
October	2	2/ 2	5
November	3	5/ 5	10
December	3	3/ 3	10
Total	13	8/13	40

SPA Meteor Section Results: January–February 1999

Alastair McBeath

Details from results and news submitted to the *SPA Meteor Section* from January and February 1999 are given. Moonlight and poor weather meant only radio data were available for the Quadrantids, which enabled a mean peak time to be determined for them around $\lambda_\odot = 283°.18 \pm 0.04$ (J2000.0), January 4, $0^h \pm 1^h$ UT, slightly later than expected. No clear Virginid radiants were apparent from meteor plots made during February, and only very low rates from this source were seen.

1. Introduction

Typically unhelpful northern winter weather combined with Full Moon to ruin views of the 1999 Quadrantids, but some minor shower coverage was possible in mid-January. February was still poorer, but some Virginid plots were made at least. Table 1 has the overall observing tallies.

Table 1 – Visual, photographic, and radio hours' totals, and visual meteor numbers recorded in each month.

Month	Visual	Meteors	Photo	Radio
January	$92^h.7$	504	$198^h.2$	4719^h
February	$35^h.7$	164	$51^h.9$	3061^h

Our photographic results came exclusively from the all-sky fireball cameras of the German *Arbeitskreis Meteore* (*AKM*) observers, which along with the other *AKM* details here were taken from their journal *Meteoros* 2:2, 2:3, and 2:5 (1999), kindly provided by photographic observer Ina Rendtel. The other photographers were Jürgen Rendtel, Jörg Strunk, and Roland Winkler.

Much of the radio reports came from *Radio Meteor Observation Bulletins* (*RMOB*s) 66–68 (February to April 1999, inclusive) which Chris Steyaert was good enough to provide. The radio observers included

> Enric Fraile Algeciras (Spain; *RMOB*), Mike Boschat (Canada; *RMOB*), Maurice de Meyere (Belgium; *RMOB*), Ghent University (Belgium; *RMOB*), Will Kelsey (California, USA; *RMOB*), Werfried Kuneth (Austria; *RMOB*), R.B. Minton (New Mexico, USA), Sadao Okamoto (Japan; *RMOB*), Chikara Shimoda (Japan; *RMOB*), Pierre Terrier (France; *RMOB*), Robert S. White (England), and Ilkka Yrjölä (Finland; *RMOB*).

An analysis of the raw data was carried out as normal. The graph given as Figure 1 here shows a reasonable overview of what was generally recorded by the majority of observers during January and February.

The visual observers were as follows:

> *AKM* members Rainer Arlt, Franziska Böttcher, Frank Enzlein, Christoph Gerber, Sylvio Lachmann, Sven Näther, Ina Rendtel, Jürgen Rendtel, Marion Rudolph, Harald Seifert, Roland Winkler (all in Germany); Tim Cooper (South Africa), Shelagh Godwin (England), and Chris Hall (England).

2. January

A moonlit Quadrantid return was predicted to begin the year, which the weather conspired with to conceal most visual shower meteors. Fortunately, radio observing was not affected and some excellent, detailed results were received. From the continuous radio data sets available, an average Quadrantid maximum time close to $\lambda_\odot = 283°.18 \pm 0°.04$ (J2000.0) was calculated based on the raw data, allowing for the radiant's normal culmination time. This equates to January 4, 1999, $0^h \pm 1^h$ UT. Enhanced echo count rates were found for several hours to either side of this time too, as expected, providing the radiant remained at a reasonable elevation above the horizon for a given site.

Although this is an excellent result, being very close to the predicted maximum time [1], with a good degree of relative agreement between the different datasets, the lack of confirming visual data makes certainty about the event's timing less than ideal. The radio peak found here is at least not inconsistent with Quadrantid returns in recent years, which have shown the radio and visual maxima to be generally coincident.

After the Quadrantid epoch, radio rates decreased to their usual January levels, as Figure 1 illustrates. All the minor echo count peaks found previously in [2] were again detected, though those around $\lambda_\odot = 289°$ (January 9-10, 1999) and $\lambda_\odot = 295°$ (January 15-16) were recorded only weakly in the available results. The $\lambda_\odot = 304°$–$305°$ period (January 24–26) first found in 1998 [3] recurred in most datasets, though it was weak in both the long-duration echo data and the observations made from Japan. Unlike in the previous year, no coincident minor fireballs were reported to us during this period in 1999, however.

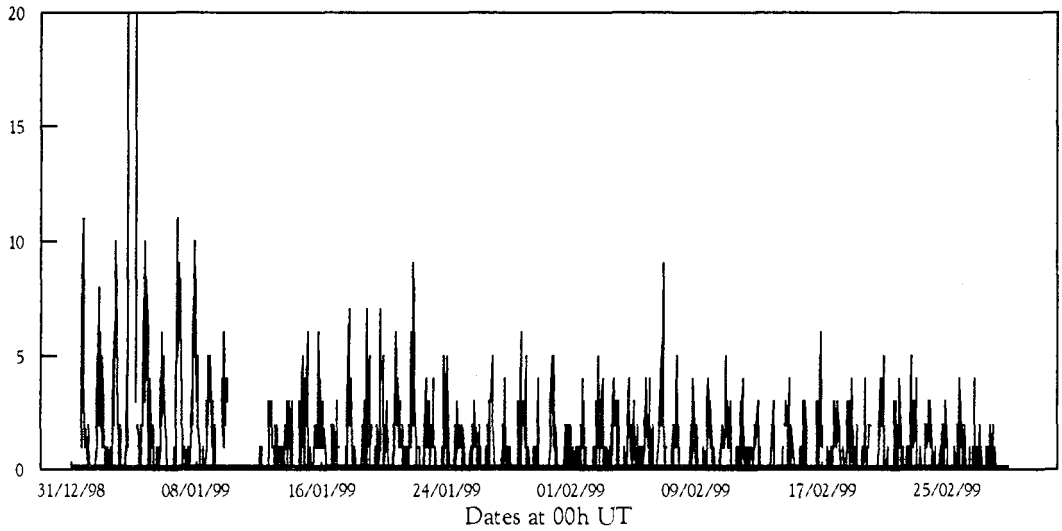

Figure 1 – Long-duration (more than 5 s) raw hourly radio meteor echo counts from 1999 January and February, in data collected by Sadao Okamoto. Sadao's radio set-up was operated virtually continuously throughout this period except when atmospheric interference intervened, and from 1^h UT on January 10 to 1^h UT on January 12, when an equipment failure caused a longer break. The peak Quadrantid echo count disappears off the top of the graph, as it was over 20 per hour from 18^h UT on January 3 to 4^h UT on January 4, peaking at 117 echoes between 22^h and 23^h UT on January 3.

Most visual observations were made by the German *AKM* watchers between January 14 and 21. These revealed only very weak minor shower activity, generally, but provided valuable details on what was happening to the sporadic rates during their annual decline to their northern spring low point.

3. February

Meteorically, February is generally a quiet month unless the α-Centaurids produce one of their rare higher outbursts for southern hemisphere observers. In 1999, the midnight-rising waning Moon was a problem for them as their roughly south-circumpolar radiant is highest after local midnight. Only Tim Cooper of our observers attempted to cover the shower, but reported no stream members in about 4 hours of watching near their expected peak, on February 6-7 and 8-9 before moonrise.

Some Virginids were seen during the month, producing weak observed rates only (about 1 or 2 per hour at best). Often poor skies meant just eleven meteor plots were available for further analysis as part of our on-going Virginid examination, but investigation of these revealed no clear radiants at all, regrettably.

As expected, no large variations in radio meteor echo counts were found during the month, as Figure 1 demonstrates. Those lesser variations seen in previous years [2] all recurred again, however. The early-month period $\lambda_\odot = 312°$–$320°$ (February 1-2 to 9-10; the extended $\lambda_\odot = 314°$–$318°$ period), notably $\lambda_\odot = 314°$–$316°$ (February 3-4 to 5-6), was particularly prominent. Of the two new solar longitudes found to yield minor peaks in 1998 [3], that at $\lambda_\odot = 325°$ (February 14-15) was not detected, while that at $\lambda_\odot = 331°$ (February 20-21) was reported only weakly in half the available data sets. As in 1998, the $\lambda_\odot = 336°$–$337°$ time (February 26–27) was the relatively strongest part of the February section of the $\lambda_\odot = 333°$–$342°$ (end-February corresponds to $\lambda_\odot = 339°$) echo-rate enhancement.

Acknowledgments

As always, I have great pleasure in thanking all our observers and correspondents. Please keep your news and data coming, and clear skies for all your work.

References

[1] A. McBeath (comp.), "Meteor Shower Calendar: October 1998–March 1999", *WGN* 26:4, August 1998, pp. 147–153.

[2] A. McBeath, "The Forward Scatter Meteor Year", in *Proceedings 1997 IMC*, Petnica, Yugoslavia, A. Knöfel, A. McBeath, eds., IMO, 1998, pp. 39-54.

[3] A. McBeath, "SPA Meteor Section Results: January-February 1998", *WGN* 26:4, August 1998, pp. 184–188.

The 1999 Draconids from the Netherlands and the Draconids of 1953

Marco Langbroek

A low-level but definite Draconid activity observed from the Netherlands in the evening of October 8, 1999, is reported. A comparison is drawn with 1953. Aspects of apparent rapid stream evolution are discussed, which have some bearing on, e.g., activity and radiant positions during "off season" years.

1. Introduction

In 1998, and connected to the perihelion-passage of the parent comet, 21P/Giacobini-Zinner that year, the Draconid stream provided a prominent display over eastern Asia, with a low-level activity tail over Europe and North America [1–3]. Subsequently, some hopes were raised for possible activity in 1999 as well [2], although there is only one clear precedent for such a multi-year occurrence, namely 1952 and 1953, [4].

2. 1999 observations by the author

Unfortunately, northwestern Europe suffered from traditional bad weather around the stream maximum of October 8-9. Clouds and rain showers, generated by an Atlantic low pressure "train," "boiled" by the warm North Sea, were all that most observers in this part of the world encountered.

Yet, this author has been lucky. In localized parts of the western Netherlands, short clearings developed on the evening of October 8. Between roughly 20^h and 21^h UT, this author at Voorschoten ($\lambda = 4°28'$ E, $\varphi = 52°07'$ N) got two periods of about 20 minutes in which clouds almost completely disappeared, allowing an unhampered although short view on the meteor activity.

Table 1 - Summary of observed Draconids (GIA) and sporadics (SPO) on October 8, 1999.

Period (UT)	T_{eff}	Lm	GIA	SPO
19^h59^m–20^h20^m	0.32	6.3	2	4
20^h38^m–20^h50^m	0.18	6.3	2	2
20^h50^m–20^h58^m	0.10	5.9	1	0
Total	0.60		5	6

Table 2 - Magnitude distributions of observed Draconids and sporadics.

Shower	+1	+2	+3	+4	+5	$\overline{m}$
Draconids	0	1	2	2	0	3.2
Sporadics	0	2	3	0	1	3.0

Unhampered observations (no cloud cover) were conducted in the periods 19^h59^m–20^h20^m UT and 20^h38^m–20^h58^m UT, with partial cloud cover in between. With a very good limiting magnitude (+6.3) for the most part, the author noted 11 meteors in 0.60 hours, all of which were plotted.

Figure 1 shows that five of these are slow meteors radiating from the head of Draco. The number of meteors is high enough to suggest that this is true Draconid activity. A sixth Draconid was seen in "unofficial time" with partial cloud cover at 20^h31^m UT, adding to this picture of low-level but significant activity. With some reservations given the low numbers, a ZHR of 11 ± 5 is suggested.

The Draconids seen were, like in 1998 [1-2], rather faint, with a mean magnitude that is, taken face value, slightly fainter than that of the sporadic background observed. To this author, the activity was strongly reminiscent of the activity he and his friends observed from the Netherlands on October 8 of the previous year (1998). This activity was part of a background tail to the prominent outburst over Asia, an extended background with (for the observational period of the Dutch observers) a ZHR of 8 ± 2 [2,3].

3. The case for "off season" activity

The plotted Draconids provide a radiant centered at approximately $\alpha = 262.^\circ9$ and $\delta = +53.^\circ5$, excluding one outlier which passes slightly more to the south. Given the inaccuracies endemic to deriving a radiant position from plottings, this is in good agreement with previously determined radiant positions for the Draconids obtained by single-station photographic and video records from 1946 and 1985 (see Figure 1).

In 1946, single-station records from the main outburst provided an intersection radiant at $\alpha = 262.^\circ1$ and $\delta = +54.^\circ1$; in 1985, four single-station photographic meteors from the main outburst component provided an intersection radiant at $\alpha = 262.^\circ4$ and $\delta = +55.^\circ8$, while seven video trails resulted in an intersection radiant at $\alpha = 262.^\circ2$ and $\delta = +55.^\circ3$ [4].

The radiant determined from my 1999 visual plottings might be located slightly more to the south (as suggested by McBeath [5]). Given the inaccuracies, this might be only an apparent deviation.

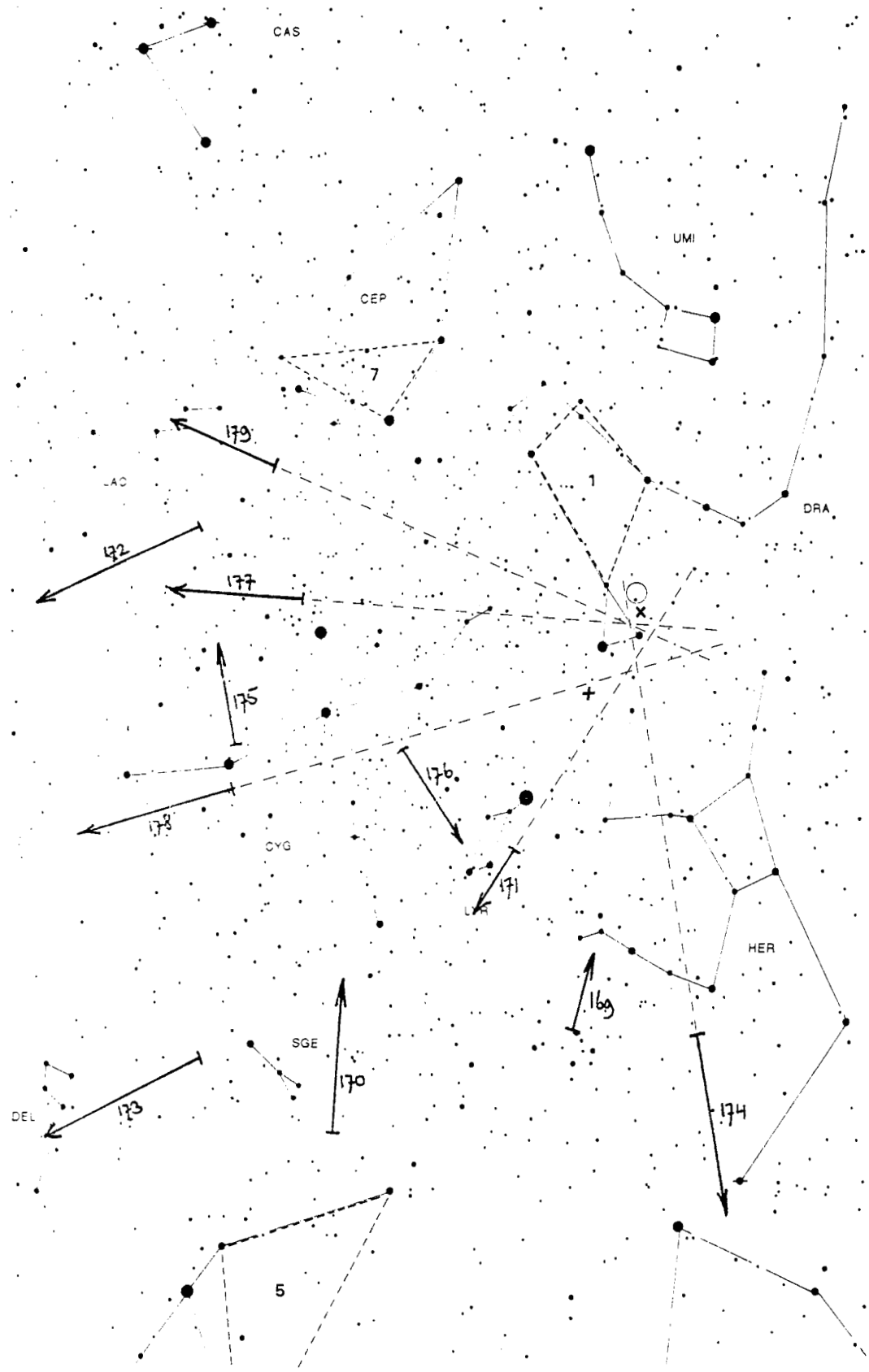

Figure 1 – Five Draconid meteors (and six sporadics) observed by the author in only 0.6 effective hours in the evening of October 8, 1999. Radiants for previous years of activity are shown: open circle, 1985 photographic and video single-station radiant; "×," 1946 single-station photographic radiant; and "+," 1953 multi-station photographic radiant.

Still, it is interesting to note that two multi-station Harvard Survey photographic records [6] of Draconids photographed within a period of 2 hours, half a day before nodal crossing on October 9, 1953 (HV 8943 328J and HV 8951 330J) and one year after the 1952 outburst, indeed have a radiant that is notably south of the 1946 and 1985 radiants [4,6], with (geocentric) coordinates $\alpha = 270\overset{\circ}{.}8$ and $\delta = +47\overset{\circ}{.}3$.

This is interesting (and has wider implications, given below), given that 1952 and 1953 is the only unambiguous precedent to 1998 and 1999 for observed Draconid activity in two consecutive years. My meteors 178 and perhaps 171 (Figure 1) might belong to such a 1953-like "southern" deviating radiant.

The 1952 and 1953 displays both occurred about half a year from nodal passage of the parent comet [4]. The 1999 activity now observed occurred considerably later (over a year after nodal passage of 21P/Giacobini-Zinner).

The apparent gradual widening of the main outburst component of the stream over the years (B = 17–24 in 1933–1952 [4]; B = 13 in 1985 [4]; and B = 8 in 1998 [1,2]) points to a gradual dispersal of dust perpendicular to the Comet's orbit (and in the plane of the ecliptic); the consecutive 1998 and 1999 activity as well as the consecutive 1952 and 1953 activity might point to a very rapid dust dispersal along the cometary orbit as well, both in front and behind the comet. And, indeed, both 1953 meteors have orbital elements with a considerably smaller semi-major axis (a shorter orbital period) and a lower inclination compared to the comet [4,6,7].

There is no reason why activity of Draconid meteors should be restricted to perihelion passage years of the parent comet, given the photographic orbits obtained in 1953; assuming that they would remain in a similar orbit, meteoroids from the dust component that provided the activity of 1953 should have reappeared at their orbital node in 1995, 3 years (half an orbital period!) in front of the comet! This might provide an argument in favor of reported activity in "off season" years (e.g., as for 1996 in [8,9], a report which sparked considerable debate at the time).

Here, it appears we are witnessing an outburst stream rapidly evolving into an annual stream. We should be on the lookout for continuing signs of activity next years, and not be surprised if we do detect such.

However, the example of 1953 shows that the radiant positions of the stream in "off-season" years might be well off from those obtained during the classic outburst displays, which is a point to bear in mind regarding meteor classifications in "off season" years. Partaking in the elusive character of the stream might be its so far unappreciated elusive radiant.

References

[1] R. Arlt, "Summary of 1998 Draconid Outburst Observations", *WGN* 26:6, 1998, pp. 256–259.

[2] M. Langbroek, "Draconiden 1998, voorlopige resultaten", *Radiant* 20:6, 1998, pp. 92–93.

[3] C. ter Kuile, M. Langbroek, "Draconiden 1998 succes!", *Radiant* 20:6, 1998, p. 89–91.

[4] P. Jenniskens, "Meteor Stream Activity II. Meteor Outbursts", *Astron. Astrophys.* 295, 1995, pp. 206–235.

[5] A. McBeath, *personal communications*, October 1999.

[6] P. Jenniskens, "On the Dynamics of Meteoroid Streams", *Earth, Planets, Space* 50, 1998, pp. 555–567.

[7] B. Lindblad (database ed.), *IAU Photographic Meteor Database*, Lund, Sweden.

[8] M. Langbroek, "1998 October Draconid Prospects?", *WGN* 25:1, 1997, p. 37–39.

[9] E.P. Bus, "Radiowaarnemingen (2), α-Monocerotiden en Draconiden", *Radiant* 19:3, 1997, pp. 58–60.

The International Meteor Organization

Council

President: Jürgen Rendtel, Seestraße 6, D-14476 Marquardt, *Germany*,
tel. +49 (332) 08 50753, e-mail: president@imo.net

Vice-Pres.: Alastair McBeath, 12A Prior's Walk, Morpeth, Northumberld. NE61 2RF, *Engl.*,
tel. +44 (1670) 518 487

Secretary-General: Robert Lunsford, Vance Street 161, Chula Vista, *CA 91910, USA*
tel. +1 (619) 585 9642, e-mail treasurer@imo.net

Treasurer: Ina Rendtel, Mehlbeerenweg 5, D-14469 Potsdam, *Germany*,
tel. +49 (331) 520 707, e-mail: treasurer@imo.net
postal (giro) account number: 5472 34-107
bank code: 100 100 10 Postbank Berlin
(bank code and postbank to be mentioned together with account number!)

Other council members:
Rainer Arlt, Friedenstraße 5, D-14109 Berlin, *Germany*
Godfrey Baldacchino, "Sirius," Triq-Il-Migbha, ZBR 10 Marsascala, *Malta*
Marc Gyssens, Heerbaan 74, B-2530 Boechout, *Belgium*
André Knöfel, Saarbrücker Straße 8, D-40476 Düsseldorf, *Germany*
Sirko Molau, Weidenweg 1, D-52074 Aachen, *Germany*

Commission Directors

Visual Commission: Rainer Arlt, e-mail: visual@imo.net

Telescopic Commission: M. Currie, 660, N'Aohoku Place, Hilo, *HI 96720, USA*,
e-mail: tele@imo.net

FIreball DAta Center: André Knöfel, e-mail: fidac@imo.net

Photographic Commission: Marc de Lignie, Prins Hendrikplein 42, NL-2264 SN Leidschendam,
the Netherlands, e-mail: photo@imo.net

Video Commission: Sirko Molau, e-mail: video@imo.net

Radio Commission: vacant, e-mail: radio@imo.net

WGN — The Journal of the International Meteor Organization and Observational Report Series

Editor-in-chief: Marc Gyssens, tel. 32 (477) 64 05 48, e-mail: wgn@imo.net
fax: 32 (11) 26 82 99 (mention "for Marc Gyssens")

Editorial board: R. Arlt, D. Asher, M. Beech, P. Brown, M. Currie, M. de Lignie, W. Elford, G. Kronk, R. Hawkes, D. Hughes, J. Jones, C. Keay, R. Koschack, A. McBeath, D. Meisel, P. Pravec, J. Rendtel, M. Šimek, G. Spalding, I. Williams.

Typesetting: Urania, the Public Observatory of Antwerp

Web Site: http://www.imo.net

Addresses of contact authors not mentioned above

P. Martin, 1847 Loranger Court, Orleans, *Ontario K1C 7H6, Canada*
P. Jenniskens, NASA/Ames Res. Ctr., Mail Stop 239-4, Moffett Field, *CA 94035-1000, USA*
J. Richardson, 1229 Clark Avenue, Tallahassee, *FL 32301, USA*
W.H. Black, P.O. Box 633, Grayson, *GA 30017, USA*
J.M. Trigo-Rodriguez, C/ Manuel de Falla 26, E-12560 Benicassim (Castelló), *Spain*
M. Langbroek, Jan Steenlaan 46, NL-2251 JH Voorschoten, *the Netherlands*

Please renew promptly your

Subscription/Membership for 2000

and save us a lot of difficulties!!!

Each year, many *WGN* subscribers renew late. As a consequence, we have serious trouble in planning the new volume. Please save us this trouble by renewing early. Early subscribers are also rewarded—read the leaflet enclosed with this issue! All subscription/membership information can be found on p. 263 en 264.

The stock of the IMO

	DEM	EUR	USD
Publications in English:			
Photographic Meteor Data Base (1986)	8	4.09	6
Proceedings International Meteor Conference 1990	10	5.11	8
Proceedings International Meteor Conference 1991	10	5.11	8
Proceedings International Meteor Conference 1992	10	5.11	8
Proceedings International Meteor Conference 1993	12	6.14	9
Proceedings International Meteor Conference 1994	10	5.11	8
Proceedings International Meteor Conference 1995	12	6.14	9
Proceedings International Meteor Conference 1996	12	6.14	9
Proceedings International Meteor Conference 1997	12	6.14	9
Proceedings International Meteor Conference 1998	12	6.14	9
Proceedings International Meteor Conference 1999	12	6.14	9
Gnomonic Atlas Brno 2000.0	5	2.56	4
Photographic Astrometry + diskette	13	6.65	10
WGN Observational Report Series:			
Vols. 1–4 (1988–91): Visual and Fireball Obs., per vol.	15	7.67	12
Vol. 5 (1992): Visual Observations	15	7.67	12
Vol. 6 (1993): Vis. Obs. and Electrophonic Fireball Cat.	20	10.23	16
Vols. 7–11 (1994–98): Visual Observations, per vol.	20	10.23	16
Backissues of the WGN Journal:			
Volumes 19–20 (1991–92): complete, per volume:	20	10.23	16
Volumes 21–22 (1993–94): complete, per volume:	25	12.78	20
Volumes 23–27 (1995–99): complete, per volume:	35	17.90	25
Backissues of Fidac News:			
Volumes 1–7 (1993–99) : complete, per volume:	15	7.67	12